Distribution Agreement

In presenting this thesis or dissertation as a partial fulfillment of the requirements for an advanced degree from Emory University, I hereby grant to Emory University and its agents the non-exclusive license to archive, make accessible, and display my thesis or dissertation in whole or in part in all forms of media, now or hereafter known, including display on the world wide web. I understand that I may select some access restrictions as part of the online submission of this thesis or dissertation. I retain all ownership rights to the copyright of the thesis or dissertation. I also retain the right to use in future works (such as articles or books) all or part of this thesis or dissertation.

Signature:

_____ _____

Alyssa Scott Date

The role of lysine specific demethylase 1 (LSD1) and the functional consequences during development

By

Alyssa Scott

Doctor of Philosophy

Graduate Division of Biological and Biomedical Sciences

Genetics and Molecular Biology

The role of lysine specific demethylase 1 (LSD1) and the functional consequences during development

By

Alyssa Scott
B.S., Marist College, 2011
Genetics and Molecular Biology

David Katz, PhD
Advisor

Jeremy Boss, PhD
Committee Member

Meleah Hickman, PhD
Committee Member

Shannon Gourley, PhD
Committee Member

Tamara Caspary, PhD
Committee Member

Accepted:

Kimberly Jabob Arriola, Ph.D.
Dean of the James T. Laney School of Graduate Studies

Date

The role of lysine specific demethylase 1 (LSD1) and the functional consequences during development

By

Alyssa Scott
B.S., Marist College, 2011

Advisor: David J. Katz, Ph.D.

An abstract of

A dissertation submitted to the Faculty of the
James T. Laney School of Graduate Studies of Emory University

in partial fulfillment of the requirements for the degree of

Doctor of Philosophy
in the Graduate Division of Biological and Biomedical Sciences

Genetics and Molecular Biology

2021

Abstract

The role of lysine specific demethylase 1 (LSD1) and the functional consequences during development

By Alyssa Scott

The importance of lysine specific demethylase 1 (LSD1) during cell fate transitions has been established as a crucial step for developmental processes. We add to the accumulating body of evidence that LSD1 is critical in erasing epigenetic memory during these cell fate transitions. In neural stem cells in mice, we have shown that LSD1 is required for survival and appropriate neurodevelopment. We also examined the role of LSD1 during the maternal-to-zygotic transition. In *C. elegans*, LSD1/KDM1A (lysine specific demethylase 1) acts as part of the CoREST repressor complex to enable this transition by removing H3K4me1/2 and preventing the transgenerational inheritance of transcription patterns. In mouse, the loss of maternal LSD1 results in embryonic arrest at the 1-2 cell stage, with arrested embryos similarly failing to undergo the maternal-to zygotic transition. This suggests that LSD1 maternal reprogramming is conserved. Moreover, partial loss of maternal LSD1 results in striking phenotypes weeks after fertilization, including perinatal lethality and abnormal behavior in surviving adults. To explore the mechanism underlying these heritable defects further, we developed a new maternally hypomorphic LSD1 allele that predominantly affects the binding of LSD1 to CoREST. This new hypomorphic allele phenocopies our mouse model with reduced LSD1, suggesting that the maternal reprogramming function of LSD1 is CoREST dependent. In addition, we find that the incidence of perinatal lethality in our new model

is higher in a mother's first litter, as well as with advanced maternal age (>9 months). This modulation of the phenotype by maternal age is reminiscent of the epidemiological data in autism, raising the possibility that defective maternal epigenetic reprogramming can contribute to neurodevelopmental disorders.

The role of lysine specific demethylase 1 (LSD1) and the functional consequences during development

By

Alyssa Scott
B.S., Marist College, 2011

Advisor: David J. Katz, Ph.D.

A dissertation submitted to the Faculty of the
James T. Laney School of Graduate Studies of Emory University

in partial fulfillment of the requirements for the degree of

Doctor of Philosophy
in the Graduate Division of Biological and Biomedical Sciences

Genetics and Molecular Biology

2021

Acknowledgements

I would first like to thank my PI, Dr. David Katz, for being a supportive mentor for over 6 years. I know that I am leaving his lab as a well-trained scientist, and he has sparked a curiosity about the world that I will take with me into my next steps. I would also like to thank my committee for their ideas and contributions to my project that have made this a stronger body of work.

I also could not have done this without the support of my friends and family. It is this support outside of the lab that made it possible to continue. I am fortunate to have met incredible people through the GMB program that will remain in my life long after graduate school. I am deeply grateful to the GMB program for this opportunity and the incredible training I have received.

Table of Contents

Chapter 1: An introduction to epigenetic mechanisms and cellular reprogramming

Chapter 2: Maternally provided LSD1 prevents defects that manifest postnatally

Chapter 3: Materials and methods

Chapter 4: SPR-5/LSD1 functions through CoREST to maternally reprogram histone methylation

Chapter 1:

An introduction to epigenetic mechanisms and cellular reprogramming

Epigenetic modifications influence gene expression

Every cell type in our body contains the same genetic information, and yet they can have vastly different transcriptional programs that translate to different functions. This difference in phenotype, despite cells having the same genotype, comes down to differences in epigenetics. The term was first established by C.H. Waddington in 1942 as a way to describe the underlying relationship between genotype and phenotype (Waddington, 1942). Epigenetics is now defined as the stably heritable phenotype resulting from changes in a chromosome without alterations in the DNA sequence (Berger et al., 2009). These changes can include modifications made directly to the DNA, or modifications to proteins that the DNA is associated with. Together, the complex of DNA and its associated proteins and modifications are what make up chromatin.

Nucleosomes are the building blocks of chromatin. They consist of an octomer of histone core proteins around which DNA is coiled. These histones have N-terminal tails that can be reversibly covalently modified through methylation, acetylation, and phosphorylation, among others (Tessarz & Kouzarides, 2014). The modifications on histones affect the way the DNA wrapped around them is packaged, making it more or less accessible for gene expression. The DNA itself can also be modified via methylation to cytosine bases. Modifications to DNA or nucleosomes are a major mechanism through which cells with the same DNA can have different gene expression

programs; cells acquire different epigenetic modifications during development, which in turn facilitates which genes are turned on or off.

Proteins that change epigenetic marks fall into one or more of three categories: writers, readers, and erasers. Writers are proteins that add epigenetic marks, erasers remove them, and readers recognize specific modifications and mediate their function (Hyun et al., 2017). These proteins often contain conserved domains that confer the function as a reader, writer, or eraser. For example, SET domains are present in almost all histone lysine methyltransferases, and allow the protein to modify different methylation states on histone tails, and therefore conferring a writer function.

The methylation of DNA typically occurs in the context of a CpG dinucleotide at the 5’ position of cytosine (5mC). However, it has also been described to occur, albeit more rarely, at CpA residues. DNA methylation has been canonically described as a repressive modification through its association with silenced genes at their promoters and at repetitive elements (Greenberg & Bourc'his, 2019). However, DNA methylation in gene bodies has been shown to be associated with active gene expression (Greenberg & Bourc'his, 2019). Therefore, the location of DNA methylation in the genome can have either an activating or repressing effect. Like other epigenetic marks, DNA methylation is reversible.

The addition of DNA methylation is catalyzed through the DNA methyltransferase (DNMT) enzymes DNMT1, DNMT3a, and DNMT3b. The removal is performed by the Ten-eleven translocation (TET) enzymes TET1, TET2, and TET3 (Wu & Zhang, 2011). The removal process from 5mC to unmethylated DNA generates several intermediate species, including 5-hydroxymethylcytosine (5hmC), 5-carboxlcytosine (5caC), and 5-

formlycytosine (5fC). While originally thought to simply be intermediate species during the process of active demethylation, they have begun to be described as having their own independent functions. For example, 5hmC seems to be playing an important role in neurodevelopment, memory formation, and neurological function (Dawlaty et al., 2013; Qiao et al., 2016; Rudenko et al., 2013).

Modifications to nucleosome tails also have varying effects on gene expression based on which residue is modified, the number of modifications added, and which modification is added. For example, modification of the same H3K9 residue is influenced by whether it is acetylation or methylation that is added; H3K9ac correlates with transcriptional activation, while H3K9me3 is associated with repression of genes (Berndsen & Denu, 2008; Du et al., 2015; Mozzetta et al., 2015). Similarly, the number of modifications can have different outcomes as well: H3K4me1 is usually enriched in the enhancers of genes and at the 3' end of gene bodies, while H3K4me3 is found at actively transcribed promoter regions and at genes that are poised for transcriptional activation (Benayoun et al., 2014; Whyte et al., 2012).

Furthermore, there is a relationship between DNA methylation and histone modifications that is still being teased out. One demonstrated example of this interplay is between the acquisition of DNA methylation and H3K4 methylation. In order for the DNA methyltransferase complex to dock onto the histone tail, a hypomethylated substrate is required; it has been shown that H3K4 methylation blocks this docking (Ooi et al., 2007). This suggests that in order for new DNA methylation marks to be laid down, H3K4 methylation must be removed first.

H3K4 methylation is an active mark

H3K4 methylation can exist in the genome as mono-, di-, or tri-methylation, with different patterns appearing at different regions in the genome. In the open reading frame of actively transcribed genes, monomethylation is most enriched at the 3' region, dimethylation is most enriched in the promoter and gene body, and trimethylation is highest at the 5' end (Li et al., 2011). In addition to the gene body, there is also H3K4me1 enrichment at enhancers, and sometimes H3K4me2 at particularly active enhancers (Heintzman et al., 2007).

As H3K4me is associated with actively transcribed genes, the question arises as to whether it is an activator or consequence of transcription. Studies in yeast indicate that the H3K4 methyltransferase, Set-1, functions in a complex with RNA Polymerase II where it is recruited to active genes (Ng et al., 2003). Additionally, in *Drosophila* S2 cells, high resolution profiling of H3K4me2 and RNA Polymerase II indicates that their distribution throughout the genome is very similar (Mito et al., 2005). Together, these data indicate that H3K4me is a consequence of transcription, and may serve as a marker for activated genes rather than functioning in *de novo* transcriptional activation.

Due to H3K4me being a consequence of transcription, a model has been proposed in which H3K4me acts as epigenetic transcriptional memory (Lee & Katz, 2020). When genes turn on, they acquire this epigenetic mark, and it serves as a memory of the transcriptional program over time or between cell divisions. If this is true, however, this modification would need to undergo extensive reprogramming during cell fate transitions such as fertilization and differentiation.

LSD1 is an amine oxidase demethylase

LSD1 was first discovered in 2004 as the first known histone demethylase, and the crystal structure was solved in 2006 (Chen et al., 2006; Shi et al., 2004). Mouse LSD1 has 852 amino acids,19 exons, and 4 isoforms. The isoforms include: LSD1, LSD1 + exon 8a (expressed in the brain only), LSD1 + 2a, and LSD1 + 2a/8a (expressed in the testis and brain only) (Maiques-Diaz & Somervaille, 2016). LSD1 is conserved from yeast to humans; the human protein has >95% conservation with mouse, and it is widely expressed in both systems.

LSD1 has several domains that have different functions (Figure 1A). The SWIRM domain contributes to histone binding, the tower domain helps control enzymatic activity and is the site for complex member binding, and the amine oxidase domain is the enzymatic site (Maiques-Diaz & Somervaille, 2016). As a member of the amine oxidase superfamily, LSD1 utilizes FAD (flavin adenine dinucleotide) as its cofactor. The amine oxidase demethylation reaction requires a protonated nitrogen as a substrate. Therefore, LSD1 is only able to demethylate mono- and di-methylated lysine residues, and not tri-methylated lysine residues since there is no protonated nitrogen (Shi et al., 2004).

A

Figure 1. LSD1 protein domains. A) N terminal (N), C terminal (C), SWIRM, Tower, and amine oxidase domains (AOD) shown for LSD1.

Binding partners affect LSD1 function

LSD1 on its own can demethylate lysine residues in peptides or bulk histones, but not in nucleosomes (Shi et al., 2004). In order to demethylate nucleosomal substrates, LSD1 is required to be in a complex. Furthermore, complex member composition confers different specificity to various substrates. Canonically, LSD1 functions as a transcriptional repressor by removing the active marks H3K4me1/2. It was first described through its association with the CoREST complex, where LSD1 removes H3K4me1/2 and represses neuronal genes in non-neuronal lineages (Shi et al., 2005). This complex includes the histone deacetylase HDAC1 or sometimes HDAC2. HDACs remove the expression-promoting acetyl groups and help provide a coordinated switch from active to repressed chromatin states. LSD1 also performs this repressive role when in complex with NuRD or PRC2 (Figure 2A) (Maiques-Diaz & Somervaille, 2016).

Alternatively, LSD1 may also act as a transcriptional activator by removing the repressive marks H3K9me1/2. *In vitro*, LSD1 can function as an activator when in complex with androgen receptor (AR) or estrogen receptor (ERa), but *in vivo* evidence of LSD1 functioning as an activator is lacking (Maiques-Diaz & Somervaille, 2016). More recently, LSD1 has also been shown to demethylate non-histone targets and is thought to affect their stability. These proteins include p53, E2F-1, DNMT1, MYPT1, HIF-1α, and STAT-3 (Amente et al., 2013). However, similar to LSD1 activator function, *in vivo* evidence for these activities is lacking.

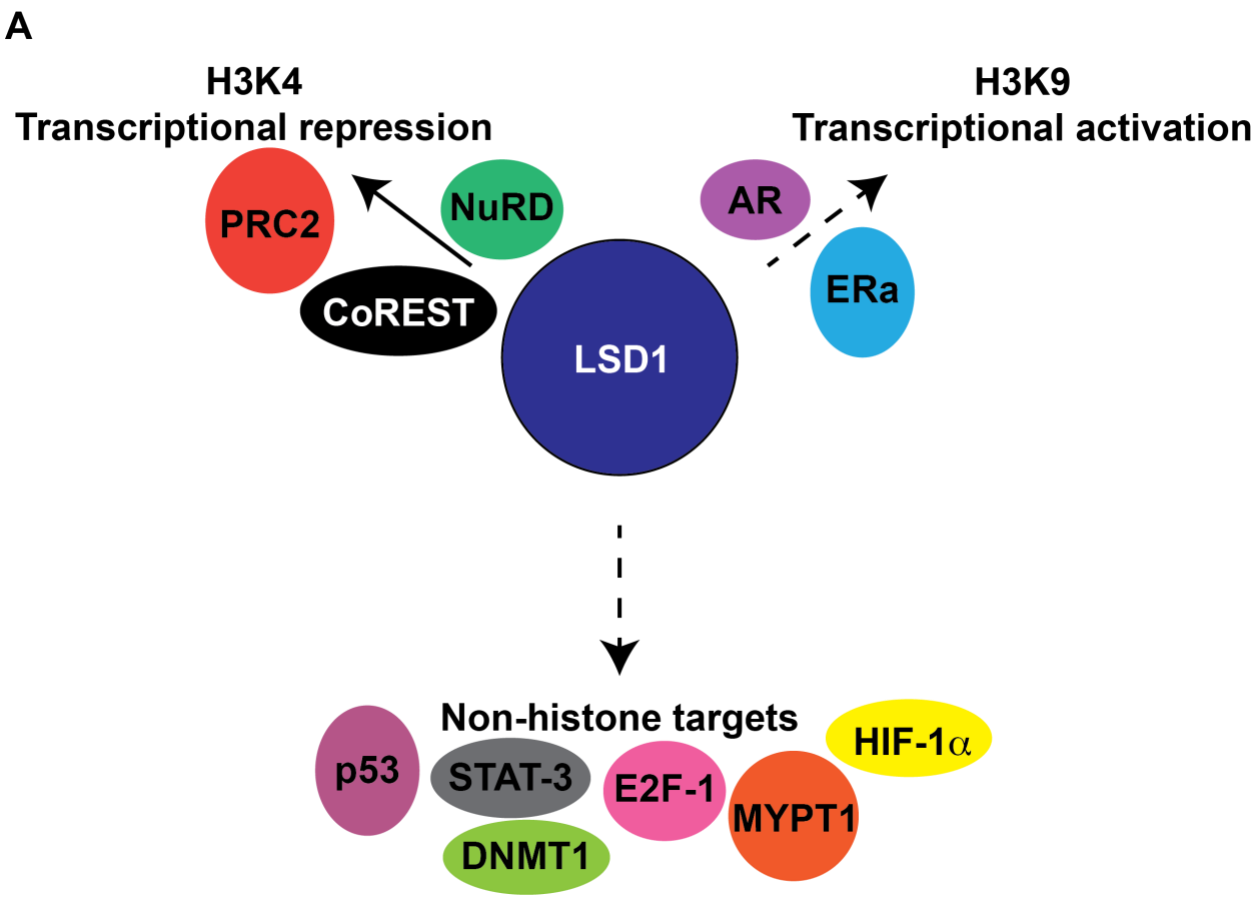

Figure 2. LSD1 demethylase specificity changes depending on complex composition. A) LSD1 either demethylates H3K4, H3K9, or non-histone targets depending on complex composition. Dashed line indicates complex members with *in vitro*, but no *in vivo*, evidence.

LSD1 decommissions enhancers in stem cell populations

In a study on mouse embryonic stem cells (mESCs), it was discovered that LSD1 occupies the enhancers of active genes that are critical for the maintenance of the stem cell (SC) state (Whyte et al., 2012). Perhaps unexpectedly, it was shown that LSD1 was not required for the maintenance of the SC gene expression profile. Instead, mESCs

that lacked LSD1 were unable to properly differentiate. The findings of this study indicate that during differentiation, LSD1 is required to remove H3K4me1 at enhancers in order for differentiation to continue. The decommissioning of enhancers of the mESC program via LSD1 is part of what allows for the transition to new cellular identities.

Since this landmark study in 2012, it has been found that LSD1 plays a similar role in stem cell populations beyond mESCs. For example, LSD1 has been deleted in testis stem cells in mice (Lambrot et al., 2015; Myrick et al., 2017). In the absence of LSD1, the ability of germ cells to differentiate into sperm was greatly reduced. Additionally, differentiating germ cells inappropriately expressed the stem cell factor OCT4. This indicates that the testis stem cell program was not adequately shut down to allow for differentiation to occur properly.

A similar phenomenon has been observed in many other SC populations *in vivo,* such as: hematopoetic (Kerenyi et al., 2013), trophoblast (Zhu et al., 2014), naïve B cells (Haines et al., 2018), and satellite SCs (Tosic et al., 2018). A knockout of LSD1 in all of these cell types results in a similar phenotype: a significant reduction in the ability of the SC populations to properly undergo differentiation.

LSD1 plays a role in neural stem cell development

Neural stem cells (NSCs) differentiate into the neurons and glia of the nervous system during embryonic development. It has been shown that LSD1 is expressed in NSCs, the expression levels decrease with differentiation, and that decrease correlates with an increase in H3K4me2 (Sun et al., 2010). *In vitro*, it was shown that either a chemical inhibition or siRNA knockdown of LSD1 leads to the inhibition of NSC

proliferation. When knocked down in adult mice *in vivo*, there is also a decrease in proliferation detected in the hippocampus (Sun et al., 2010). This suggests that LSD1 may be playing a similar role in NSCs as other stem cell populations, however prior to this thesis work, the knockout of *Lsd1* in NSCs during embryonic development had not been investigated.

The maternal to zygotic transition requires extensive epigenetic regulation

Post-fertilization differentiation is inherently epigenetic since all cells are derived from the same genome. This includes gametes, which contain cell type specific histone methylation (Xu et al., 2021). However, at fertilization those highly differentiated gametes must fuse to form the totipotent zygote. This suggests that histone methylation may need to be reprogrammed between generations to erase those cell type specific epigenetic patterns.

The importance of epigenetic reprogramming at fertilization has been illustrated since 1958, when it was demonstrated in *Xenopus* that an enucleated oocyte had the capacity to reprogram a differentiated somatic nucleus to a totipotent state (Gurdon et al., 1958). This reprogramming has been shown to be largely controlled by maternally deposited RNAs and proteins in the oocyte. These maternally deposited components are important for switching the transcriptional program of a highly differentiated oocyte to a zygotic transcriptional program, otherwise known as the maternal-to-zygotic transition. Furthermore, it was often the case that the reprogrammed nucleus retained a “memory” of the somatic cell type it used to be; the somatic cell nucleus that was derived from endodermal tissue that was reprogrammed would often still misexpress

endodermal genes (Gurdon et al., 1958). It was later found that this epigenetic memory was largely dependent on lysine 4 of histone H3.3 (Ng & Gurdon, 2008). Therefore, if H3K4 methylation is functioning in the maintenance of transcriptional programs, then this mark may need to be reprogrammed after fertilization.

The maternal-to-zygotic transition occurs at different time points in various model organisms, but in mice it occurs during the 1-2 cell stage. During this time, ~15% of the mouse genome is expressed in a process known as zygotic genome activation (ZGA) (Jukam et al., 2017). In mice, there is a minor and a major wave of ZGA. In the minor wave at the one cell stage, maternal factors are responsible for the initiation of zygotic transcription. During the major wave of ZGA between the one and two cell stage, chromatin is extensively remodeled. In humans, ZGA occurs during the 4-8 cell stage (Jukam et al., 2017).

Epigenetic factors play a major role during the maternal-to-zygotic transition. In *C. elegans*, worms lacking the H3K9 methyltransferase, MET-2, become increasingly sterile across many generations. This sterility is caused by a loss of the repressive mark H3K9me2, which indirectly leads to the gradual accumulation of the active mark H3K4me2 (Andersen & Horvitz, 2007; Kerr et al., 2014; Lee & Katz, 2020). This is similar to the phenotype of worms when they lose the H3K4 demethylase SPR-5, which is increasing sterility across many generations accompanied by the misexpression of spermatogenesis genes in somatic tissues (Katz et al., 2009). The *spr-5* and *met-2* mutants together become sterile in a single generation, indicating that the enzymes work together to reprogram the embryo (Carpenter et al., 2021; Kerr et al., 2014).

While development is able to proceed in the absence of those reprogramming factors in *C. elegans*, the phenotypes are much more severe in mammals. In the maternal mutant in mice of the MET-2 homolog, SETDB1, embryos are delayed and die by the blastocyst stage (Eymery et al., 2016; Kim et al., 2016). There are other examples of maternally-provided epigenetic enzyme mutations causing embryonic arrest phenotypes: the H3K4 methyltransferase, *Kmt2d,* causes embryonic arrest at the 1-2 cell stage (Andreu-Vieyra et al., 2010), the H3K9 methyltransferase *G9a* causes arrest of preimplantation embryos (Au Yeung et al., 2019; Zylicz et al., 2018), and the H3K36 methyltransferase *Setd2* causes arrest at the one-cell stage (Xu et al., 2019), among several other examples. Overall, the severity of these phenotypes indicate the importance of epigenetic reprogramming during the maternal-to-zygotic transition.

DNA methylation is inherited between generations and must be reprogrammed

DNA methylation is primarily found at CpG residues and can be stably inherited between cell divisions by the maintenance DNA methyltransferase, DNMT1 (Yoder et al., 1997). During DNA replication, DNMTt1 will methylate hemi-methylated DNA. CpG methylation is found at repeat sequences such as retrotransposons, and is thought to be partially responsible for stably repressing those regions. DNA methylation is also found at imprinted genes, which are genes with mono-allelic expression depending on the parent-of-origin. At these genes, methylation is usually found at CpG islands, otherwise known as imprinting control regions (ICRs), that are either maternally or paternally methylated (Bartolomei, 2009).

During the maternal-to-zygotic transition, DNA methylation also needs to be reprogrammed between generations. There is a genome-wide wave of DNA demethylation that occurs post-fertilization; in the maternal genome, this occurs passively between cell divisions, but in the paternal genome this demethylation occurs actively by the TET family proteins (Mayer et al., 2000; Oswald et al., 2000). The maternal knockout of *Tet3* in mice results in a failure to demethylate the paternal genome resulting in embryonic lethality (Gu et al., 2011). This indicates that maternally-provided TET3 is responsible for the active demethylation of the paternal genome post-fertilization.

While there is a wave of demethylation that occurs after fertilization, some ICRs are protected from this event. This resistance to demethylation is crucial to retain their parent-of-origin pattern of methylation at imprinted genes. The resistance to demethylation is dependent upon the protein STELLA; in its absence, many imprinted genes become demethylated (Nakamura et al., 2007). Maternally-provided TRIM28 is also required to protect certain sites from demethylation (Messerschmidt et al., 2012). The ICRs not only need to be able to resist demethylation during fertilization, but they also need to maintain their methylation between cell divisions during this stage. DNMT1 is critical for maintaining DNA methylation at ICR CpG residues (Howell et al., 2001). ZFP57 is also important for maintenance at maternal and paternally imprinted loci (Li et al., 2008; Quenneville et al., 2011). The selective reprogramming of DNA methylation at fertilization is a tightly regulated process that is crucial for proper development.

While it is known that both histone methylation and DNA methylation must be reprogrammed between generations, the relationship between the two processes is less

well understood. However, there does seem to be some evidence of interplay between the epigenetic marks. One example of this is through the protein DNMT3L, which is a protein responsible for stimulating *de novo* DNA methylation. DNMT3L docks on histone H3 to perform its function, but it requires a hypomethylated H3K4 residue to perform its activity (Ooi et al., 2007). The methylation of H3K4 strongly inhibits its DNA methyltransferase function. Additionally, LSD2 is a homolog of LSD1 that is also an H3K4 demethylase. LSD2 is only expressed in the oocyte, and must be functional during oogenesis for DNMT3A to *de novo* methylate imprinted alleles (Ciccone et al., 2009). In the absence of maternal LSD2, there is an increase of H3K4me2 and a failure to set up DNA methylation marks at certain imprinted loci (Ciccone et al., 2009). Interestingly, imprinted genes in the oocyte not affected by LSD2 are not controlled by LSD1 (Stewart et al., 2015) These examples provide insight into a possible mechanism in which defects in histone methylation can have secondary effects on DNA methylation.

LSD1 is required for the maternal to zygotic transition

The LSD1 homolog in *C. elegans*, SPR-5, has been shown to play an important role in epigenetic reprogramming at fertilization. When *spr-5* is mutated, it is no longer able to erase H3K4me1/2 at fertilization between generations. This correlates with an accumulation of H3K4me2 and ectopic spermatogenesis gene expression across ~30 generations. This indicates the requirement for SPR-5 to prevent the inappropriate inheritance of previously specified transcriptional states between generations.

To examine the requirement of LSD1 during the maternal to zygotic transition in mice, *Lsd1* was deleted specifically in the oocyte in mice and crossed to wild type males

(Ancelin et al., 2016; Wasson et al., 2016). Since zygotic copies of *Lsd1* are not expressed until the blastocyst stage of development, any defects observed during early embryonic development in the offspring would be due to losing the maternally provided protein. Without maternal LSD1, all embryos die at the 1-2 cell stage (Figure 3A-B). Furthermore, after hierarchal cluster dendrogram analysis, RNA sequencing on arrested embryos looked more transcriptionally similar to oocytes than to wild type embryos. Arrested embryos, compared to wild type controls, overexpressed >1500 genes and underexpressed >2700 genes. GO analysis of over and under expressed genes show an enrichment for genes normally expressed in unfertilized oocytes and a reduction of genes associated with embryonic development (Wasson et al., 2016). This indicates that without maternally-provided LSD1, embryos failed to undergo the maternal to zygotic transition.

Oocytes deficient in LSD1 showed a modest change in gene expression; overall there were less than 400 genes misregulated in *Lsd1*-deficient oocytes (Wasson et al., 2016). However, one group examined oocyte meiotic progression and determined that *Lsd1*-deficient oocytes resulted in a failure of some oocytes to complete meiosis I and led to apoptosis (Kim et al., 2015). To determine whether the 2-cell arrest phenotype observed was due to defective oocytes or the role of LSD1 post-fertilization, a chemical inhibitor of enzymatic activity of LSD1 was applied to wild type zygotes (Ancelin et al., 2016). The resulting embryos phenocopied the 1-2 cell arrest, indicating that the phenotype is most likely due to the lack of LSD1 post-fertilization, and not due to the loss of the protein in the oocyte.

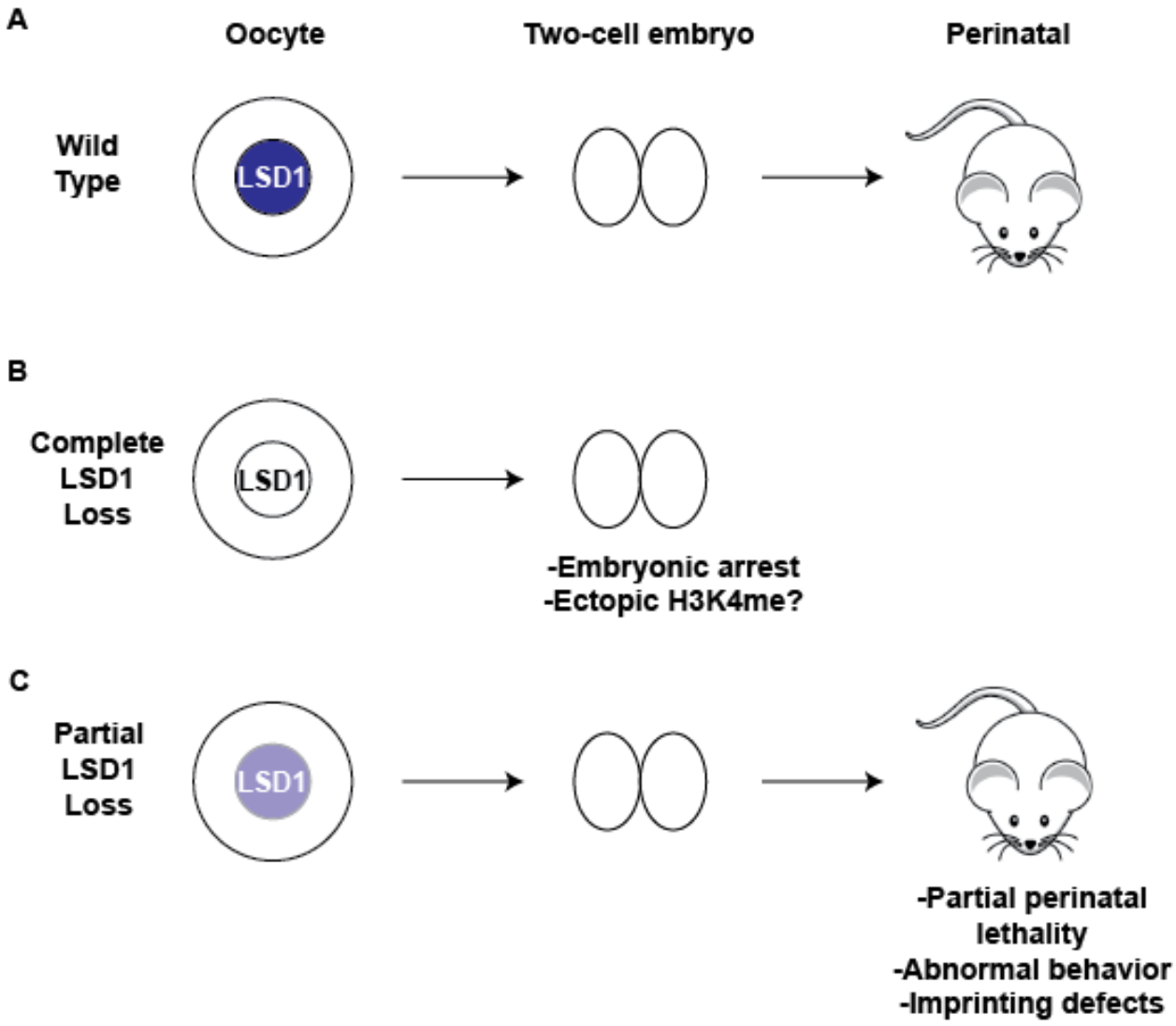

Figure 3. Maternally-provided LSD1 is required for epigenetic reprogramming at fertilization. A) In a wild type oocyte, LSD1 is deposited maternally and leads to normal development. B) A complete loss of LSD1 in the oocyte leads to 1-2 cell arrest, possibly due to ectopic H3K4 methylation. C) A partial loss of LSD1 maternally leads to offspring that bypass the 1-2 cell arrest. Those that make it out to birth have phenotypes such as perinatal lethality, abnormal behavior, and imprinting defects.

A partial loss of LSD1 maternally results in defects that manifest postnatally

Several different *Cre* lines were used to inducibly delete *Lsd1* from oocytes. Using *Zp3-* and *Gdf9-Cre*, the result was offspring with 100% lethality at the 1-2 cell stage. However, for reasons that remain unclear, *Vasa-Cre* functioned abnormally. 1/3 of the time, oocytes completely lacked LSD1, but 2/3 of the time oocytes retained a low level of LSD1 (Wasson et al., 2016). This incomplete effect is surprising because the *Vasa-Cre* transgene is reported to be expressed earlier in the germline than either *Gdf9-* or *Zp3-Cre*. Nonetheless, when this partial loss of maternal LSD1 protein occurred, some animals were able to bypass the 1-2 cell arrest and make it out to birth (Figure 3C). Compared to controls, these maternal mutants had higher levels of perinatal lethality. Of the few animals that survived to adulthood, all displayed striking repetitive and anxiety-like behaviors, which were identified in assays such as the open field test, food grinding, and marble-burying (Wasson et al., 2016).

The RNA sequencing from the arrested 2-cell embryos was utilized to uncover what could be responsible for these heritable defects. There were several genes misexpressed that are involved in the regulation of imprinted genes: *Tet1, Trim28, Zfp57,* and *Stella.* Additionally, the DNA methyltransferase *Dnmt1* was overexpressed. While the function of DNMT1 is primarily as the maintenance DNA methyltransferase, when overexpressed it has been shown to have *de novo* DNA methyltransferase activity (Vertino et al., 1996). Taken together, these data suggested that imprinted genes may be misregulated in maternal mutants, either directly or indirectly. To test this, bisulfite

PCR was performed at several candidate genes and it was found that at several loci, imprinted gene expression was severely affected in mutants (Wasson et al., 2016).

Mutations in epigenetic proteins cause human disease

Human mutations in epigenetic enzymes frequently cause deleterious effects, illustrating their importance during human development. One of the earliest known examples is mutations in the *Mll* gene, which is an H3K4 methyltransferase. The gene was named after the phenotype when mutated, which was mixed lineage leukemia (Slany, 2009). Mutations in the H3K36 methyltransferase, NSD1, cause Sotos syndrome, which is characterized by excessive growth during childhood, macrocephaly, and learning disabilities (Baujat & Cormier-Daire, 2007). Mutations in the H3K27 demethylase, UTX, or the H3K4 methyltransferase, KMT2B, both cause Kabuki syndrome (Arnaud et al., 2015). Kabuki syndrome is characterized by intellectual disability, developmental delay, and craniofacial abnormalities, among other characteristics. Additionally, mutations in LSD1 have been discovered that also contribute to Kabuki-like phenotypes (Chong et al., 2016; Tunovic et al., 2014).

In all of these cases, the mutations observed in humans are dominant. This is perhaps surprising, because often in heterozygous mouse models, losing one copy of an epigenetic enzyme is not sufficient to cause a phenotype. When losing both copies, the phenotype is often severe with early embryonic arrest; this makes it unlikely that the nature of the mutations observed in humans are a complete loss of function of the enzymes. One possibility is that a mutation in one allele is not sufficient to cause the phenotype on its own, but rather it creates a sensitized background which, in the

presence of another defect or mutation, uncovers the neurodevelopmental phenotype (Lee & Katz, 2020). This is supported by two pedigrees in which hypomorphic mutations in LSD1 have been described (Wei et al., 2018). These individuals have an increased risk for developing leukemia, but no neurodevelopmental phenotypes have been described. Based on LSD1 mutations conferring different phenotypes in humans, a two-hit hypothesis of epigenetic reprogramming has been proposed: at key developmental time points, such as fertilization or stem cell differentiation, a loss of function mutation in an epigenetic enzyme may synergize with other defects to affect reprogramming at those stages past a certain threshold. Other defects that could contribute to this could be genetic background, parental age, or other environmental factors.

Outstanding questions

(1) The role of LSD1 during cell fate transitions is still being teased out. Particularly, the function of LSD1 during neural stem cell differentiation *in vivo* has yet to be established. The work presented in this thesis addresses this gap (Chapter 5). (2) The important role of LSD1 maternally has been established through previous work that it is essential during the maternal-to-zygotic transition. A complete loss of the protein maternally leads to embryonic arrest at the 1-2 cell stage (Ancelin et al., 2016; Wasson et al., 2016). However, in humans, a complete loss of the protein in the oocyte may not be what occurs naturally. In mice, it has been shown that levels of LSD1 in the oocyte decrease with maternal age (Shao et al., 2015). Additionally, a partial loss of LSD1 maternally leads to phenotypes that can manifest postnatally (Wasson et al., 2016). In my work, I

sought to expand upon that work to determine what phenotypes were possible resulting from a partial loss of function of LSD1 maternally (Chapter 2).

Chapter 2:

Maternally provided LSD1 prevents defects that manifest postnatally

David Katz and I conceived and designed this study. Marcus Curlee and I performed experiments under the direction of D.K. D.K. and I analyzed data and interpreted results. I wrote the manuscript.

Generation of a novel hypomorphic LSD1 allele

Previous work has shown that a partial reduction in the amount of LSD1 protein in the oocyte can lead to defects that manifest postnatally (Wasson et al., 2016). This opened the door to a new model wherein incomplete reprogramming at fertilization could lead to inappropriately inherited histone methylation, which in turn causes phenotypes later on in development. Could this be underlying neurodevelopmental defects we see in humans? It has been shown that mutations in LSD1 lead to Kabuki syndrome-like phenotypes (Chong et al., 2016; Tunovic et al., 2014), although it is unclear whether those mutations arose in the maternal or paternal germline. It is also possible this phenomenon can occur without a mutation; it has been shown in mice that levels of LSD1 in the oocyte decrease with maternal age (Shao et al., 2015). The link between maternal age and risk of having a child with neurodevelopmental disorders in humans has been well described (Newschaffer et al., 2007). Therefore, we are proposing a new disease paradigm where changes in the levels of maternally deposited LSD1 due to advanced maternal age can alter the epigenetic landscape and lead to defects postnatally. We initially discovered this new paradigm serendipitously, with the partial loss of maternal LSD1 due to a defective *Cre* allele (Wasson et al., 2016). Unfortunately, this reduction in protein levels occurred very rarely and unpredictably,

with very few mice to study. In order to circumvent this issue, I generated a new mouse model using CRISPR-Cas9.

The purpose of the new model was to use a partial loss of function allele to mimic the partial loss of LSD1 protein levels. Using CRISPR, a point mutation (M448V) was introduced in the tower domain of the *Lsd1* gene at the endogenous locus (Figure 1A-C). This allele will be referred to as $Lsd1^{M448V}$. The tower domain is the site of protein-protein interactions (Forneris et al., 2007; Stavropoulos et al., 2006; Yang et al., 2006), and M448V resides in a residue that binds CoREST (Shi et al., 2005). Previous studies have shown that this mutation reduces the ability of LSD1 to demethylate histones *in vitro* slightly (85% demethylase activity compared to wild-type LSD1) (Nicholson et al., 2013). This modest reduction in LSD1 function is unlikely to compromise maternal reprogramming. However, the M448V mutation severely reduces the ability of LSD1 to bind CoREST (35% binding activity compared to wild type *in vitro*) (Nicholson et al., 2013).Thus, the M448V mutation serves as a separation-of-function allele between demethylase activity and CoREST binding.

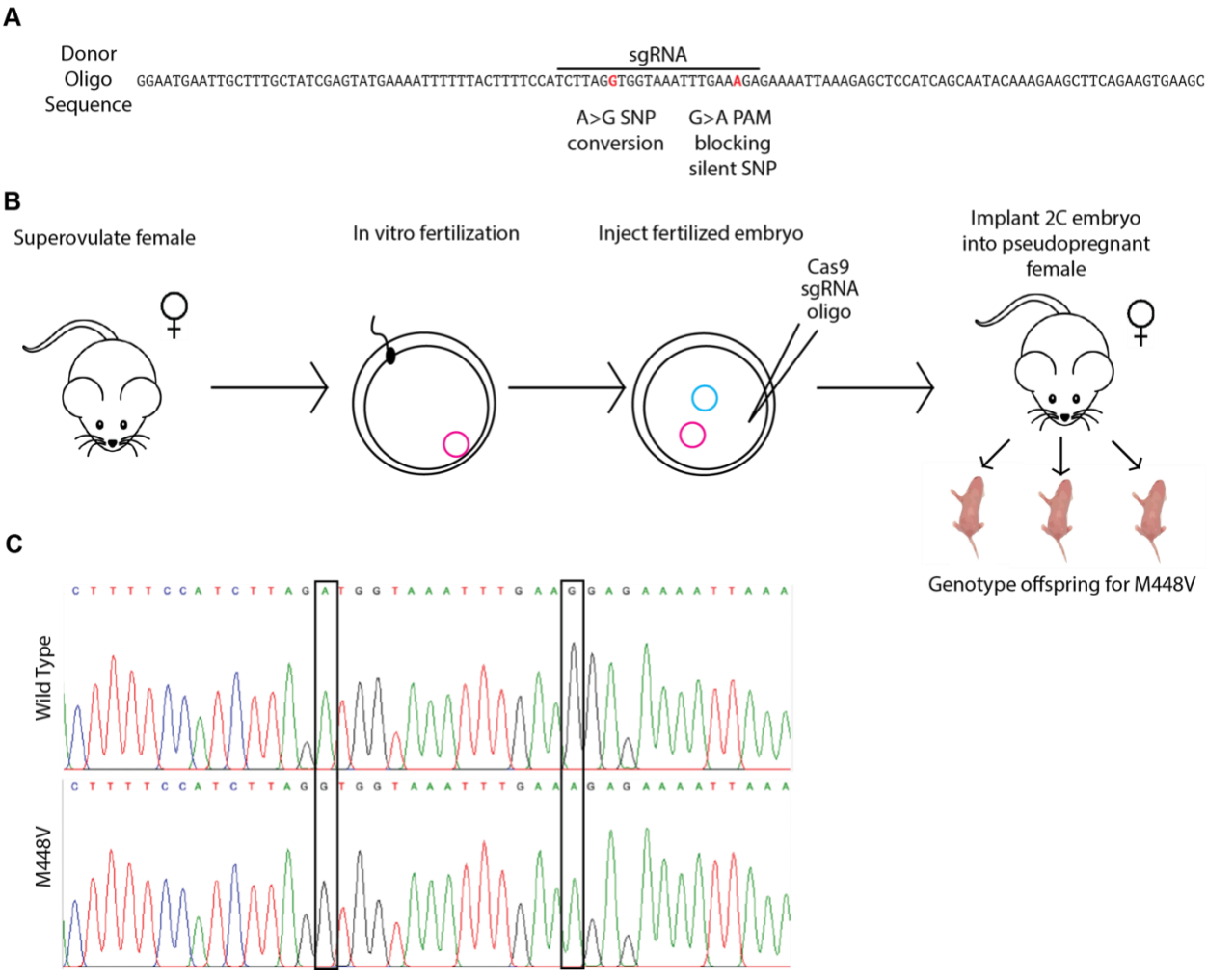

Figure 1. Generation of M448V hypomorphic allele. A) Donor oligo sequence with the sgRNA sequence denoted. Two point mutations being introduced are colored in red: A>G SNP and G>A PAM blocking silent SNP. B) Workflow for introducing M448V mutation into mice. C) Wild-type chromatogram versus validated A>G SNP and G>A silent SNP in the newly generated mutants.

Maternally hypomorphic LSD1 leads to perinatal lethality which may be modified by maternal age

To determine what the phenotypic effects would be of having maternally hypomorphic LSD1, I generated mice with the *Lsd1*^{M448V} allele over a floxed allele of

the *Lsd1* gene. In the presence of an oocyte-specific *Zp3-Cre* allele that expresses prior to the first meiotic division, the floxed allele recombines to a null allele in the oocyte. As a result, the only maternal contribution of LSD1 is from the $Lsd1^{M448V}$ allele, which produces LSD1 with a reduced ability to bind CoREST (Figure 2A). The F1 offspring from this cross will be referred to as $Lsd1^{M448V}$ progeny. Importantly, the mothers have a normal copy of the *Lsd1* gene in every other cell type throughout the mouse, and heterozygous *Lsd1* animals have been shown to have no phenotypic defects (Engstrom et al., 2020; Foster et al., 2010; Jin et al., 2013; Wang et al., 2007). In addition, mothers with a compromised maternal *Lsd1* allele are crossed to wild-type males, so the progeny have normal zygotic LSD1 activity from their paternal allele after transcription begins at the 2-cell stage. This mating scheme enables us to determine the specific effect of compromising LSD1 activity maternally in the oocyte (Figure 2).

In one set of controls, the mother has the $Lsd1^{M448V}$ allele over a floxed allele of LSD1 and is *Zp3Cre* negative (Figure 2B). The maternal contribution in this case would be one functional copy of LSD1 and one hypomorphic $Lsd1^{M448V}$ copy. These control F1 offspring will be referred to as $Lsd1^{+}$. In the other set of controls, the mother has a wild-type copy of the *Lsd1* gene over a floxed allele of *Lsd1* and are *Zp3Cre* positive (Figure 2C). The maternal contribution will be just one functional copy of the *Lsd1* gene. Previous studies have shown animals that are heterozygous for the *Lsd1* null allele have 70% protein levels (30% reduction) compared to homozygotes (Engstrom et al., 2020). These control F1 offspring will be referred to as $Lsd1^{het}$. Therefore, there is an allelic series of maternal LSD1 activity, with $Lsd1^{M448V}$ progeny having the least, $Lsd1^{het}$ having an intermediate amount, and $Lsd1^{+}$ having the most.

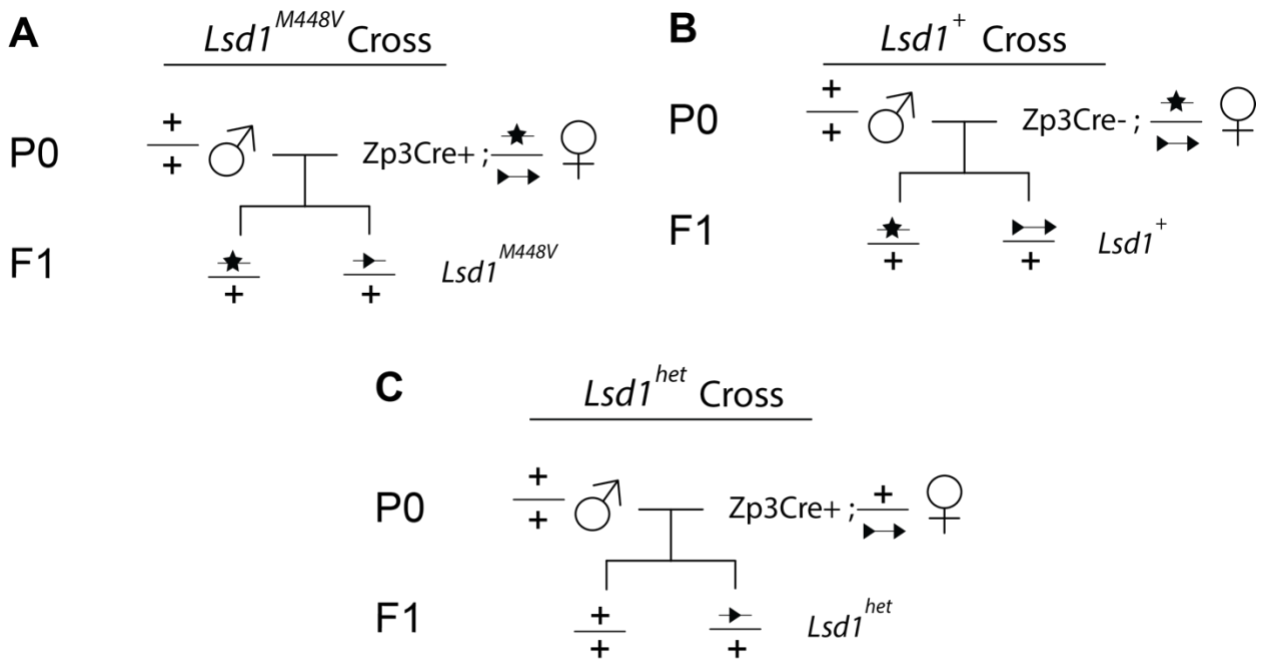

Figure 2. Genetic crosses to obtain mutant and control progeny. A-C) Genetic crosses showing wild type (+), loxP sites (triangles), and M448V (star) alleles. In all cases, P0 females are crossed to wild-type males, so that F1 progeny have normal zygotic LSD1 activity from their paternal allele after transcription begins at the 2-cell stage. A) In the *Lsd1*^{M448V} cross, P0 mothers are *Zp3-Cre*+, contributing only the hypomorphic allele maternally. B) In the *Lsd*$^{+}$ control cross, P0 mothers are *Zp3-Cre*-, contributing a wild-type and hypomorphic allele maternally. C) In the *Lsd1*^{het} control cross, P0 mothers are *Zp3-Cre*+, contributing one wild-type copy of *Lsd1* maternally.

It has been shown previously that losing both copies of *Lsd1* maternally leads to embryonic arrest at the 1-2 cell stage. Therefore, it was important to determine whether *Lsd1*^{M448V} progeny had enough maternal LSD1 activity to bypass that arrest. To test

this, litter sizes from *Lsd1*^{M448V} mothers were counted and compared to both controls. On average, there were 6 pups per litter from *Lsd1*$^{+}$, *Lsd1*^{het}, and *Lsd1*^{M448V} mothers (Figure 3A). Since there was no difference between the experimental and control groups, this indicates that there was no embryonic lethality, and *Lsd1*^{M448V} animals are indeed able to bypass the 1-2 cell arrest.

Previously, partial maternal loss of LSD1 progeny were able to bypass the 1-2 cell arrest, but once they were born ~30% of them died (Wasson et al., 2016). To determine whether maternally hypomorphic LSD1 would phenocopy this effect, progeny were closely monitored after birth from mothers <8 months of age. *Lsd1*$^{+}$ progeny had perinatal lethality rates of 9% (Figure 3B). *Lsd1*^{het} progeny had elevated rates of lethality wherein 18% of animals died after birth (Figure 3B). *Lsd1*^{M448V} progeny had the highest rates of perinatal lethality with 35% of animals dying after birth (Figure 3B). Importantly, the level of perinatal lethality does not depend on which allele the pup inherited from the mother (Figure 3C). These results indicate that maternally hypomorphic LSD1 phenocopies the partial loss of LSD1 protein levels maternally. Since disrupting the LSD1-CoREST interaction in the oocyte phenocopies partial loss of LSD1 protein levels, this suggests that LSD1 may be functioning in a complex with CoREST in the oocyte. Consistent with this, our lab has found that LSD1 is functioning through CoREST in *C. elegans* as well (BioRxiv 444472). Additionally, my discovery that the perinatal lethality rates get more severe with the dosage of LSD1 in the allelic series indicates that the epigenetic reprogramming step at fertilization is highly sensitive to the dosage of LSD1. This result has implications for maternal age, since LSD1 levels decrease with higher maternal age in mice (Shao et al., 2015). Based on these data, we might predict that in

our mouse model, the phenotype of perinatal lethality would get more severe with higher maternal age in all genotypes. This is indeed what we see; in both *Lsd1*$^{+}$ and *Lsd1*^{M448V} progeny from mothers 7-10 months of age, 70% of animals die after birth (Figure 3D). Interestingly, in *Lsd1*^{M448V} progeny, there is a higher rate of perinatal lethality in younger maternal age (<3 months old) as well, with 52% of animals dying compared with 11% in controls (Figure 3D). At intermediate maternal age (3-7 months), *Lsd1*$^{+}$ progeny have a 6% rate of lethality and *Lsd1*^{M448V} progeny have a 27% rate of lethality (Figure 3D).

In summary, *Lsd1*$^{+}$ animals start at low rates of lethality that jump up by the time the mothers reach advanced maternal age. *Lsd1*^{M448V} animals, on the other hand, have high rates of lethality early, rates drop down during intermediate maternal age, and increase again by advanced maternal age. This mirrors what happens in humans, wherein both lower and higher maternal age have increased risk of having a child with a neurodevelopmental disability (Newschaffer et al., 2007). Why is this pattern only seen in the mutants and not the controls? It is possible that the *Lsd1* hypomorphic mutation sensitizes the background enough to uncover the phenotype at the younger maternal age. It is unknown whether LSD1 levels are lower at a younger maternal age, but if it is that would provide a “second hit” which could increase the severity of the lethality phenotype. Alternatively, it is possible that this phenomenon is related specifically to the function of CoREST, rather than LSD1 levels. To distinguish between these possibilities, we would delete CoREST maternally.

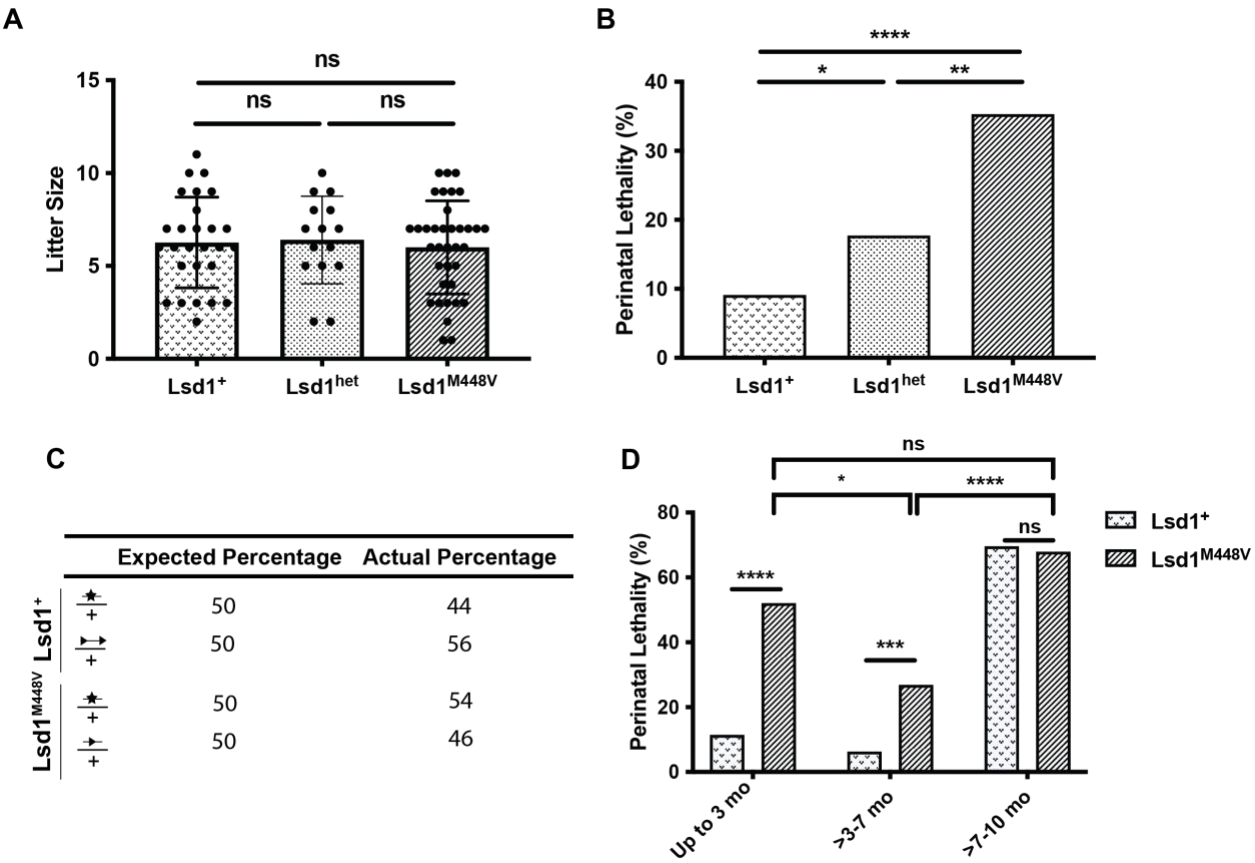

Figure 3. Maternally hypomorphic LSD1 leads to higher rates of perinatal lethality.

A) Litter sizes of Lsd1+, Lsd1^{het}, and Lsd1^{M448V} where each dot represents one litter and bars represent standard deviation. Data collected from maternal age <7 months. Bars represent standard deviation. n= 169 pups from 27 litters (Lsd1^{+}), 96 pups from 15 litters (Lsd1^{het}), and 216 pups from 36 litters (Lsd1^{M448V}). p values calculated using an unpaired t-test. B) Percent perinatal lethality by experimental condition. Data are collected from maternal age <7 months. n= 146 pups from 22 litters (Lsd1^{+}), n= 82 pups from 12 litters (Lsd1^{het}), n= 162 pups from 26 litters (Lsd1^{M448V}). p values calculated using a chi-square test. C) Percent perinatal lethality per litter by experimental condition. Data are collected from maternal age up to 3 months, >3-7 months, and litters from maternal age >7-10 months. n= 35, 111, 23 pups from 7, 16, 4 litters (Lsd1^{+}), n= 25,

138, 54 pups from 6, 22, 9 litters (Lsd1^{M448V}). p values calculated using a chi-square test. **** = p <.0001, *** = p < .001, ** = p <.01, * = p <.05, ns= not significant.

Reasons underlying perinatal lethality are unclear

While high levels of progeny died postnatally in *Lsd1*^{M448V} progeny, it was unclear what was causing them to die. It would often occur within the first 24 hours after birth, and animals that died were often missing their milk spot, indicating that they were unable to eat. One reason that could cause the inability to eat would be craniofacial abnormalities. This was a particularly appealing hypothesis due to craniofacial abnormalities being a hallmark of individuals with human mutations in *Lsd1* (Tunovic et al., 2014*)*. To test this possibility, skeletal preps were made of entire litters of *Lsd1*$^{+}$, *Lsd1*^{het}, and *Lsd1*^{M448V} progeny (Figure 4A). These were performed at postnatal day 0 (P0), and therefore it was unknown whether the animals were ones that would go on to die or not. After the skeletal preps were made, various craniofacial measurements were taken (Figure 4B-C). There were no significant differences in any of the measurements taken between any of the experimental groups (Figure 4B). This is still a particularly interesting result, as it indicates that the lethality is not due to craniofacial defects. It suggests that the phenotype observed in humans is more likely due to zygotic defects rather than defects in LSD1 maternally.

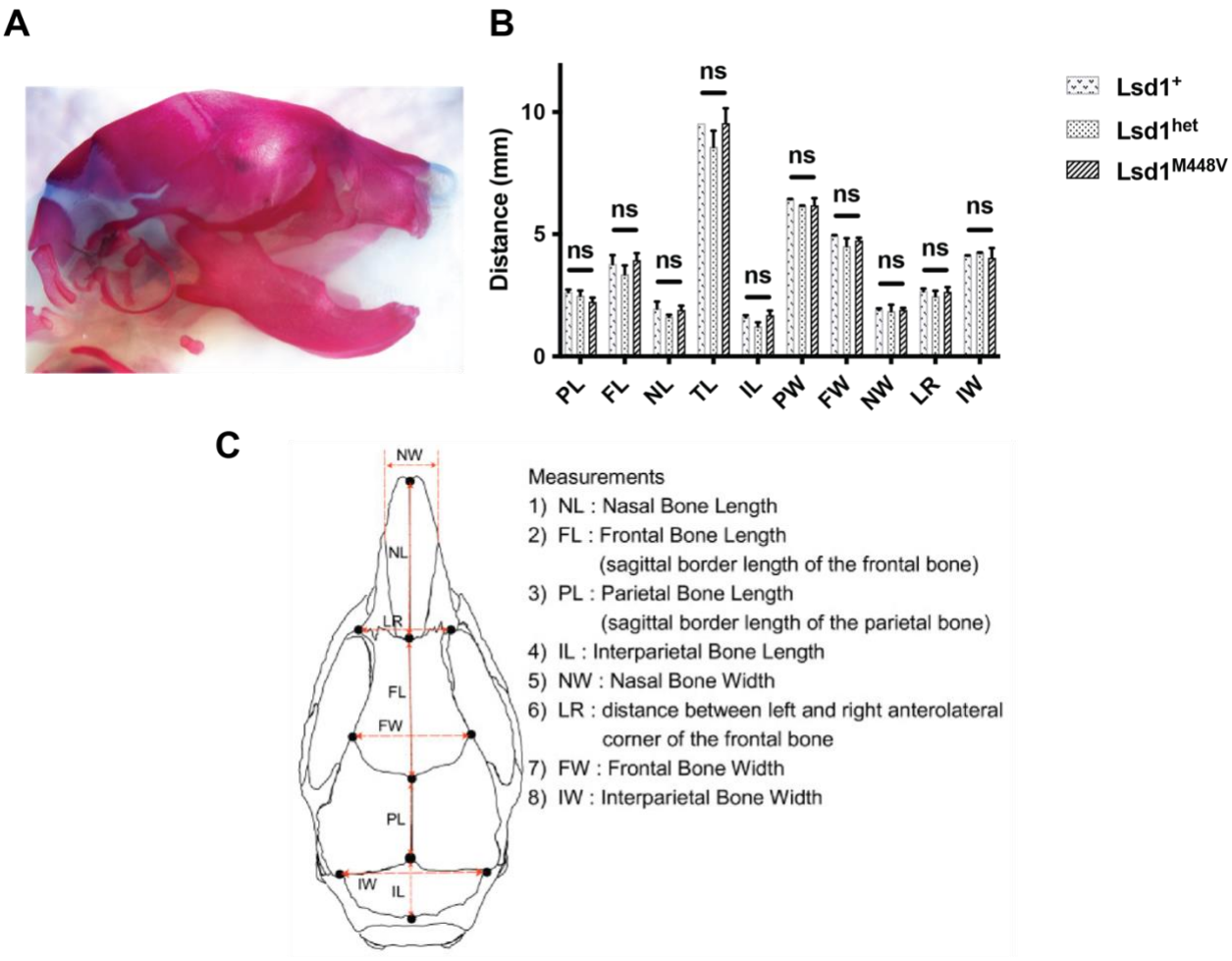

Figure 4. Maternal mutants do not have craniofacial defects. A) Representative skeletal prep image that craniofacial measurements were taken from. B) Craniofacial measurements for different experimental groups. n= 2 ($Lsd1^{+}$), n=2 ($Lsd1^{het}$), and n=7 ($Lsd1^{M448V}$). p values calculated using an unpaired t test. ns= not significant. C) Image representing measurements taken adapted from (Kawakami & Yamamura, 2008).

Another method to determine what could be underlying the lethality was to look at gene expression changes between mutants and controls. Since LSD1 is responsible for removing active marks at fertilization, we predicted that in mutants it would be unable to do that job efficiently, and we would see the inappropriate expression of

germline genes in the embryo that should have been turned off during the maternal to zygotic transition (MZT) in transcription. To test this, two replicates of each genotype at the blastocyst stage were sent for sequencing. Clustered normalized read counts were determined for each of the replicates (Figure 5A). Unfortunately, the replicates did not cluster together by genotype, indicating either there are not uniform gene expression changes based on genotype, or that the collection method of the blastocysts was not successful. More replicates will be collected and sequenced to determine which of these it is. With the data we had, we performed differential gene expression analysis between *Lsd1*$^{+}$ blastocysts and *Lsd1*^{M448V} blastocysts (Figure 5B). There were 30 differentially expressed genes in *Lsd1*^{M448V} progeny, with roughly an equal number up- or down-regulated. GO analysis determined that those genes were involved in metabolic process and the regulation of histone methylation, among other functions (Figure 5C). Intriguingly, all of the genes misregulated are expressed at some point in either the male or female germline.

We had the advantage of having the RNA sequencing data from the 2-cell arrested embryos from *Lsd1*$^{-/-}$ mothers to compare our sequencing data to (Wasson et al., 2016). Since we were looking at blastocysts, we could look at the overlap between the 2-cell dataset and our misexpressed genes at the blastocyst to determine which genes remain misexpressed between cell divisions. The overlap between the two datasets was statistically significant, and there were 9 genes that remained misexpressed between 2-cell arrested embryos and maternally hypomorphic blastocysts (Figure 5D): *Trim43b, Lss, Gm15698, Xlr4a, Appl2, Slc33a1, Erdr1, Zfp53*, and *Gm26825*. These genes represent the most promising targets for which may be

underlying the perinatal lethality later on in development. However it will be important to obtain additional high quality replicates before these candidates are pursued further.

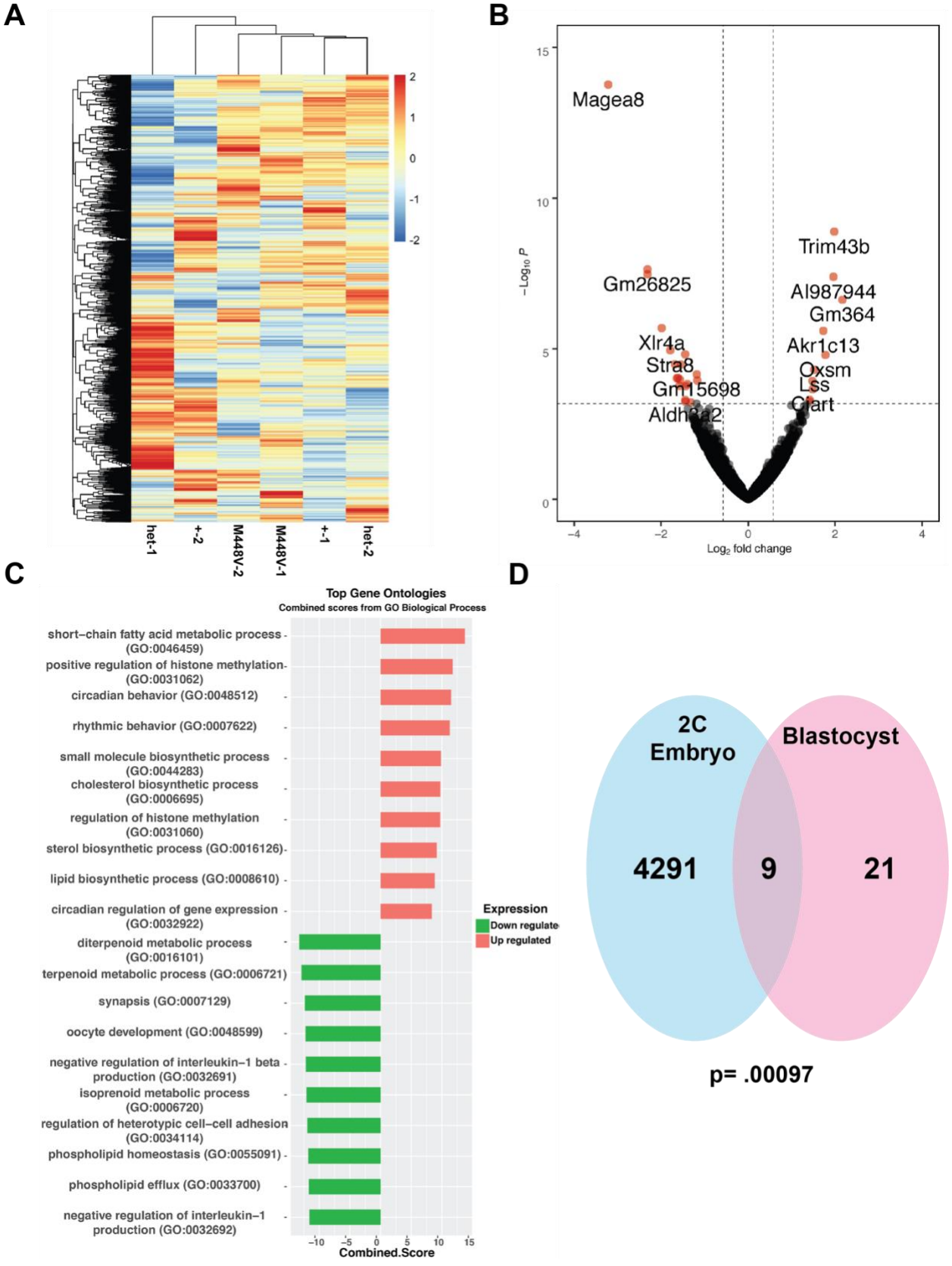
A
2
1
0
-1
-2
het-1
+2
M448V-2
M448V-1
+1
het-2
B
Magea8
Trim43b
Gm26825
AI987944
Gm364
Xlr4a
Akr1c13
Stra8
Oxsm
Gm15698
Lss
Cfart
Aldh3a2
−Log10 P
Log2 fold change
C
Top Gene Ontologies
Combined scores from GO Biological Process
short−chain fatty acid metabolic process (GO:0046459)
positive regulation of histone methylation (GO:0031062)
circadian behavior (GO:0048512)
rhythmic behavior (GO:0007622)
small molecule biosynthetic process (GO:0044283)
cholesterol biosynthetic process (GO:0006695)
regulation of histone methylation (GO:0031060)
sterol biosynthetic process (GO:0016126)
lipid biosynthetic process (GO:0008610)
circadian regulation of gene expression (GO:0032922)
diterpenoid metabolic process (GO:0016101)
terpenoid metabolic process (GO:0006721)
synapsis (GO:0007129)
oocyte development (GO:0048599)
negative regulation of interleukin−1 beta production (GO:0032691)
isoprenoid metabolic process (GO:0006720)
regulation of heterotypic cell−cell adhesion (GO:0034114)
phospholipid homeostasis (GO:0055091)
phospholipid efflux (GO:0033700)
negative regulation of interleukin−1 production (GO:0032692)
Expression
Down regulated
Up regulated
Combined.Score
D
2C Embryo
Blastocyst
4291
9
21
p= .00097

Figure 5. RNA sequencing analysis of blastocysts. A) Clustered normalized read counts for each replicate. B) Volcano plot showing $\log_2$ fold change in gene expression of significantly up and down regulated genes in *Lsd1*^{M448V} blastocyst compared to *Lsd1*$^{+}$ blastocysts. C) Gene ontology scores for biological processes of the significantly different genes in *Lsd1*^{M448V} blastocyst compared to *Lsd1*$^{+}$ blastocysts. D) Overlap of significantly misexpressed genes from 2 cell arrested embryos from *Lsd1*$^{-/-}$ mothers (Wasson et al., 2016) compared to misexpressed genes from *Lsd1*^{M448V} mothers.

Lsd1^{M448V} progeny may have imprinting defects

While it remains unclear why animals were dying perinatally, the next step was to determine whether there were any defects in the animals that survived. We first wanted to examine developmental delay, since that is another phenotype associated with the human *Lsd1* mutations (Tunovic et al., 2014). To measure developmental delay in mice, their body weight was measured each day from birth to weaning, as well as the day that each pup reached certain developmental milestones. There were no significant differences in body weight between any of the experimental groups (Figure 6A). There were also no significant differences between *Lsd1*^{M448V} progeny and controls on the postnatal day that they reached eye opening, pinnae detachment, upper incisor eruption, or ear opening (Figure 6B-E). This indicates that maternally hypomorphic mutant survivors do not display developmental delay. This indicates that the developmental delay observed in the corresponding human patients may be due to the zygotic role of the protein, rather than the maternal one.

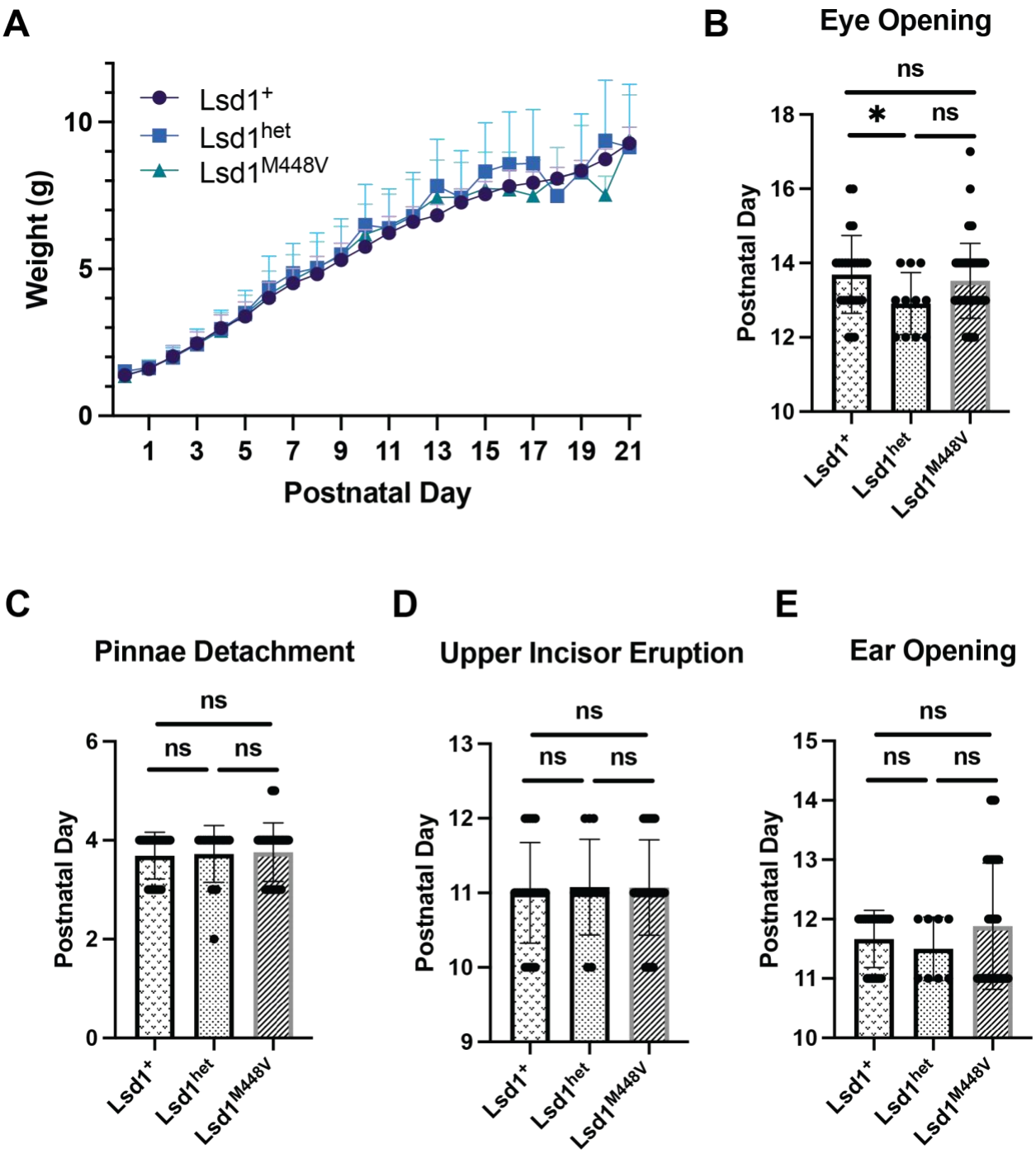

Figure 6. Maternal mutants do not display developmental delay. A) Weights of animals from postnatal day 0-21. n= 5 ($Lsd1^{+}$), n= 3 ($Lsd1^{het}$), and n= 8 ($Lsd1^{M448V}$). B) Postnatal day when eyes opened. n= 26 ($Lsd1^{+}$), n=11 ($Lsd1^{het}$), and n=48 ($Lsd1^{M448V}$). C) Postnatal day when pinnae detached. n= 29 ($Lsd1^{+}$), n=18 ($Lsd1^{het}$), and n=50

(Lsd1^{M448V}). D) Postnatal day when upper incisors erupted. n= 23 (Lsd1^{+}), n=13 (Lsd1^{het}), and n=42 (Lsd1^{M448V}). E) Postnatal day when ears opened. n= 21 (Lsd1^{+}), n=8 (Lsd1^{het}), and n=42 (Lsd1^{M448V}). All p values calculated using an unpaired t test. * = p<.05, ns= not significant.

Previous studies on the partial loss of maternal LSD1 showed that mutants have defects in DNA methylation at some imprinted genes (Wasson et al., 2016). For example, when performing allele-specific bisulfite sequencing, it was found that there was an increase in DNA methylation on the paternal allele in mutants (Wasson et al., 2016). This provided support that there may also be DNA methylation defects in maternally hypomorphic mutants. To test this, mutant or control mothers were crossed to *Castaneous* (CAST) mice in order to perform the allele-specific analysis. Tissues from the heart, brain, and liver were taken from adult progeny and allele-specific bisulfite sequencing was performed on the *Zac1* gene. *Zac1* is a maternally methylated and paternally expressed gene. A single nucleotide polymorphism (SNP) was used to distinguish between the maternal (B6 background) and paternal (CAST background) alleles. The preliminary results show that in *Lsd1*$^{+}$ and *Lsd1*^{het} progeny, the maternal allele is methylated and the paternal allele is unmethylated, as it should be (Figure 7A-D). However, in the *Lsd1*^{M448V} progeny, there appears to be a loss of maternal methylation at the 3’ end of the *Zac1* gene in some replicates (Figure 7E). There is also a gain in methylation in some replicates on the paternal allele at the 5’end of the *Zac1* gene (Figure 7F). While more data needs to be collected on other imprinted genes, it appears that hypomorphic maternal LSD1 may cause DNA methylation defects that

persist throughout development in mammals. To pursue this further, we are carrying out genome-wide allele specific bisulfite sequencing.

These results hold broad implications for the relationship between histone methylation and DNA methylation. H3K4 methylation has been shown to block *de novo* DNA methylation (Ooi et al., 2007), so it possible that the effect could be direct. Alternatively, loss of maternal LSD1 has been shown to affect multiple genes that regulate DNA methylation, so the effect could be indirect. For example, loss of maternal LSD1 causes overexpression of the maintenance DNA methyltrasferase DNMT1, which can lead to *de novo* DNA methylation (Vertino et al., 1996; Wasson et al., 2016). Regardless, the persistent DNA methylation defects that we observe preliminarily indicate that the defects in DNA methylation can be very long lasting; we perturbed the ability of a histone demethylase to perform its function at fertilization, which in turn affected DNA methylation, whose defects were subsequently maintained throughout millions of cell divisions. It is unclear whether the human *Lsd1* mutation patients have DNA methylation defects, but DNA methylation defects are associated with many other neurodevelopmental disorders (Kubota et al., 2013).

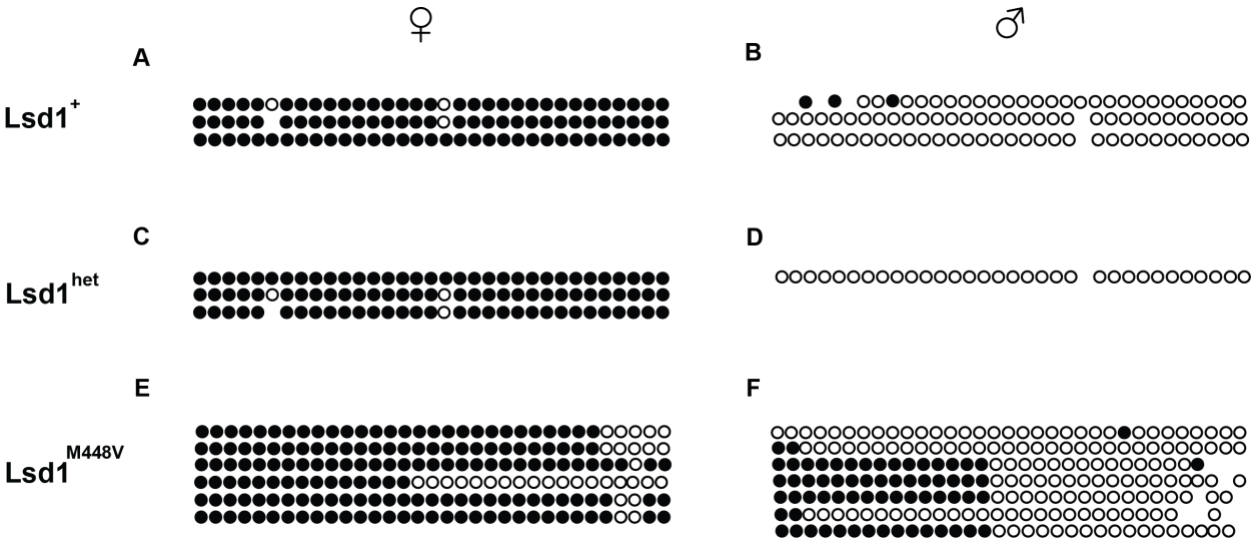

Figure 7. *Zac1* imprinting is defective in maternal mutants. Allele-specific bisulfite analysis of the *Zac1* gene in *Lsd1*$^{+}$ progeny (A-B), *Lsd1*^{het} progeny (C-D), and *Lsd1*^{M448V} progeny (E-F) separated by maternal and paternal alleles, respectively. Each line represents a clone of one allele. Each circle represents a CpG dinucleotide. Close circles signify methylation and open circles signify a lack of methylation. No circle indicates a lack of sequencing data.

Maternal mutant behavioral phenotypes are modified by genetic background

Due to human *Lsd1* mutation patients having abnormal behavior, we wanted to test whether there were any behavioral defects in our maternal mutants. To test learning and memory, we performed the Morris water maze assay in *Lsd1*$^{+}$ and *Lsd1*^{M448V} progeny in the B6 background. There were no differences in the latency to reach the platform during any of the training phase days between mutants and controls (Figure 8A). This indicates that mutants and controls were able to learn equally well. Once the platform was removed, both experimental groups spent the same amount of time in the target quadrant (Figure 8B). This indicates that both groups shared similar levels of

memory of where the platform used to be. Therefore, there were no defects in learning and memory in *Lsd1*^{M448V} progeny.

Next, we wanted to assess whether there was elevated anxiety-like behavior in maternal mutants. To test this, we performed the open field test. There was no significant difference between mutants and controls in the time spent in the center of the test chamber (Figure 8C), indicating that there was not elevated anxiety-like behavior in *Lsd1*^{M448V} progeny. Finally, to test for repetitive behavior, time spent grooming was assessed in mutants and controls. There was no significant difference between the groups (Figure 8D). Overall, there were no behavioral defects detected in any of the assays used on animals in the B6 background. Based on the following results, this suggests that genetic background plays an important role in the phenotypes that develop. This result could be extrapolated to humans, where genetic background may also be playing a role in how severe a mutation in LSD1 ends up becoming.

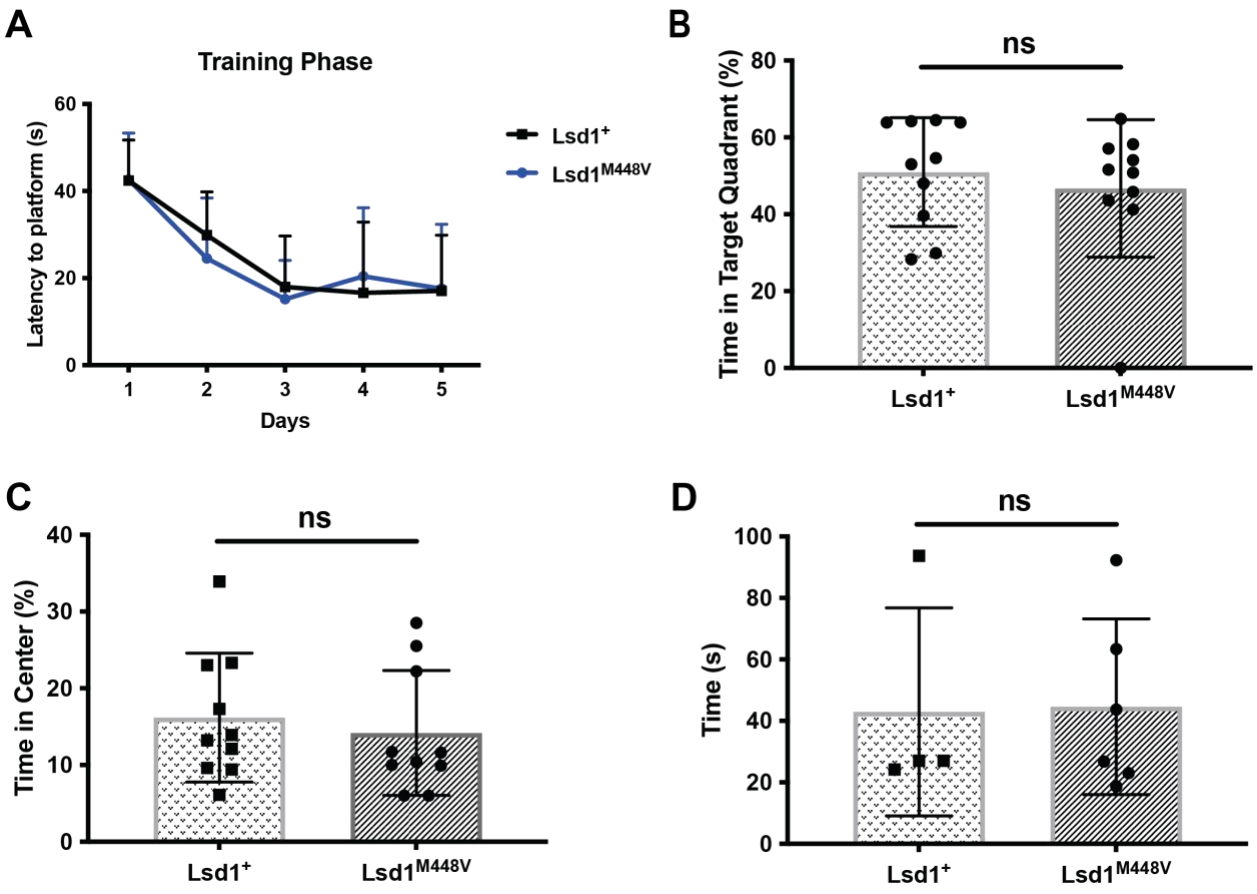

Figure 8. There are no detectable behavioral differences in maternal mutants in the B6 background. A-B) Morris water maze data during the training phase (A) and probe trial (B). n=10 ($Lsd1^{+}$ and $Lsd1^{M449V}$). C) Open field test percentage of time spent in center of chamber. n=10 ($Lsd1^{+}$ and $Lsd1^{M449V}$). D) Time spent grooming per 10 minutes. N= 4 ($Lsd1^{+}$) and n= 6 ($Lsd1^{M448V}$). All p values calculated using an unpaired t test. ns= not significant.

In addition to crossing *Lsd1*$^{+}$ and *Lsd1*^{M448V} mothers to B6 fathers, I also crossed those mothers to CAST males. The resulting progeny were CAST/B6 hybrids. After setting up a video camera to observe their behavior overnight, it was discovered that these animals displayed a repetitive looping behavior (Figure 9A). Individual animals

were taped from mutants and controls, and their number of loops per 10 minutes were scored. In *Lsd1*$^{+}$ progeny, 1 out of 4 animals (25%) assayed displayed looping behavior (Figure 9B). In *Lsd1*^{M448V} progeny, 4 out of 5 animals (80%) assayed displayed looping behavior (Figure 9C). While there is some looping present in control CAST/B6 hybrids, this repetitive behavior appears to be exacerbated in mutant hybrids. This is an interesting contrast to B6 background animals, where repetitive behavior assayed by grooming time did not show any significant differences. This suggests that the genetic background of *Lsd1*^{M448V} progeny may modify the behavioral phenotype observed. Based on this finding, we predict that differences in genetic background in humans may contribute to the different outcomes observed, where some individuals develop craniofacial defects and abnormal behaviors, while others are phenotypically normal. Consistent with this possibility, a pedigree was recently identified with LSD1 mutations that are similar to those found in LSD1 patients with Kabuki Syndrome-like abnormalities (Wei et al., 2018). The individuals in this pedigree have a susceptibility to cancer due to somatic mutation of the unaffected LSD1 allele. However, these patients do not have any neurodevelopmental defects. This indicates that the LSD1 mutation may not be sufficient to produce neurodevelopmental defects.

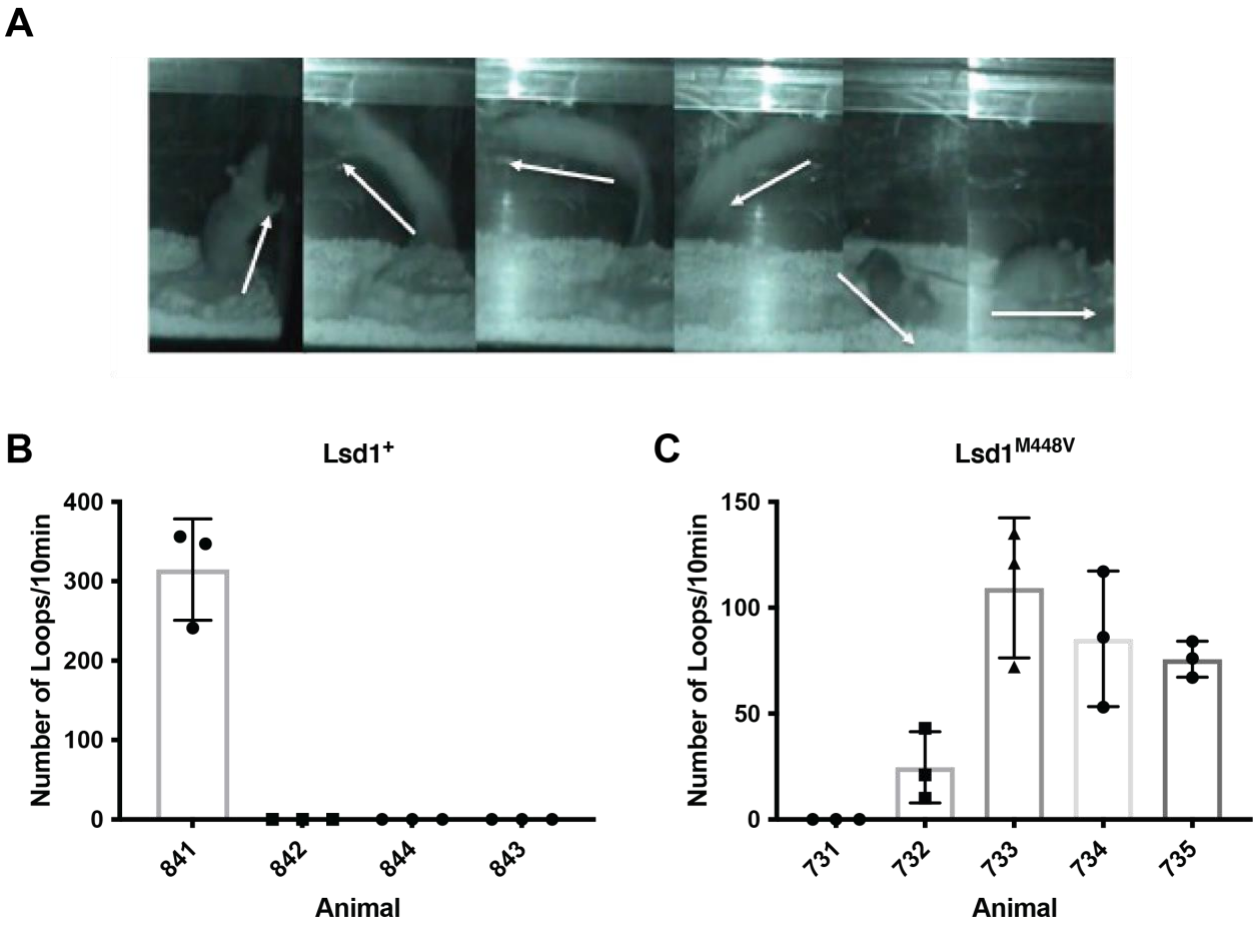

Figure 9. Maternal mutants in the CAST background display looping behavior. A) Screen capture of video of *Lsd1*^{M448V} progeny taken during the dark cycle. Time course takes place in <1 second. White arrows indicate the direction of movement. B) Looping per minute of *Lsd1*$^{+}$ progeny. Bars represent standard deviation. C) Looping per minute of *Lsd1*^{M448V} progeny.

Chapter 3:

Materials and Methods

Solutions and buffers

0.1 M Phosphate buffer

0.2 M Solution A: NaH_2PO_4 24.0 g/L

0.2 M Solution B: Na_2HPO_4 28.4 g/L

To 1,000 mL Solution B, add Solution A slowly to bring pH to 7.3 (about 220 mL Solution A).

Dilute 1/2 with diH_2O when needed to make 0.1 M

Tail prep buffer

10 mL 1 M Tris-Cl

2 0mL 5 M NaCl

20 mL 0.5 M EDTA

50 mL 10% SDS

900 mL diH_2O

1X TBS

7.88 g Tris-Cl

9.0 g NaCl

1,000 mL diH_2O

10X Citrate Buffer

2.0 g Citrate Monohydrate

1000 mL diH2O

pH to 6.0 with NaOH

dilute 1:10 for working 1X solution

H20 Brij

1,000 mL of diH2O

2.5 mL of 30% Brij 35 solution (Sigma)

Tris Brij

100 mL 1 M Tris-Cl pH 7.5

100 mL 1 M NaCl

5 mL 1 M MgCl2

2.5 mL 30% Brij 35

797.5 mL diH2O

Alcian Blue Stain

800 mL 80% EtOH

100 mL 20% Acetic Acid

150 mg/L Alcian Blue

Alizarin Red Stain

50 mg Alizarin Red

10 g KOH

Up to 1L H_2O

Mouse lines

Lsd1$^{M448V/+}$ mice were backcrossed 4 times and are continuing to be backcrossed to B6 animals. *Lsd1*$^{M448V/+}$ mice were maintained as heterozygotes. To generate

animals used for experiments, they were crossed to *Lsd1*$^{fl/fl}$ animals to generate *Lsd1*$^{M448V/fl}$. Those mice were crossed to *Zp3-Cre; Lsd1*$^{fl/fl}$ animals to generate the genotypes necessary for experiments.

Mouse genotyping by PCR

At weaning, a 5 mm piece of mouse tail was removed with a razor blade and digested overnight in a 50 °C water bath with 500 µL tail prep buffer and 5 µL of 20 mg/mL protease K (Ambion). This digest was then phenol/chloroform extracted by adding 500 µL phenol/chloroform and vigorously vortexing followed by separation of the aqueous and organic layers by centrifugation (5 minutes). The 250 µL of the aqueous (top) layer was extracted, brought back up to 500 µL with water, and then re-extracted with 500 µL phenol/chloroform. The aqueous layer of the second extraction was recovered (400 µL) and DNA was precipitated with ethanol by adding 40 µL of 3 M sodium acetate and 800 µL of ice cold 100% ethanol, followed by inversion. The mixture was then centrifuged at 4 °C for 10 minutes to produce a pellet and the supernatant was discarded. The pellet was washed with 150 µL of 70% ethanol (room temperature) and centrifuged again for 5 minutes, followed by careful removal of the ethanol and allowed to dry at room temperature for 5 minutes and finally reconstituted with water. This DNA served as the template for genotyping PCR reactions.

For genotyping, each PCR reaction contained 3 µL of template DNA diluted either 1/100 (Cre, Tau) or 1/1000 (Lsd1) and 22 µL of PCR reaction mix. Each PCR reaction mix contained 2.5 µL 10X AmpliTaq Gold 360 buffer, 0.5 µL 10mM dNTPs, 1.0 µL each primer (50 µM stock, Table 2-1), 35.0 µL 25mM MgCl2, 0.2 µL AmpliTaq Gold

360 Polymerase and water. The Lsd1genotyping reaction yields two possible products: 483bp for wildtype and 289bp for deleted. The Cre genotyping reaction yields a positive control product (250bp) and 320bp product when the Cre transgene is present. The hypomorphic allele genotyping results in a 386bp product. The point mutation removes a restriction site, so mutants versus wild type were determined by incubating PCR products at 37°C with the HpyAV restriction enzyme for one hour. Wild type band sizes: 72bp, 81bp, 209bp, 24bp. M448V band sizes: 72bp, 290bp, 24bp. Each genotyping reaction is optimized for the specific primer set. Detailed protocol (reagent concentrations can vary) for each genotyping PCR reaction are in the protocols binder for all mouse work.

Morris water maze

A cohort of 10 control and 10 mutant mice training was carried out in a round, water-filled tub (52 inch diameter). Mice were trained with 4 trials per day for 5 days with a maximum trial length of 60 s and a 15 minute intertrial interval. Subjects that did not reach the platform in the allotted time were manually guided to it. Mice were allowed 5 seconds on the platform to survey spatial cues. Following the 5 day training period, probe trials were performed by removing the escape platform and measuring the amount of time spent in the quadrant that originally contained the escape platform over a 60 s trial. All trials were recorded and performance analyzed by determining the mean values of latency to mount the platform and tracking mice with MazeScan (Clever Sys, Inc.).

Skeletal preps

Skeletal prep protocol was received from the Caspary lab. P0 pups were euthanized by freezing and then severance of the head. Pups were skinned and internal organs removed. They were then washed in 95% ethanol overnight. The next day, they were washed in 100% acetone for 1-2 hours, then fresh acetone was added and samples were washed overnight. On day 3, samples were washed in water for 1-2 hours, rinsed in water briefly, then washed in Alcian blue stain and washed overnight. On day 4, samples were washed 4 x 1hr in 70% ethanol. They were removed from the rocker and wahed 1 hour in 1% KOH, then washed overnight in Alizarin red stain. Finally, samples were put in storage solution. They can then be stored indefinitely at room temperature.

To quantify facial bone lengths for craniofacial analysis, calipers were used for measurements. The bones to measure were adapted from Balemans et al. 2014.

Developmental delay

Developmental delay was assed from P0-P21. Toe clips were performed on pups at P0 to distinguish between animals. Weight was recorded daily and the day of the appearance of physical traits were recorded: pinnae detachment, eye opening, and incisor eruption.

Flushing blastocysts for RNA seq

Pregnant mice were euthanized by cervical dislocation at e3.5 before 12pm. Uterus was dissected out into m2 buffer. Fat was removed from uterus and uterus was

cut to have an open tube at both ends. Using a 1ml syringe with a 30 ½ G needle bent 30 degrees and filled with m2 buffer, uterus was flushed to collect blastocysts. To move embryos, a petri dish had 10ul droplets of m2 media and embryos were mouth pipeted to droplets. Embryos were transferred to droplets to be washed before being collected for sequencing. For sequencing, a 10X reaction buffer was made: 19ul 10X lysis buffer + 1ul RNase inhibitor. Then each 1X reaction buffer was 1 blastocyst + 1ul 10X reaction buffer + 9.5ul nuclease-free water.

RNA library preparation and sequencing were performed by UGA Genomic Services Lab. We used Illumina NextSeq submitting cells for cDNA synthesis with the Clonetech kit. Output flow cell was PE 75 Mid.

RNA sequencing analysis

The RNA sequencing data described in Chapter 4 were analyzed as follows: The sequencing data were uploaded to the Galaxy web platform, and we used the public server at usegalaxy.org to analyze the data. FASTQ files were quality assessed using FASTQC (v.0.11.7), trimmed using Trimmomatic (v.0.36.5) and minimum QC score of 20 and minimum read length of 36bp. Paired-end reads were subsequently mapped to the GRCm38 genome using HISAT2 (v.2.1.0). Unmapped, unpaired and multiply mapped reads were removed using Filter SAM or BAM (v.1.1.2). Assignment of transcripts to GRCm38 genomic features was performed using Featurecounts (v.1.6.0.6) and the Ensembl GRCm38.93 gtf file. Differentially expressed transcripts were determined using DESEQ2 (v.2.11.40.2). For all datasets, a cutoff of adjusted p-value < 0.3 and abs (log_2 fold change) > 0.58 was applied. TPM values were calculated

from raw data obtained from Featurecounts output. Subsequent downstream analysis was performed using R and normalized counts and adjusted P-values from DESEQ2 (v.2.11.40.2). Heatmaps were produced and hierarchical clustering was done using the gplots package (v. 3.0.1) and normalized counts. Volcano plots were produced using the enhanced volcano package (v.0.99.16) and adjusted p-values. Additionally, Gene Set Enrichment Analysis (Pre-ranked list) was performed using the online platform WebGestalt. Custom R-scripts available upon request.

Chapter 4:

SPR-5/LSD1 functions through CoREST to maternally reprogram histone methylation

Brandon S. Carpenter[1,#], Alyssa Scott[1,#], Robert Goldin[2], Sindy R. Chavez[1], Dexter A. Myrick[1], Marcus Curlee[1], Karen Schmeichel[3], David J. Katz[1*]

[1]Department of Cell Biology, Emory University School of Medicine, Atlanta GA 30322, USA.

[2]Uniformed Services University School of Medicine, Bethesda MD 20814, USA.

[3]Natural Sciences Division, Oglethorpe University, Atlanta GA 30319, USA.

[#]Authors contributed equally

*corresponding author:
David J. Katz
Associate Professor
Department of Cell Biology
Room 443, Whitehead Biomedical Research Building
Emory University School of Medicine
Atlanta, GA 30322, USA
Phone: (404) 727-3403
djkatz@emory.edu

B.S.C., A.S. and D.J.K. conceived and designed the study and wrote the manuscript. B.S.C., A.S., R.G., S.R.C, M.C, and K.S. performed experiments under the direction of D.J.K. B.S.C, A.S., and D.J.K. analyzed data and interpreted results. D.A.M. helped with RNAseq analysis and visualizations. All authors discussed the results.

ABSTRACT

Maternal reprogramming of histone methylation is critical for reestablishing totipotency in the zygote, but how histone modifying enzymes are regulated during maternal reprogramming is not well characterized. To address this gap, we asked whether maternal reprogramming by the H3K4me1/2 demethylase SPR-5/LSD1/KDM1A, is regulated by the co-repressor protein, SPR-1/CoREST in *C. elegans* and mice. In *C. elegans,* SPR-5 functions as part of a reprogramming switch together with the H3K9 methyltransferase MET-2. By examining germline development, fertility and gene expression in double mutants between *spr-1* and *met-2,* we find that *spr-1* mutants are partially compromised for *spr-5; met-2* reprogramming. In mice, we generated a separation of function *Lsd1* M448V point mutation that compromises CoREST binding, but only slightly affects LSD1 demethylase activity. When maternal LSD1 in the oocyte is derived exclusively from this allele, the progeny phenocopy the increased perinatal lethality that we previously observed when LSD1 was reduced maternally. Together, these data are consistent with CoREST having a conserved function in facilitating maternal LSD1 epigenetic reprogramming.

INTRODUCTION

Re-establishing the transcriptional ground state to enable embryonic development in a newly formed zygote requires extensive maternal reprogramming of chromatin at fertilization (Burton & Torres-Padilla, 2014; Hemberger et al., 2009; Li, 2002; Morgan et al., 2005; Seisenberger et al., 2012). Maternal reprogramming of chromatin is accomplished by the deposition of enzymes into the oocyte that covalently

modify histones. The combination of these histone modifications contributes to developmental cell fates by regulating the accessibility of chromatin for transcription. For example, methylation of either lysine 9 or 27 on histone H3 (H3K9me and H3K27me) is generally associated with repressed transcription, whereas methylation of either lysine 4 or 36 on histone H3 (H3K4me and H3K36me) is associated with active transcription (Bannister et al., 2005; Barski et al., 2007; Bernstein et al., 2002; Bernstein et al., 2005).

Accumulating evidence suggests that patterns of histone modifications can be maintained through cell divisions to help maintain cell fate. For example, during early patterning in *Drosophila*, the expression of homeotic genes is modulated by segmentation transcription factors. After the segmentation factors turn over, the continued maintenance of homeotic gene expression through development is dependent on the H3K27 and H3K4 methyltransferases, Polycomb and Trithorax (Coleman & Struhl, 2017; Moehrle & Paro, 1994; Simon & Tamkun, 2002). Likewise, in *C. elegans*, the Polycomb Repressive Complex 2 (PRC2), which includes MES-2/3/6, maintains paternally inherited H3K27me3 during embryogenesis (Gaydos et al., 2014; Kaneshiro et al., 2019; Tabuchi et al., 2018). In addition to H3K27me3, the maternally deposited H3K36 methyltransferase, MES-4, maintains H3K36me2/3 at a subset of germline genes (MES-4 germline genes) in a transcriptionally independent manner to help reestablish the germline in the next generation (Furuhashi et al., 2010; Rechtsteiner et al., 2010). Furthermore, the transgenerational inheritance of repressive histone modifications occurs in *C. elegans* mutants lacking the COMPASS complex component, WDR-5. *wdr-5* mutants transgenerationally extend lifespan due to the

accumulation of H3K9me2 across generations (Greer et al., 2010; Lee et al., 2019). Histone methylation may also be transmitted across generations in vertebrates (Brykczynska et al., 2010; Hammoud et al., 2009; Wu et al., 2011; Zheng et al., 2016; Zhu et al., 2014). Together these findings suggest that inherited histone methylation patterns are conserved across multiple phyla, and that the inheritance of the proper chromatin state is critical for normal function of the offspring.

Despite the importance of inherited histone methylation in contributing to the maintenance of cell fates, there are developmental transitions where the inheritance of histone methylation may need to be prevented. For example, in *C. elegans,* the histone demethylase SPR-5, must remove H3K4me1/2 at fertilization to prevent the inappropriate inheritance of previously specified transcriptional states. Failure to erase H3K4me1/2 at fertilization between generations in *spr-5* mutants correlates with an accumulation of H3K4me2 and ectopic spermatogenesis gene expression across ~30 generations. This accumulation of H3K4me2 leads to progressively increasing sterility, which is defined as germline mortality (Katz et al., 2009). SPR-5 reprogramming at fertilization functions together with the addition of H3K9 methylation by the methyltransferase MET-2 (Greer et al., 2014; Kerr et al., 2014). *spr-5; met-2* mutants have a synergistic sterility where progeny are sterile in a single generation, rather than over many generations (Kerr et al., 2014). Together this work supports a model in which SPR-5 and MET-2 are maternally deposited into the oocyte, where they reprogram histone methylation at fertilization to prevent defects caused by inappropriately inherited transcriptional states. Furthermore, in *C. elegans* the transgenerational maintenance of

H3K36me3 by MES-4 functions to antagonize SPR-5/MET-2 repression, enabling the proper specification of the germline in the progeny (Carpenter et al., 2021).

SPR-5/MET-2 epigenetic reprogramming at fertilization is conserved in mammals. When the *met-2* ortholog *Setdb1* is maternally deleted in mice, zygotes develop slowly and die by the blastocyst stage (Eymery et al., 2016; Kim et al., 2016). Similarly, when the *spr-5* ortholog *Lsd1* is maternally deleted in mice, embryos die at the 1-2 cell stage, and these mutants are more transcriptionally similar to an oocyte than a wild type 1-2 cell embryo (Ancelin et al., 2016; Wasson et al., 2016). Thus, without maternally provided LSD1, embryos are unable to undergo the maternal-to-zygotic transition. Moreover, when maternal LSD1 protein levels are decreased, some animals can bypass the 1-2 cell arrest and survive until birth. However, progeny that are born exhibit lethality shortly after birth (perinatal lethal), indicating that incomplete reprogramming at fertilization can have phenotypes that manifest postnatally (Wasson et al., 2016). The 1-2 cell arrest and perinatal lethality phenotypes potentially occur through the inappropriate inheritance of histone methylation.

Although the evidence for maternal reprogramming across multiple taxa is mounting, it is not clear how histone modifying enzymes like LSD1 are regulated during this process. Recently, studies have implicated the co-repressor CoREST in broadly regulating LSD1 function. In mice, LSD1 and CoREST are often found in the same transcriptional corepressor complex together (Hakimi et al., 2003; Humphrey et al., 2001; Shi et al., 2003; You et al., 2001). In addition, LSD1 and CoREST have been co-crystallized, (Yang et al., 2006) and CoREST is required for the stability of LSD1 (Foster et al., 2010; Shi et al., 2005). CoREST may also be required for full LSD1 function,

because although LSD1 can demethylate H3K4 peptides or bulk histones *in vitro*, it is only capable of demethylating nucleosomes when in complex with CoREST (Lee et al., 2005; Shi et al., 2005; Yang et al., 2006). Additionally, LSD1 and CoREST phenocopy each other in multiple organisms. In *Drosophila,* LSD1 and CoREST have overlapping functions in spermatogenesis and in ovary follicle progenitor cells (Lee & Spradling, 2014; Macinkovic et al., 2019). In *C. elegans*, the homolog of CoREST, SPR-1, was identified, along with SPR-5, in a suppressor screen for the ability to rescue the egg-laying defect (Egl) associated with loss of SEL-12, a presenilin protein (Wen et al., 2000). Furthermore, SPR-1 has been shown to physically interact with SPR-*5 in vitro* and *in vivo* (Eimer et al., 2002; Kim et al., 2018*)*. Together, these data raise the possibility that LSD1 could be functioning through CoREST to maternally reprogram histone methylation, but this hypothesis has not yet been tested.

Here, we utilize both mouse and *C. elegans* to test whether LSD1 and CoREST function together maternally. We demonstrate that *C. elegans* lacking SPR-1 display a reduction in brood size that is between wildtype and *spr-5* mutants. Unlike *spr-5* mutants, *spr-1* mutants do not become increasingly sterile across ~30 generations. However, when maternal reprogramming is sensitized by loss of the *met-2* gene, *met-2; spr-1* mutants reveal intermediate sterility and gene expression changes that are exacerbated compared to single mutants, but less affected than *spr-5; met-2* mutants. We also demonstrate that *met-2; spr-1* mutants misexpress MES-4 germline genes in somatic tissues at intermediate levels compared to *spr-5; met-2* mutants. In mice, we find that LSD1 and CoREST are both expressed in mouse oocyte nuclei. In addition, we generated a separation of function *Lsd1* point mutation that compromises CoREST

binding, but only slightly affects LSD1 demethylase activity. When this mutation is inherited maternally, the progeny phenocopy the increased perinatal lethality that we previously observed when LSD1 was reduced maternally. Together, these data are consistent with CoREST having a conserved function in facilitating maternal LSD1 epigenetic reprogramming.

RESULTS

spr-1 mutants have reduced fertility but do not exhibit germline mortality

Previously, we demonstrated that populations of *spr-5* mutants become increasingly sterile over ~30 generations (Katz et al., 2009). Therefore, if SPR-1 is required for SPR-5 maternal reprogramming activity, it is possible that *spr-1* mutants might phenocopy the germline mortality across generations observed in *spr-5* mutants. To address this possibility, we performed germline mortality assays on wild type (Bristol N2 strain, hereafter referred to as wild type), *spr-1* mutant, and *spr-5* mutant animals (Fig. 1A). Wild type hermaphrodites gave rise to ~300 progeny in the first generation (F1) and this average number of progeny was maintained through 50 generations (Fig. 1A). Similar to what we previously reported, progeny from F1 *spr-5* mutants average ~150-200 progeny, and by generation 23 (F23), the average number of progeny declined to ~60 animals (Fig. 1A). *spr-1* mutants averaged ~250 progeny in the first generation. This average number of progeny is intermediate between *spr-5* mutants and wild type. But unlike *spr-5* mutants, *spr-1* mutants never became sterile across generations (Fig. 1A).

met-2; spr-1 double mutants exhibit germline mortality

Previously we demonstrated that SPR-5 synergizes with the H3K9me2 methyltransferase, MET-2, to regulate maternal epigenetic reprogramming (Kerr et al., 2014). Progeny of mutants lacking both SPR-5 and MET-2 are completely sterile in a single generation (Kerr et al., 2014). If SPR-1 is partially required for SPR-5 maternal reprogramming, then it is possible that *spr-1* mutants will exhibit a synergistic phenotype when combined with a *met-2* mutation. To determine whether *spr-1* mutants display any abnormal phenotypes in a *met-2* mutant background, we individually cloned out 288 progeny from first generation (F1) *met-2; spr-1* double mutants and examined each animal for sterility (Fig. 1B-D). Of the 288 individually cloned *met-2; spr-1* F1 mutant progeny, 208 were fertile (Fig. 1B,C) and 80 were sterile (Fig. 1D). We also observed that 76 of the 208 fertile F1 progeny die as young adults due to defects in egg laying (Fig. 1C). To determine whether fertile *met-2; spr-1* mutants become germline mortal, we counted the average number of progeny from *met-2; spr-1* mutants over successive generations and compared them to wild type, *spr-1* and *met-2* mutants (Fig. 1E; Fig. S1A,C). As observed previously, the average number of progeny from *spr-1* and *met-2* mutants were lower than wild type, but remained consistent over 10 generations, and neither mutant gave rise to sterile animals over that time frame (Fig. 1E,F; Fig. S1A,B). Fertile *met-2; spr-1* mutant progeny produced an average of ~70 progeny in the first generation. However, by generation 10 the average number of progeny declined to ~30 (Fig. 1E; Fig. S1C). Consistent with this germline mortality phenotype, the number of completely sterile animals in *met-2; spr-1* mutants increased across successive generations from ~30% at early generations to ~60% by F10 (Fig. 1F; Fig. S1D).

Together, these results show that *met-2; spr-1* mutants display a germline mortality phenotype that is intermediate between the maternal effect sterility of *spr-5; met-2* mutants in a single generation and the germline mortality of *spr-5* and *met-2* single mutants over ~30 generations.

The sterility of *met-2; spr-1* mutants resembles *spr-5; met-2* mutants

We also examined the gonads of sterile *met-2; spr-1* mutants to determine if the sterility resembles the sterility of *spr-5; met-2* mutants. *spr-5; met-2* mutants have a squat germline, with both gonad arms failing to elongate (Fig. S2A,B; Kerr et al., 2014). Within the squat germline there are proliferating germ cells, sperm and oocytes, indicating that the germline has proceeded through normal transitions. However, these cell types are inappropriately interspersed (Carpenter et al., 2021; Katz et al., 2009). Unlike *spr-5; met-2* mutants, F1 sterile *met-2; spr-1* mutants have elongated gonad arms. However, within these sterile F1 gonads, we observed a similarly disorganized mixture of germ cells, sperm and oocytes (Fig. S2C,D). In addition, after several generations the germlines of sterile *met-2; spr-1* mutants resembled the squat germlines of *spr-5; met-2* mutants, although unlike *spr-5; met-2* mutants, some animals remained partially fertile at later generations (Fig. 1E; Fig. S2A,B,E,F). Thus, the sterility of *met-2; spr-1* mutants at late generations phenocopies the maternal effect sterility of *spr-5; met-2* mutants observed in the first generation.

Transcriptional misregulation in *met-2; spr-1* progeny resembles that observed in *spr-5; met-2* progeny but is less affected

Since the severity of the germline mortality phenotype of *met-2; spr-1* mutants is between *spr-5; met-2* mutants and *spr-1* or *met-2* single mutants, it raises the possibility that maternal SPR-5 reprogramming may be partially dependent upon the SPR-5 interacting partner SPR-1. If mutating *spr-1* partially compromises SPR-5 maternal reprogramming, we would expect that the genes that are misexpressed in *met-2; spr-1* mutants would be similar to *spr-5; met-2* mutants, but that the gene expression changes would be less affected in *met-2; spr-1* mutants. To test this possibility, we performed RNA-seq on F7 *spr-1*, *met-2*, and *met-2; spr-1* mutant L1 progeny compared to wild type L1 progeny. We chose to perform the analysis on F7 *met-2; spr-1* mutants because this generation precedes the increase in sterility that we observed in our germline mortality assay after F7 (Fig. 1F; Fig. S1A). Thus, by performing the analysis at F7, it allowed us to observe primary effects from the loss of MET-2 and SPR-1, rather than secondary effects due to the sterility. In addition, we utilized starved L1 larvae for our RNA-seq analysis for two reasons. First, starved L1 larvae only have two germ cells that are not undergoing transcription. As a result, performing RNA-seq on these larvae allows us to exclusively examine somatic transcription. Second, we have previously performed RNA-seq and differential gene expression analysis on the L1 stage of *spr-5; met-2* mutant progeny, so performing the RNA-seq analysis on *met-2; spr-1* mutants at the L1 stage allows us to compare to our previously published data set (Carpenter et al., 2021). We identified 1,787 differentially expressed genes (DEGs) in *met-2; spr-1* mutant progeny compared to wild type (Fig. S3A; Fig. S4C,F), and most of these genes are differentially expressed in *met-2* (856/1327)(Fig. S3A,B; Fig. S4B,E) and *spr-1* single mutants (40/60)(Fig. S3A,B; Fig. S4A,D) compared to wild type (Fig. S3B).

To determine whether gene expression changes in *met-2; spr-1* mutants resemble those in our previously published *spr-5; met-2* mutant RNA-seq data set, we first compared DEGs between the two data sets. We identified 1,787 DEGs in *met-2; spr-1* mutant progeny compared to wild-type. 1,010 (57%) of these significantly overlapped with the 4,223 DEGs that we previously identified in *spr-5; met-2* mutant progeny compared to wild-type (Fig. 2A, hypergeometric test, P-value < 1.28E-270, (Carpenter et al., 2021), and the gene ontology categories of DEGs in both data sets are similar (Fig. S3C,D; Carpenter et al., 2021). We also examined the overlapped gene expression changes between up-regulated and down-regulated DEGs in both datasets separately. Of the 1,067 up-regulated DEGs in *met-2; spr-1* mutant progeny, 676 (63%) of these overlap with the 2,330 up-regulated DEGs in *spr-5*; *met-2* mutant progeny (Fig. 2B, hypergeometric test, P-value < 2.61E-392; Carpenter et al., 2021). Of the 720 down-regulated DEGs in *met-2; spr-1* mutant progeny, 236 (33%) of these overlap with the 1,893 DEGs down-regulated DEGs in *spr-5*; *met-2* mutant progeny (Fig. 2C, hypergeometric test, P-value < 2.16E-72; Carpenter et al., 2021).

If mutating *spr-1* partially compromises SPR-5 maternal reprogramming, we would expect that the gene expression changes in *met-2; spr-1* mutants would be less affected in *spr-5*; *met-2* mutants. To determine if this is the case, we compared the average log2 fold change (FC) of the upregulated and downregulated DEGs separately. The average log2 (FC) of DEGs that are up-regulated in *met-2; spr-1* mutant progeny is 2, compared to 3.1 in *spr-5; met-2* mutant progeny (Fig. 3D; Carpenter et al., 2021). Similarly, the average log2(FC) of DEGs that are down-regulated in *met-2; spr-1* mutant progeny is -1, compared to -1.4 in *spr-5; met-2* mutant progeny (Fig. 3E; Carpenter et

al., 2021). Together, these data demonstrate while the same genes are differentially expressed in *spr-5; met-2* and *met-2; spr-1* mutant progeny, the changes are smaller in *met-2; spr-1* mutant progeny.

MES-4 germline genes are enriched in *met-2; spr-1* mutants, but less affected compared to *spr-5; met-2* mutants

MES-4 germline genes are genes that are expressed in the parental germline and acquire H3K36 methylation, which is maintained by a transcription independent methyltransferase MES-4 in the embryo of the progeny. Recently, we demonstrated that *spr-5; met-2* mutants ectopically express 112 (57%) out of the 196 MES-4 germline genes in somatic tissues (Carpenter et al., 2021). If the loss of SPR-1 partially compromises SPR-5 function, we would expect that MES-4 germline genes would also be ectopically expressed in *met-2; spr-1* mutants, though to a lesser degree. Of 196 MES-4 germline genes, 45 (23%) MES-4 germline genes were misexpressed in *met-2; spr-1* mutant progeny compared to wild type (Fig. 3A, hypergeometric test, P-value < 1.41E-9). All of these 45 MES-4 germline genes overlap with the 112 MES-4 germline genes that are misregulated in *spr-5; met-2* mutants (Fig. 3B; Carpenter et al., 2021). Thus, like *spr-5; met-2* mutants, *met-2; spr-1* mutants ectopically express MES-4 germline genes. However, when we compared the log2(FC) in expression of all of the MES-4 germline genes in *spr-1*, *met-2*, *met-2*; *spr-1*, and *spr-5; met-2* mutant progeny compared to wild type, we observed that the changes in the levels of gene expression are less affected in *met-2*; *spr-1* mutants than *spr-5; met-2* mutants (Fig. 3C; Carpenter et al., 2021).

LSD1 and CoREST are expressed during each stage of mouse oocyte development

Taken together, our results are consistent with SPR-5/LSD1 functioning maternally through SPR-1/CoREST in *C. elegans*. To determine whether there is a role for CoREST in LSD1 maternal reprogramming in mammals, we also sought to investigate the maternal interaction between LSD1 and CoREST in mice. Previous studies have shown that LSD1 is expressed during all stages of mouse oocyte development (Wasson et al. 2016, Ancelin et al. 2016, Kim et al. 2015). If LSD1 and CoREST function together in a complex, we would expect them to be expressed during the same stages of oogenesis. Previously CoREST was shown to be expressed in mouse oocytes, but the precise stages of oogenesis in which CoREST is expressed were not characterized (Ma et al., 2012). Thus, to determine whether CoREST is expressed at the same time as LSD1 in mouse oogenesis, we performed immunofluorescence experiments and examined CoREST and LSD1 protein at the primary, secondary, and antral stages of oocyte development (Fig. 4). Identical to what we and others previously observed with LSD1 (Fig. 4 A-I; Ancelin et al., 2016; Kim et al., 2015b; Wasson et al., 2016), CoREST was also highly expressed in the oocyte nucleus and in the surrounding follicle cells during all stages of oocyte development (Fig. 4 J-R).

Reducing the function of maternally-provided LSD1 causes perinatal lethality

Since CoREST has the same expression pattern as LSD1 in mouse oocytes, we wanted to test whether LSD1 functions through CoREST by specifically disrupting the presumptive CoREST-LSD1 interaction in the mouse oocyte. To do this, we utilized CRISPR to generate a point mutation, M448V, in the tower domain of the *Lsd1* gene at the endogenous locus (Fig. 5A; Fig. S5). This allele will be referred to as *Lsd1*^{M448V}. The tower domain is the site of protein-protein interactions (Forneris et al., 2007; Stavropoulos et al., 2006; Yang et al., 2006), and M448V resides in a residue that binds CoREST (Shi et al., 2005). Previous studies have shown that this mutation reduces the ability of LSD1 to demethylate histones *in vitro* (85% demethylase activity compared to wild-type LSD1) (Nicholson et al., 2013). This modest reduction in LSD1 function is unlikely to compromise maternal reprogramming. However, the M448V mutation severely reduces the ability of LSD1 to bind CoREST (35% binding activity compared to wild type *in vitro*) (Nicholson et al., 2013). Thus, the M448V mutation serves as a separation-of-function allele between demethylase activity and CoREST binding.

To interrogate the interaction between LSD1 and CoREST specifically in oocytes, we utilized our newly generated M448V *Lsd1* mutation. Previous studies have shown that a complete loss of LSD1 protein in the mouse oocyte results in embryonic arrest of offspring at the 1-2 cell stage (Ancelin et al., 2016; Wasson et al., 2016). This arrest is due to a failure to undergo the maternal-to-zygotic transition in gene expression. When LSD1 protein levels are decreased in the mouse oocyte, embryos can bypass the embryonic arrest, but ~30% of animals die perinatally, shortly after birth (Wasson et al., 2016). Our results in *C. elegans* suggest that loss of CoREST results in a partial loss of LSD1 function. Therefore, if LSD1 function partially requires CoREST maternally in mice,

we would expect that having only the *Lsd1*^{M448V} allele maternally would result in offspring that phenocopy the perinatal lethality observed from a partial loss of maternal LSD1. To test this possibility, we generated mice with the *Lsd1*^{M448V} allele over a floxed allele of the *Lsd1* gene. In the presence of an oocyte-specific *Zp3-Cre* allele that expresses prior to the first meiotic division, the floxed allele recombines to a null allele in the oocyte. As a result, the only maternal contribution of LSD1 is from the *Lsd1*^{M448V} allele, which produces LSD1 with a reduced ability to bind CoREST (Fig. 5B). The F1 offspring from this cross will be referred to as *Lsd1*^{M448V} progeny. Importantly, the mothers have a normal copy of the *Lsd1* gene in every other cell type throughout the mouse, and heterozygous *Lsd1* animals have been shown to have no phenotypic defects (Engstrom et al., 2020; Foster et al., 2010; Jin et al., 2013; Wang et al., 2007). In addition, mothers with a compromised maternal *Lsd1* allele are crossed to wild-type males, so the progeny have normal zygotic LSD1 activity from their paternal allele after transcription begins at the 2-cell stage. This mating scheme enables us to determine the specific effect of compromising LSD1 activity maternally in the oocyte. In one set of controls, the mother has the *Lsd1*^{M448V} allele over a floxed allele of LSD1 and is *Zp3Cre* negative (Fig. 5C). The maternal contribution in this case would be one functional copy of LSD1 and one hypomorphic *Lsd1*^{M448V} copy. These control F1 offspring will be referred to as *Lsd1*$^{+}$*.* In the other set of controls, the mother has a wild-type copy of the *Lsd1* gene over a floxed allele of *Lsd1,* and are *Zp3Cre* positive (Fig. 5D). The maternal contribution will be just one functional copy of the *Lsd1* gene. Previous studies have shown animals that are heterozygous for the *Lsd1* null allele have 70% protein levels (30% reduction) compared to homozygotes (Engstrom et al., 2020). These control F1 offspring will be referred to as *Lsd1*^{het}*.*

If disrupting the interaction between LSD1 and CoREST specifically in the oocyte phenocopies the perinatal lethality that we previously observed when LSD1 is hypomorphic maternally, it would provide further evidence that LSD1 functions in a complex with CoREST in the oocyte. To address this possibility, we examined perinatal lethality between postnatal day 0 (P0) and P1 in *Lsd1*^{M448V} progeny versus *Lsd1*$^{+}$ and *Lsd1*^{het} controls. All litters were generated from mothers that were less than 8 months old, to avoid any complications associated with advanced maternal age. Overall, we observe increasing perinatal lethality with increasingly compromised maternal LSD1. In *Lsd1*$^{+}$ control progeny, when one allele of *Lsd1* lacks the ability to bind CoREST, we observe 9% (N=24) perinatal lethality during the first 48hrs after birth. When one copy of *Lsd1* is fully deleted maternally (*Lsd1*^{het} progeny), the perinatal lethality increased to 18% (N=15), and when maternal LSD1 is solely provided from the *Lsd1*^{M448V} allele, perinatal lethality further increases to 35% (N=32)(Fig. 6E). The 35% perinatal lethality, when LSD1 completely lacks the ability to bind CoREST maternally, is similar to the ~30% perinatal lethality that we previously observed when LSD1 is partially lost maternally (Wasson et al., 2016). Importantly, the level of perinatal lethality does not depend on which allele the pup inherits from its mother (Fig. S6). Moreover, the entire litter died in 10 litters of *Lsd1*^{M448V} progeny out of 32 total (31.2%), versus only 2 litters out of 14 (14.2%) in *Lsd1*^{het} animals, and 0 out of 24 litters (0%) in *Lsd1*$^{+}$ controls (Supplemental file 1). The 31% of *Lsd1*^{M448V} litters in which all of the animals within the litter die is similar to the 10 out of 20 litters (50%) in which the entire litter died that we previously observed upon partial loss of maternal LSD1 (Wasson et al., 2016). Thus,

the loss of LSD1's ability to bind CoREST maternally phenocopies the perinatal lethality observed in progeny from mothers with partial loss of LSD1 protein in the oocyte.

DISCUSSION

CoREST regulates LSD1 maternal reprogramming of histone methylation

Despite our increasing knowledge of the enzymes involved in maternal epigenetic reprogramming, how these enzymes are regulated remains unclear. To begin to address this question, we asked whether maternal epigenetic reprogramming by the H3K4me1/2 demethylase SPR-5/LSD1/KDM1A is dependent on SPR-1/CoREST. In *C. elegans,* we find that the fertility of *spr-1* mutants is intermediate between *spr-5* mutants and wild type, which raises the possibility that loss of the *spr-1* gene partially compromises SPR-5 maternal reprogramming. However, *spr-1* mutants do not phenocopy the germline mortality phenotype of *spr-5* mutants. This suggests that if SPR-1 contributes to SPR-5 reprogramming, SPR-5 function is not completely dependent upon SPR-1.

Because SPR-5 and the H3K9 methyltransferase MET-2 function together in maternal reprogramming (Carpenter et al., 2021; Kerr et al., 2014; Greer et al., 2014), it provides a unique opportunity to ask whether SPR-1 functions in maternal SPR-5 reprogramming by making double mutants between *spr-1* and *met-2*. If loss of SPR-1 partially compromises SPR-5 reprogramming, then *spr-1* mutants might also display a synergistic sterility phenotype when combined with a mutation in *met-2*. Consistent with this possibility, *met-2; spr-1* double mutants had a germline mortality phenotype that is intermediate between the maternal effect sterility of *spr-5; met-2* mutants and the

germline mortality of *spr-5* and *met-2* single mutants. To determine if this synergistic sterility phenotype is due to loss of SPR-1 partially compromising SPR-5 reprogramming, we performed two additional experiments. First, we examined the gonads of *met-2; spr-1* double mutants to determine if the germline phenotype resembles the germline phenotype of *spr-5; met-2* mutants. This analysis demonstrated that the germline phenotype of *met-2; spr-1* mutants at late generations, with a squat gonad and disorganized germline cell types, is similar to *spr-5; met-2* mutants. This is consistent with the possibility that loss of SPR-1 partially compromises SPR-5 reprogramming. Second, we performed RNA-seq on F7 *met-2; spr-1* mutants. If SPR-1 functions specifically with SPR-5, we would expect that the genes that are misexpressed in *met-2; spr-1* mutants to be similar to the genes that are affected in *spr-5; met-2* mutants. Consistent with this possibility we observe a significant overlap in differentially expressed genes between *met-2; spr-1* mutants and *spr-5; met-2* mutants. In addition, the gene expression pathways affected in *met-2; spr-1* mutants are similar to those affected in *spr-5; met-2* mutants. However, if loss of SPR-1 only partially compromises SPR-5 function, we would expect that the magnitude of the gene expression changes in *met-2; spr-1* mutants would be less changed than in *spr-5; met-2* mutants. Strikingly, we find that the gene expression changes in *met-2; spr-1* mutants are consistently less affected than those that we observed previously in *spr-5; met-2* mutants.

MES-4 germline genes become ectopically expressed in the absence of SPR-5/MET-2 reprogramming. If SPR-1 partially compromises maternal reprogramming, we would expect that MES-4 germline genes would also be ectopically expressed in the

soma of *met-2; spr-1* mutants. The starved L1 larvae that we used for *met-2; spr-1* mutant RNA-seq only have two germ cells that are not undergoing transcription. Despite this, we observe the expression of MES-4 germline genes in L1 *met-2; spr-1* mutants. This suggests that, like we previously observed in *spr-5; met-2* mutants, *met-2; spr-1* mutants ectopically express MES-4 germline genes in somatic tissues. In addition, the fact that the MES-4 germline genes that are affected by loss of SPR-1 are the same as those affected by the loss of SPR-5 suggests that they function together on the same MES-4 targets. The ectopic expression of MES-4 germline genes in *met-2; spr-1* mutants provides further evidence that SPR-1 is functioning in maternal SPR-5 reprogramming. However, the magnitude of the ectopic expression of MES-4 genes in *met-2; spr-1* mutants is intermediate between *spr-5; met-2* double mutants and *spr-1* or *met-2* single mutants. Taken together, these data suggest that SPR-5 functions maternally through its interaction with SPR-1, with loss of SPR-1 partially compromising SPR-5 reprogramming. Consistent with this conclusion, SPR-1 and SPR-5 have been shown to directly interact with one another in *C. elegans* (Eimer et al., 2002; Kim et al., 2018), and both were identified in a screen for suppressors of presenilin (Wen et al., 2000).

In mammals, epigenetic reprogramming at fertilization also requires LSD1/SPR-5 and SETDB1/MET-2. To determine whether LSD1 reprogramming in mammals requires CoREST, we addressed the maternal role of CoREST in mice. We found that CoREST and LSD1 are both expressed during all stages of mouse oocyte development, indicating that both proteins are spatially and temporally positioned for LSD1 to be functioning through CoREST in maternal reprogramming. This is consistent with

previous literature describing the expression of LSD1 (Ancelin et al., 2016; Kim et al., 2015b; Wasson et al., 2016) and CoREST (Ma et al., 2012) in the mouse oocyte. Previously, we found that decreased levels of LSD1 protein in the oocyte results in ~30% perinatal lethality in progeny derived from these mothers (Wasson et al., 2016). Here we show that a M448V mutation, that reduces the ability to bind CoREST, phenocopies the perinatal lethality phenotype observed when LSD1 maternal protein is partially decreased, including the observation that many times all of the animals in a particular litter die. This suggests that the partial requirement for CoREST in maternal LSD1 reprogramming is conserved in mammals. In addition, we detect an allelic series in which the percentage of perinatal lethality increases from *Lsd1*$^{+}$ to *Lsd1*^{het} progeny, and increases again from *Lsd1*^{het} to *Lsd1*^{M448V} progeny. The finding that the extent of perinatal lethality is more severe in *Lsd1*^{het} progeny compared to *Lsd1*$^{+}$ progeny, provides further evidence that the *Lsd1*^{M448V} allele only partially compromises maternal LSD1 activity. In addition, we find that further compromising maternal LSD1 reprogramming in *Lsd1*^{M448V} progeny compared to *Lsd1*^{het} progeny leads to a further increase in perinatal lethality. This strengthens the link that we previously observed (Wasson et al., 2016) between maternal epigenetic reprogramming and defects that manifest postnatally. However, it remains to be determined whether these defects are due to the direct inheritance of inappropriate histone methylation or due to an indirect effect through some other epigenetic mechanism.

Evidence from diverse developmental processes across multiple phyla support a role for CoREST in LSD1 function

Across multiple phyla, the function of CoREST extends beyond the female germline. In *Drosophila*, loss of *Lsd1* results in sterility in both males and females (Reuter et al. 2007, Di Stefano et al. 2007, Szabad et al. 1988). However, CoRest and Lsd1 also function in the germline support cells. Lsd1 is required in escort cells that support early female germline differentiation (Eliazer et al., 2011), and knockdown of either Lsd1 or CoRest protein causes a number of phenotypes in ovarian follicle cells (Domanitskaya & Schüpbach, 2012; Lee & Spradling, 2014). The requirement for CoRest in cells that support oogenesis causes sterility in female CoRest mutants. Together, these data potentially implicate CoRest in regulating Lsd1 function, but the direct role of CoRest has yet to be determined during oogenesis. Furthermore, knockdown of CoRest in *Drosophila* males phenocopies the male infertility observed in LSD1 knockdown testes (Mačinković et al., 2019). The overlap in phenotypes between Lsd1 and CoRest mutants in the *Drosophila* spermatogenesis provides further evidence that *CoRest* may function with LSD1, but it is unclear if that function is in the germline, germline support cells, or both.

Analogous to the partial role for CoREST in *C. elegans* and mouse LSD1 maternal reprogramming, LSD1 may also be partially dependent on CoREST during mouse embryonic development. The phenotype of homozygous deletion of the *Lsd1* gene in mice is lethality by embryonic day 7.5 (e7.5) (Wang et al., 2007; Wang et al., 2009), while the *CoREST* deleted mice die by e16.5 (Yao et al., 2014). It is possible that the later embryonic lethality caused by loss of CoREST could result from the partial loss of LSD1 function, but this remains to be determined.

Potential roles for CoREST in regulating LSD1 activity

There are two main possibilities for how CoREST may partially regulate LSD1 during maternal reprogramming in *C. elegans* and mice. One possibility is that CoREST is required for LSD1 activity at a subset of LSD1 targets. For example, it is possible that LSD1 needs CoREST to gain access to chromatin at certain targets that normally exist in more repressed chromatin. Consistent with this possibility, *in vitro* biochemical experiments showed that while LSD1 can demethylate H3K4 peptides or bulk histones, it is only capable of demethylating nucleosomes when in complex with CoREST (Lee et al., 2005; Shi et al., 2005; Yang et al., 2006). If CoREST is required for helping LSD1 gain access to certain chromatin targets, we would expect that the gene expression changes at these targets would also be completely affected by loss of CoREST. In contrast, at other genes where LSD1 does not need CoREST to gain access to chromatin, the loss of CoREST would not have the same effect as losing LSD1. However, we observe that most genes affected by the loss of LSD1 are also affected by the loss of CoREST, when sensitized by the loss of *met-2*. Furthermore, the gene expression changes caused by loss of CoREST are less affected than when LSD1 is lost. This is consistent with an alternative possibility, that CoREST helps LSD1 more efficiently access chromatin genome-wide. In this case, it is possible that SPR-5 maintains sufficient demethylase activity to prevent accumulation of H3K4me1/2 methylation in the absence of SPR-1. For this reason, mutation of SPR-1 alone would not result in a germline mortality phenotype. However, when MET-2 maternal reprogramming is lost, the inability to reprogram active chromatin states with H3K9me1/2 creates a chromatin environment where optimal SPR-5 activity is required.

Without SPR-1, the reduced activity of SPR-5 is not sufficient to prevent the germline mortality phenotype that arises in *met-2; spr-1* double mutants. Thus, our data are more consistent with a model where CoREST is required maternally to help LSD1 more efficiently access chromatin genome-wide.

Potential implications for CoREST function in humans

Taken together, our data in *C. elegans* and mice suggest that CoREST has a conserved role in maternal LSD1 reprogramming. The partial requirement for COREST in LSD1 function has potential implications for putative patients with mutations in *COREST*. The first human patients with *de novo* mutations in LSD1 have been identified. These patients display phenotypes that are similar to Kabuki Syndrome, which is characterized by developmental delay and craniofacial abnormalities (Chong et al., 2016; Tunovic et al., 2014). The *Lsd1* human mutations appear to be dominant partial loss of function mutations. It is possible that only partial loss of function mutants are viable because of the requirement for LSD1 in embryonic development and in stem cell populations (Haines et al., 2018; Kerenyi et al., 2013; Lambrot et al., 2015; Myrick et al., 2017; Tosic et al., 2018; Zhu et al., 2014). However, if CoREST is also required to help LSD1 more efficiently access chromatin genome-wide in humans, either maternally or zygotically, we might expect that loss of CoREST would readily give rise to similar developmental defects as those caused by partial loss of LSD1 function. As a result, we are actively searching for such potential human COREST patients.

ACKNOWLEDGEMENTS

We are grateful to members of the Katz lab, as well as T. Caspary, T. Lee, and C. Bean, for their helpful discussion and critical reading of the manuscript; and the *Caenorhabditis* Genetics Center (funded by NIH P40 OD010440) for strains. **Funding:** This work was funded by a grant to D.J.K. (NSF IOS1931697); B.S.C. was supported by the Fellowships in Research and Science Teaching IRACDA postdoctoral program (NIH K12GM00680-15) and by NIH F32 GM126734-01. A.S. was supported by NIH F31 5F31HD098816-03 and the GMB training grant (T32GM008490-21). D.A.M. was supported by a research supplement to promote diversity in health-related research from NINDS (1R01NS087142). This study was supported in part by the Mouse Transgenic and Gene Targeting Core (TMF), which is subsidized by the Emory University School of Medicine and is one of the Emory Integrated Core Facilities. Additional support was provided by the National Center for Advancing Translational Science of the National Institutes of Health (UL1TR000454). **Author Contributions:** B.S.C., A.S. and D.J.K. conceived and designed the study and wrote the manuscript. B.S.C., A.S., R.G., S.R.C, M.C, and K.S. performed experiments under the direction of D.J.K. B.S.C, A.S., and D.J.K. analyzed data and interpreted results. D.A.M. helped with RNAseq analysis and visualizations. All authors discussed the results. **Data availability**: Raw and processed genomic data has been deposited with the Gene Expression Omnibus (www.ncbi.nlm.nih.gov/geo) under accession code GSE168081.

MATERIALS AND METHODS

***C. elegans* Strains.** All *Caenorhabditis elegans strains* were grown and maintained at 20° C under standard conditions, as previously described (Brenner, 1974). The *C.*

elegans spr-5 (by101)(I) strain was provided by R. Baumeister. The N2 Bristol wild-type (WT), *spr-1 (ar200)(V)*, and *et1(*III) ; *et1 [umnls 8 (myo-2p :: GFP + NeoR, III: 9421936)](V)* strain was provided by the *Caenorhabditis* Genetics Center. The *met-2 (n4256)(III) strain* was provided by R. Horvitz. From these strains we generated *spr-1 (ar200) (V)/ et1 [umnls 8 (myo-2p :: GFP + NeoR, III: 9421936)](V)* and *met-2 (n4256) (III) / et1 [umnls 8 (myo-2p :: GFP + NeoR, III: 9421936)](V); spr-1 (ar200)(V)/ et1 [umnls 8 (myo-2p :: GFP + NeoR, III: 9421936)](V)*. For genotyping, single animals were picked into 5-10ul of lysis buffer (50mM KCl, 10mM Tris-HCl (pH 8.3), 2.5mM $MgCl_2$, 0.45% NP-40, 0.45% Tween-20, 0.01% gelatin) and incubated at 65°C for 1 hour followed by 95°C for 30 minutes. PCR reactions were performed with AmpliTaq Gold (Invitrogen) according to the manufacturer's protocol and reactions were resolved on agarose gels.

Generation of M448V hypomorphic allele. Oligos were designed to include an A>G SNP conversion which removed an HpyAV restriction site, and a G>A PAM blocking silent SNP. C57BL/6 females were superovulated by injecting 0.1mL/head of CARD HyperOva (i.p.) on day 1. After 48 hours, females were injected with 7.5IU human chorionic gonadotropin (hCG, i.p.). Oocytes were collected 13 hours after the administration of hCG and fertilized with C57BL/6 sperm in vitro. Five hours postfertilization, 50ng/uL Cas9mRNA, 50ng/uL oligo, and 50ng/uL sgRNA were injected into the cytoplasm of embryos. Injected embryos were incubated at 37°C overnight. Two-cell embryos were then transferred into the oviducts of pseudopregnant females. Progeny of those females were genotyped for the point mutation, mated, and progeny were genotyped again to ensure the mutation passed through the germline. Mutant

animals were backcrossed at least s two times to C57BL/6 animals before being used in experiments.

Mouse husbandry and genotyping. The following mouse strains were used: *Zp3-Cre* MGI:2176187 (de Vries et al. 2000), *Lsd1*$^{fl/fl}$ MGI: 3711205 (Wang et al. 2007), C57BL/6 MGI: 3715241, and *Lsd1*^{M448V}. Primers for Lsd1 forward (F): GCACCAACACTAAAGAGTATCC, Lsd1 reverse (R): CCACAGAACTTCAAATTACTAAT. A wild type allele of Lsd1 results in a 720 base pair (bp) product, the floxed allele is 480 bp, and the deleted allele is 280 bp. Primers for Cre F: GAACCTGATGGACATGTTCAGG, Cre R: AGTGCGTTCGAACGCTAGAGCCTGT, Cre ctrl F: TTACGTCCATCGTGG ACAGC

Cre ctrl R: TGGGCTGGGTGTTAGCCTTA. If Cre+, this results in a 302 bp product, and Cre ctrl F/R primers are an internal control that yields a 250bp product. Primers for M448V F: CCCAAATGGCATGACATAAA, M448V R: TAAGGCACCAAACCCCTTCT resulting in a 386bp product. The point mutation removes a restriction site, so mutants versus wild type were determined by incubating PCR products at 37°C with the HpyAV restriction enzyme for one hour. Wild type band sizes: 72bp, 81bp, 209bp, 24bp. M448V band sizes: 72bp, 290bp, 24bp. All mouse work was performed under protocols approved by the Emory University Institutional Animal Care and Use Committee.

Immunofluorescence. Mice were sacrificed by cervical dislocation and ovaries were isolated. Ovaries were then fixed in 4% PFA for one hour, followed by four PBS washes over two hours. Tissues were cryoprotected in 30% sucrose at 4°C overnight and then embedded in O.C.T. Compound (Tissue Tek). Cryosections were obtained at 10µm and immunostaining was performed using rabbit polyclonal anti-LSD1 (1:200, ab17721),

rabbit polyclonal anti-CoREST (1:100, LS-B8140-50), and Alexa fluor conjugated secondary antibodies (1:500).

Perinatal lethality. Breeding cages were observed daily for new litters and number born alive were scored at P0. At P1, litter sizes were scored again, and percent lethality was calculated by determining the number of animals that died divided by the original size of the litter. Those that died due to failure to thrive shortly after birth were often missing visible milk spots. Only litters from mothers <8 months of age were used to avoid complications due to advanced maternal age.

Germline mortality assay. The germline mortality experiments were performed as described by Katz and colleagues (Katz et al., 2009). In brief, worms were maintained at 20^{o} C and three fertile young adults with visible embryos were transferred to new NGM plates every four days. The total number of progeny from wild type, *spr-1* mutants, and *spr-5* mutants was counted every third generation until generation 17, after which counts were completed every other generation. Average number of progeny from *spr-5* mutants was calculated from 10 animals until counts were stopped at generation 41 due to the inability to maintain fertile animals. For wild type, the average number of progeny was calculated from five animals until generation 41 when the average number of progeny was calculated from six animals. The average number of progeny from *spr-1* mutants was calculated from ten animals throughout the entirety of the experiment. The same germline morality assay was adapted to evaluate the germline mortality of wild-type, *spr-1* and *met-2* single mutants, and *met-2; spr-1* double mutants. Here, the number of progeny were counted every generation, except from *spr-1* mutants which was counted every fourth generation. The average number of progeny from wild type,

spr-1 mutants and *met-2* mutants was calculated from ten animals, while *met-2; spr-1* was calculated from 30 animals. The standard error of the mean (SEM) was calculated for each generation the number of progeny were averaged.

RNA sequencing and analysis. Total RNA was isolated using TRIzol reagent (Invitrogen) from ~500-1000 starved L1 larvae hatched at room temperature (21°C - 22°C) overnight in M9 Buffer. L1 larvae from wild type, *spr-1*, *met-2*, and *met-2; spr-1* were isolated at generation 7 (F7) prior to the observed decrease in sterility. For each genotype, 2 biological replicates were obtained. Sequencing reads were checked for quality using FastQC (Wingett and Andrews, 2018), filtered using Trimmomatic (Bolger et al., 2014), and remapped to the *C. elegans* transcriptome (ce10, WS220) using HISAT2 (Kim et al., 2015a). Read count by gene was obtained by FeatureCounts (Liao et al., 2014). Differentially expressed transcripts (significance threshold, Wald test, p-value < 0.05) were determined using DESEQ2 (v.2.11.40.2) (Love et al., 2014). Transcripts per million (TPM) values were calculated from raw data obtained from FeatureCounts output. Subsequent downstream analysis was performed using R with normalized counts and p-values from DESEQ2 (v.2.11.40.2). Heatmaps were produced using the ComplexHeatmap R Package (Gu et al., 2016). Data was scaled and hierarchical clustering was performed using the complete linkage algorithm. In the linkage algorithm, distance was measured by calculating pairwise distance. Volcano plots were produced using the EnhancedVolcano package (v.0.99.16). Additionally, Gene Ontology (GO) Pathway analysis was performed using the online platform WormEnrichr (Chen et al., 2013; Kuleshov et al., 2016). An additional heatmap comparison of differentially expressed genes between *spr-1*, *met-2*, *met-2; spr-1* and

spr-5; met-2 progeny compared to wild type progeny was generated in Microsoft Excel using log2 fold change values from the DESEQ2 analysis. Differentially expressed genes in *spr-5; met-2* double mutants compared to wild type examined in this manuscript were obtained from a separate RNAseq analysis performed under the same conditions (Carpenter et al., 2021). Because transcript isoforms were ignored, we discuss the data in terms of “genes expressed” rather than “transcripts expressed”.

Differential interference contrast (DIC) microscopy. Worms were immobilized in 0.1% levamisole and placed on a 2% agarose pad for imaging at either 10x, 40x, or 100x magnification.

Figures

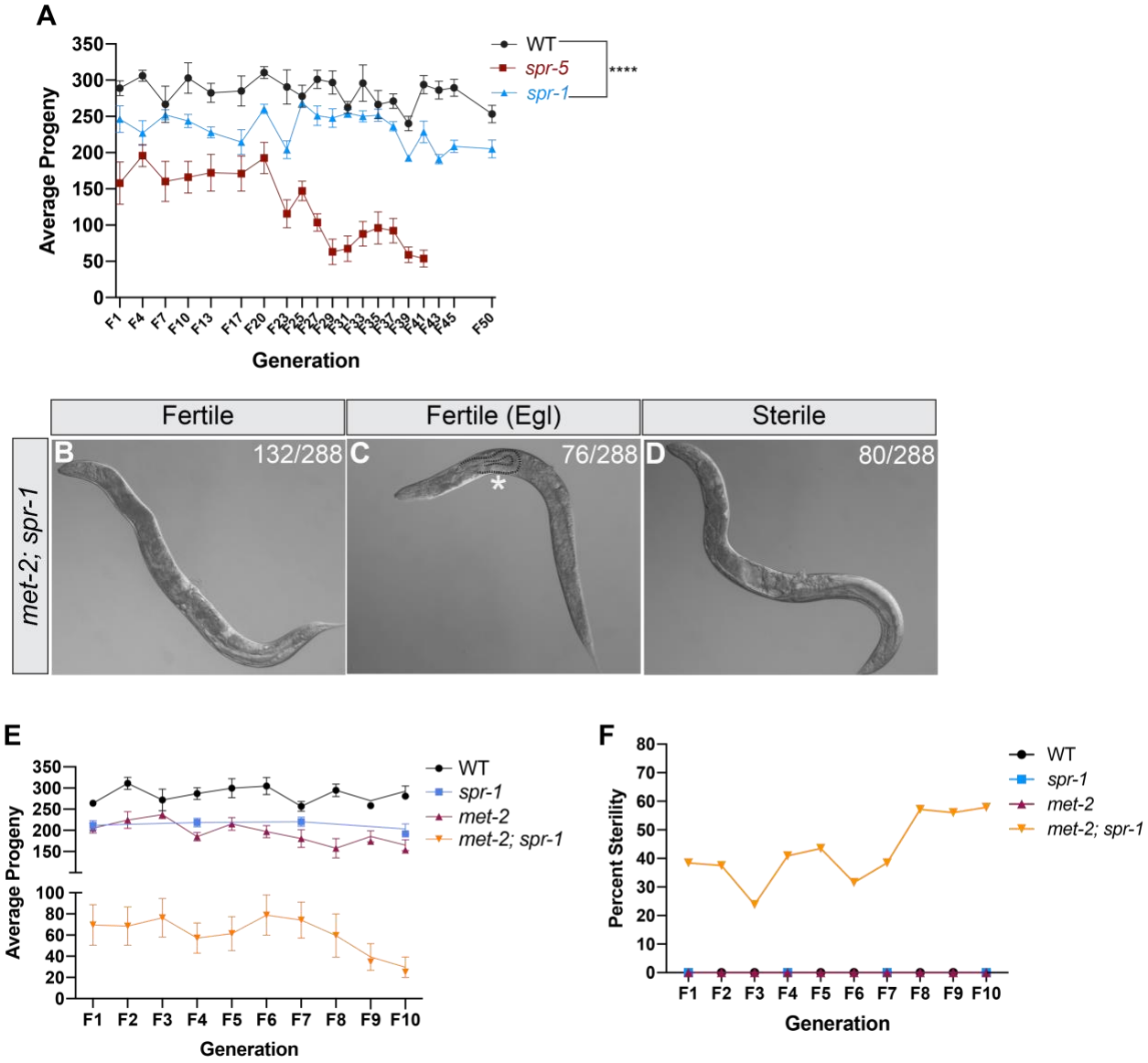

Figure 1. Germline mortality in *spr-1* and *met-2; spr-1* mutants. (A) The average number of total progeny from wild type (WT), *spr-5*, and *spr-1* mutants over progressive generations. The average number of progeny from *spr-1* mutants (N=192, N= total number broods counted) was significantly decreased compared to WT animals (N=92) across 50 generations (unpaired student t-test, **** p-value <0.0001). 10x DIC images of first generation (F1) *met-2; spr-1* mutants scored as either fertile (B), fertile (Egl) (C), or sterile (D). Asterisk denotes hatched larvae outlined by a dashed line inside of a *met-2; spr-1* mutant scored as fertile (Egl)(C). (E) The average number of total progeny from WT, *spr-1*, *met-2* and *met-2; spr-1* mutants over progressive generations. Error bars in (A, E) represent the standard error of the mean (SEM). (F) Percent of animals cloned out for experiment in (E) scored for sterility over progressive generations. *spr-1* mutant progeny were only scored at F1, F4, F7, and F10 generations in (E, F).

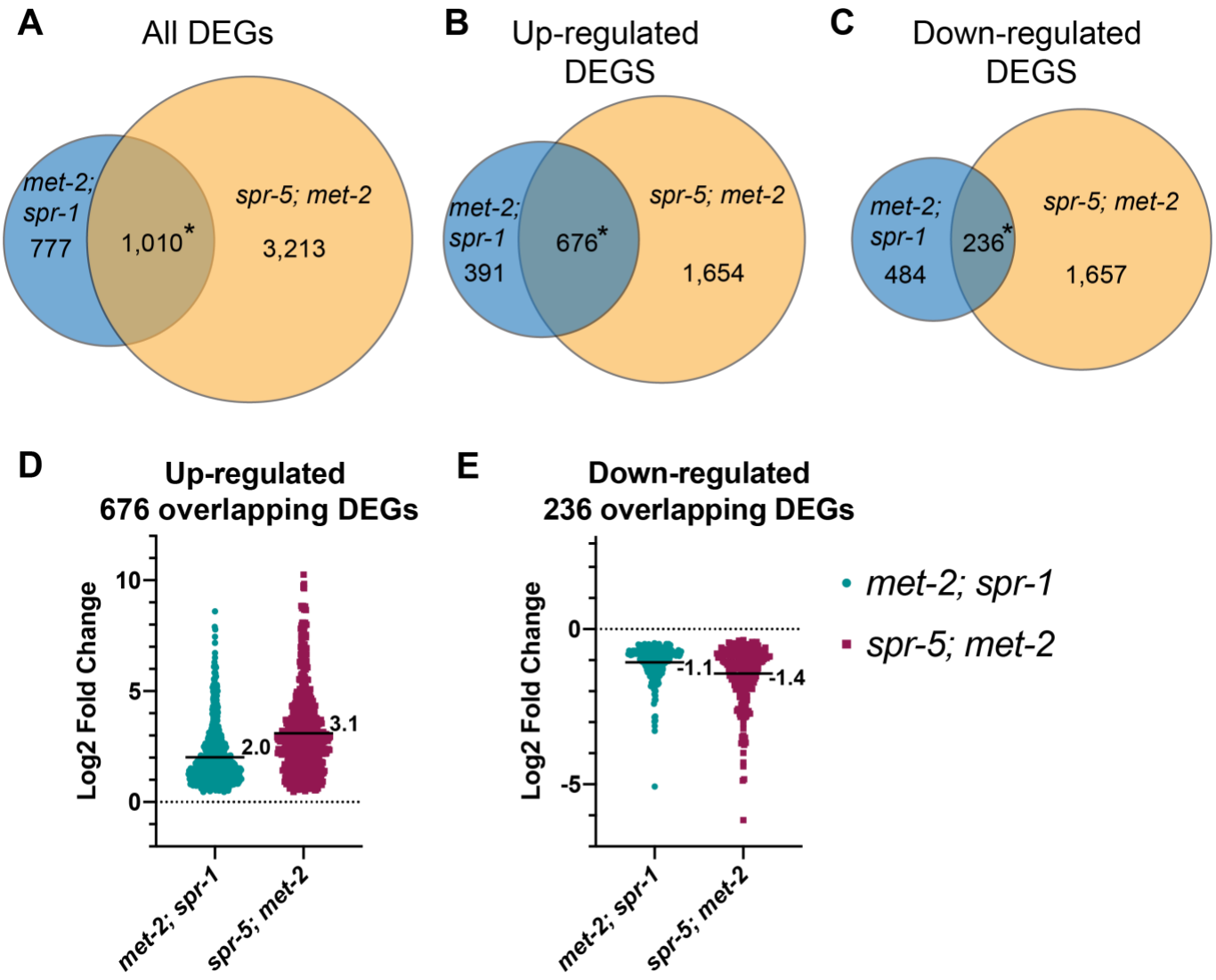

Figure 2. Transcriptional misregulation in *met-2; spr-1* progeny resembles that observed in *spr-5; met-2* progeny but is less affected. Overlap between all (A), up-regulated (B), and down-regulated (C) differentially expressed genes (DEGs) in *met-2; spr-1* and *spr-5; met-2* L1 progeny. Significant over-enrichment in A-C was determined by the hypergeometric test (*P-value < 1.28E-270, *P-value < 2.61E-392, *P-value < 2.16E-72, respectively). Scatter dot plots displaying the log2 fold change of the 676 up-regulated (D), and 236 down-regulated (E) overlapping DEGs between *met-2; spr-1* and *spr-5; met-2* progeny. (D, E) Numbers and solid black lines represent the mean log2 fold change. DEGs in *spr-5; met-2* progeny were obtained from (Carpenter et al., 2021).

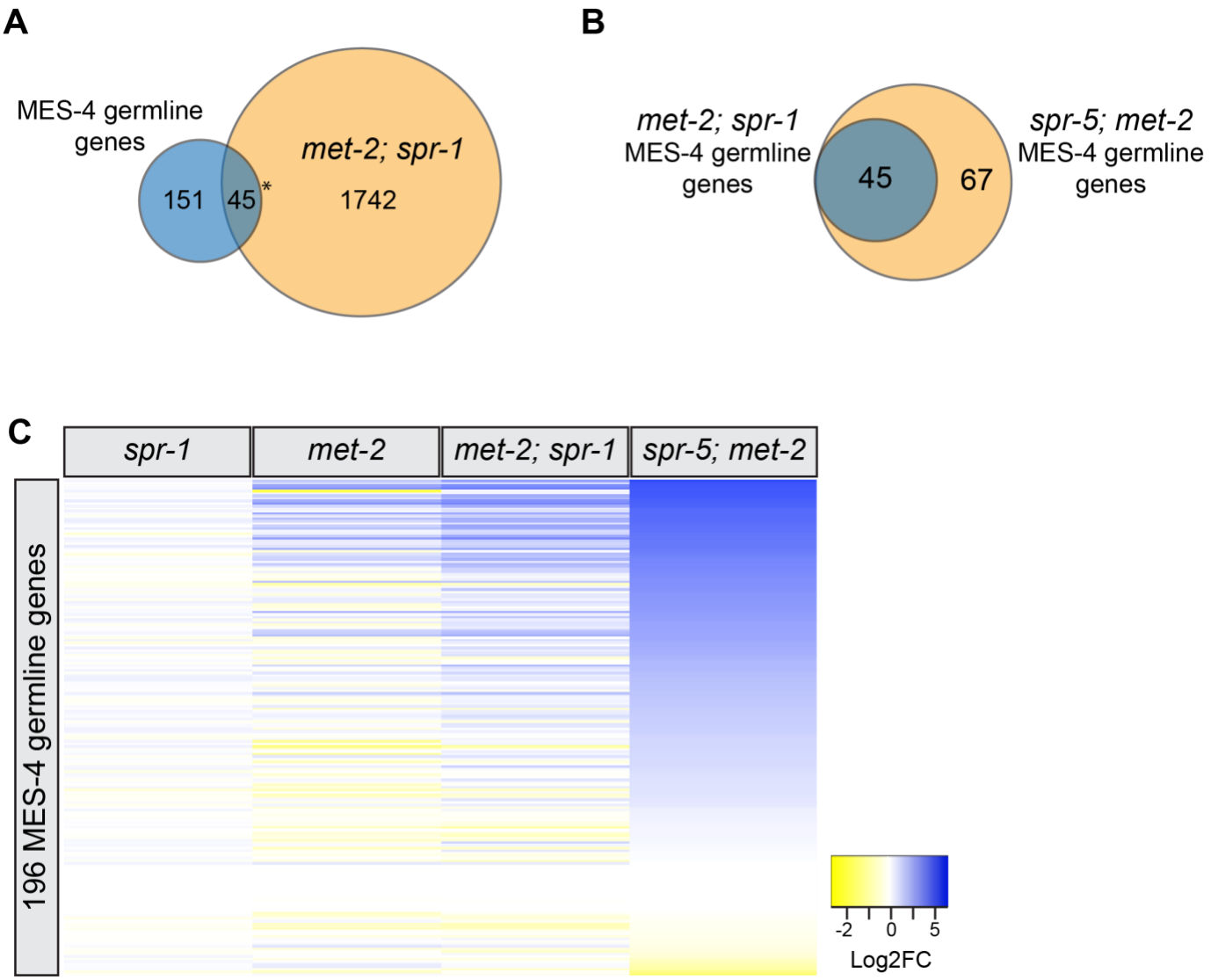

Figure 3. MES-4 germline genes are enriched in *met-2; spr-1* mutants, but less affected compared to *spr-5; met-2* mutants. (A) Overlap between MES-4 germline genes and differentially expressed genes (DEGs) in *met-2; spr-1* L1 progeny. Asterisks denotes significant over-enrichment in A as determined by a hypergeometric test (P-value < 1.41E-9). (B) Overlap between MES-4 germline genes differentially expressed in *met-2; spr-1* and *spr-5; met-2* L1 progeny. (C) Heatmap of log2 fold change (FC) of all 196 MES-4 germline genes in *spr-1*, *met-2*, *met-2; spr-1* and *spr-5; met-2* mutants compared to wild type. log2(FC) values are represented in a yellow to blue gradient with a range of -2 to 5. Yellow represents genes with negative log2(FC) values and blue represents genes with positive log2FC values compared to wild type.

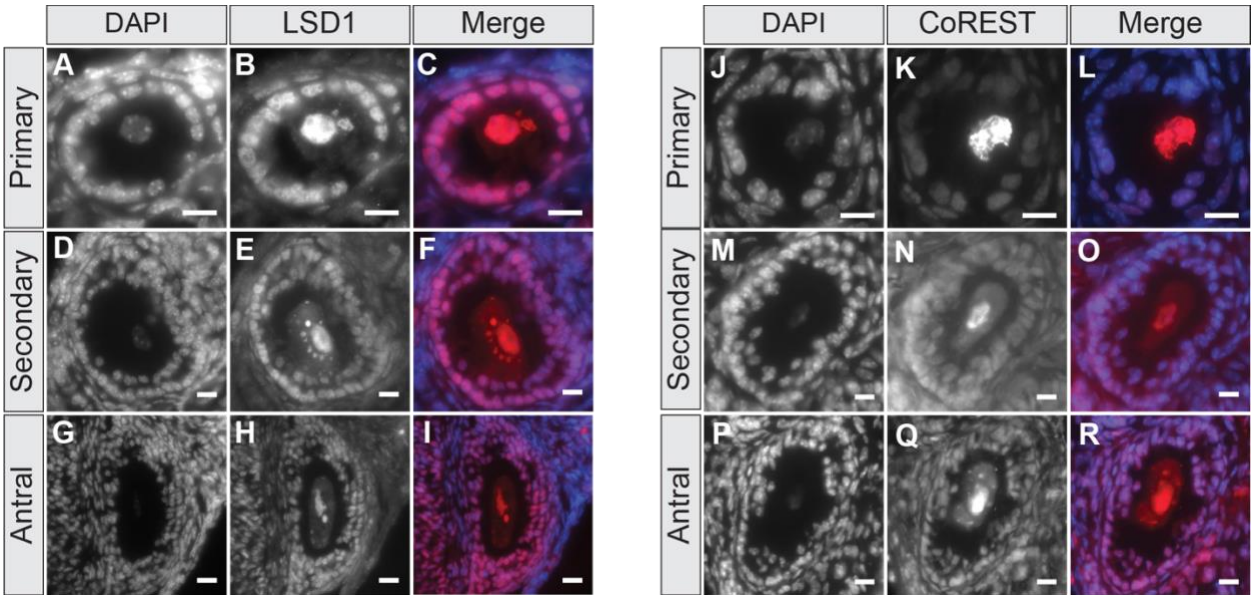

Figure 4. LSD1 and CoREST are expressed during each stage of mouse oocyte development. Representative immunofluorescence images of various stages of the mouse oocyte: primary (A-C, J-L), secondary (D-F, M-O), and antral (G-I, P-R). DAPI (A, D, G, J, M, P), LSD1 (B, E, H) CoREST (K, N, Q), and Merge (C, F, I, L, O, R). Both LSD1 and CoREST are expressed in the oocyte nucleus and surrounding follicle cells during each stage of oocyte development. Scale bars= 25um.

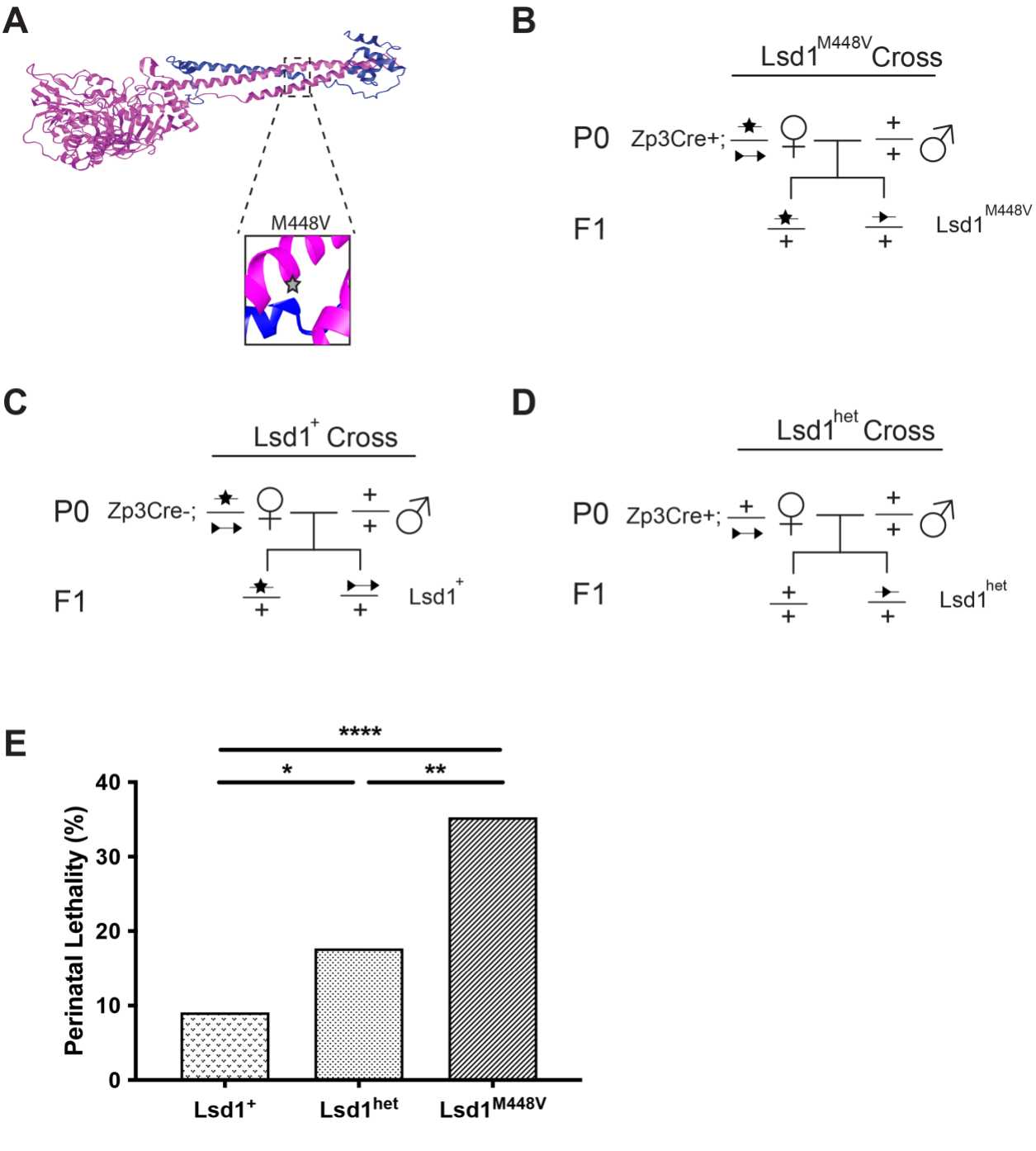
A
M448V
B
Lsd1M448V Cross
P0 Zp3Cre+;
F1
Lsd1M448V
C
Lsd1+ Cross
P0 Zp3Cre-;
F1
Lsd1+
D
Lsd1het Cross
P0 Zp3Cre+;
F1
Lsd1het
E
****
*
**
Perinatal Lethality (%)
40
30
20
10
0
Lsd1+
Lsd1het
Lsd1M448V

Figure 5. Hypomorphic maternal LSD1 results in perinatal lethality. (A) Crystal structure of LSD1 (pink) in complex with CoREST (blue) from Nicholson et al., 2013. The M448V mutation is in a CoREST binding site (star). (B-D) Genetic crosses showing wild type (+), loxP sites (triangles), and M448V (star) alleles. In all cases, P0 females are crossed to wild-type males, so that F1 progeny have normal zygotic LSD1 activity from their paternal allele after transcription begins at the 2-cell stage. (B) In the *Lsd1*^{M448V} cross, P0 mothers are Zp3Cre+, contributing only the hypomorphic allele maternally. (C) In the Lsd1^{+} control cross, P0 mothers are Zp3Cre-, contributing a wild-type and hypomorphic allele maternally. (D) In the Lsd1^{het} control cross, P0 mothers are Zp3Cre+, contributing one wild-type copy of *Lsd1* maternally. (E) Percent perinatal lethality per litter by experimental condition, n= 154 pups from 24 litters (Lsd1^{+}), n= 96 pups from 15 litters (Lsd1^{het}), and n= 187 pups from 32 litters (Lsd1^{M448V}). See Supplemental file 1 for the list of individual litters. p values calculated using a chi-square test, **** = p<.0001, ** = p<.01, *= p<.05.

Supplemental Material

Supplemental Figure 1

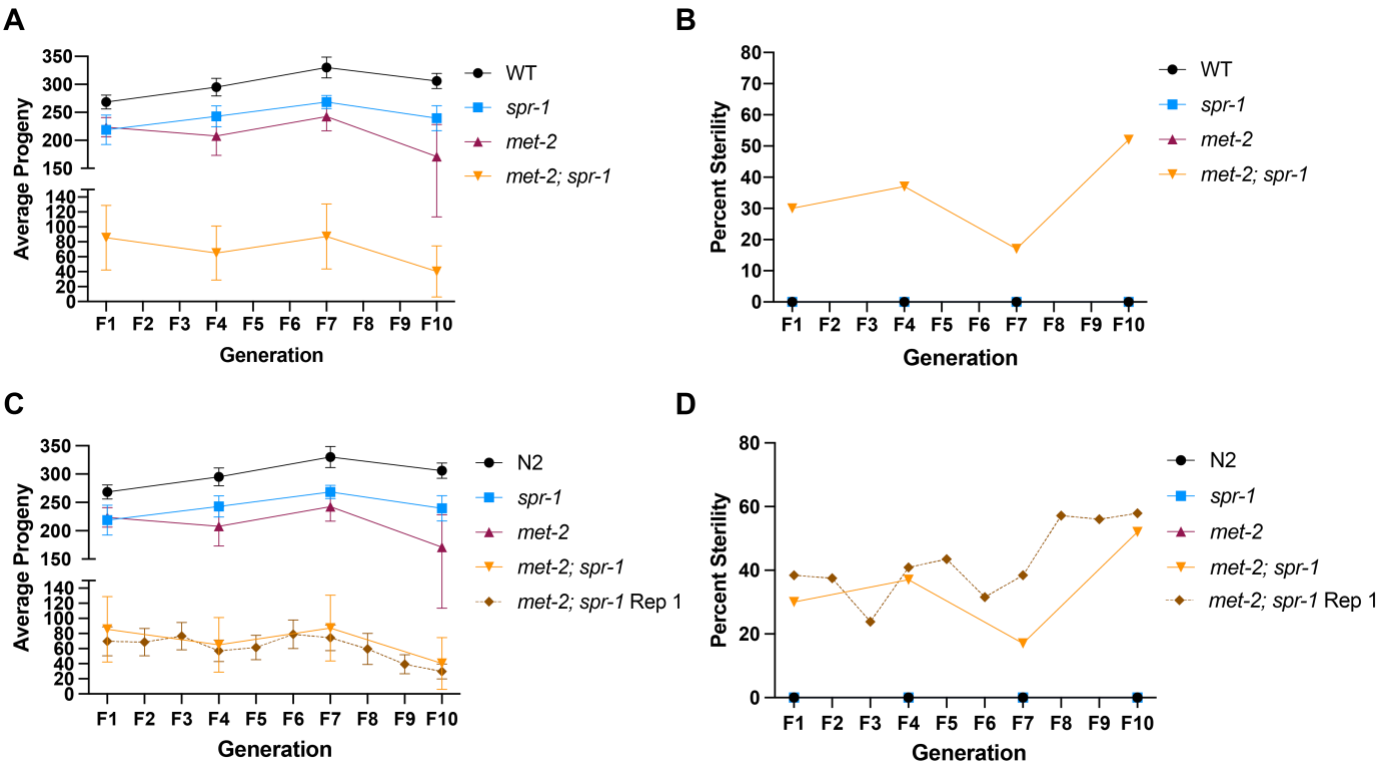

Figure S1. Germline mortality in *spr-1* and *met-2; spr-1* mutants replicate experiment. (A) The average number of total progeny from wild type (WT), *spr-1*, *met-2* and *met-2; spr-1* mutants over progressive generations in a repeat experiment (see Fig. 1E for comparison). (B) Percent of animals cloned out for repeat experiment in (A) scored for sterility over progressive generations (see Fig. 1F for comparison). (C) Same as (A) with overlay of total progeny from *met-2; spr-1* (*met-2; spr-1* Rep 1) mutants from germline mortality experiment in Figure 1E. (D) Same as (B) with overlay of percent sterile *met-2; spr-1*(*met-2; spr-1* Rep 1) mutants in Figure 1F. Error bars in (A, C) represent the standard error of the mean (SEM). Animals cloned out for the replicate germline mortality experiment were only scored at F1, F4, F7, and F10 generations in (A-D).

Supplemental Figure 2

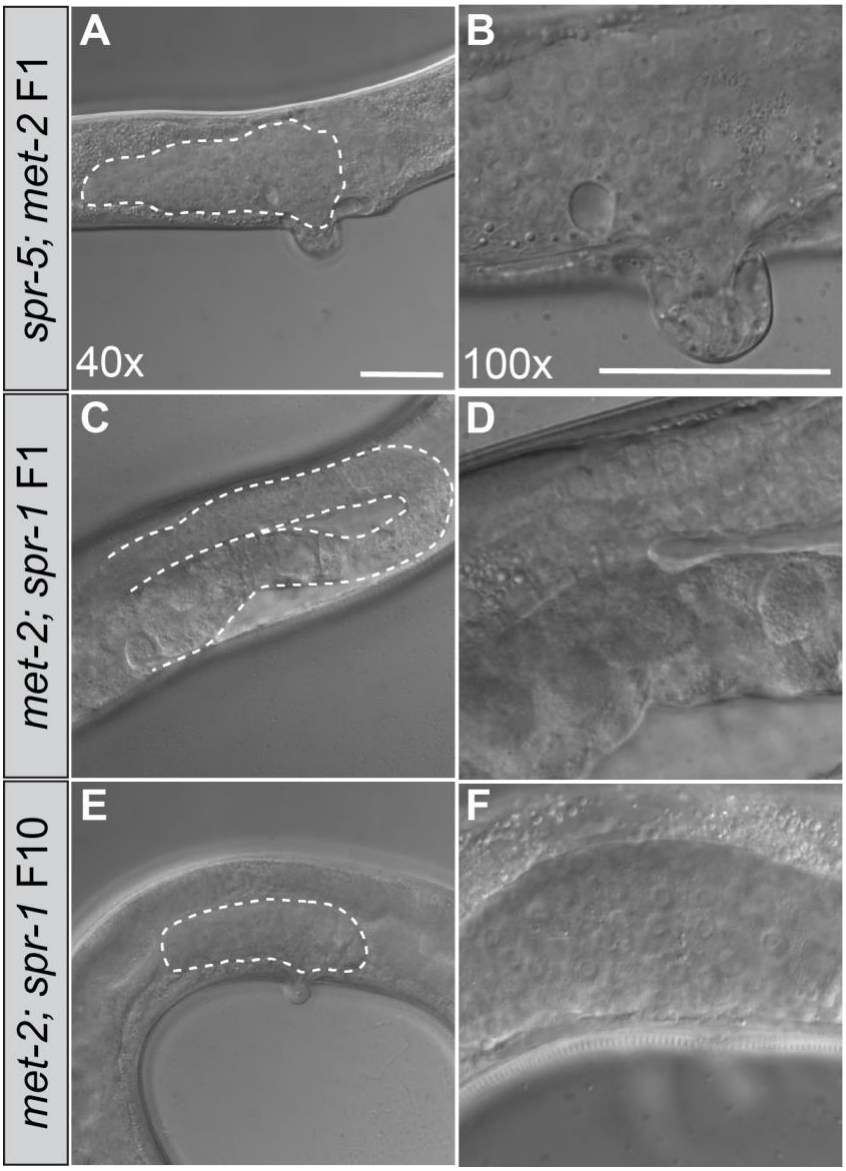

Figure S2. Sterile *spr-5; met-2* and *met-2; spr-1* double mutant gonads.
40x Differential Interference Contrast (DIC) images of F1 *spr-5; met-2* (A) *F1 met-2; spr-1* (C), and F10 *met-2; spr-1* (E) adult germlines. White dotted lines denote germlines. 100x DIC images of F1 *spr-5; met-2* (B) F1 *met-2; spr-1* (D), and F10 *met-2; spr-1* (F) adult germlines. Scale bar: 100μm.

Supplemental Figure 3

A

Genotype	Total # of differentially expressed genes	Up-regulated	Down-regulated
spr-1	60	41	19
met-2	1327	713	614
met-2; spr-1	1787	1067	720

B

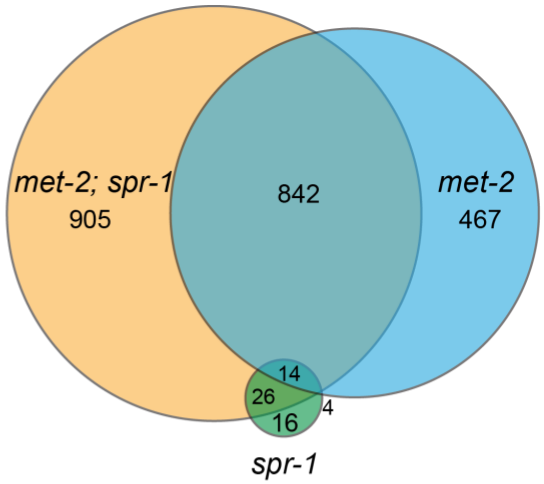

C

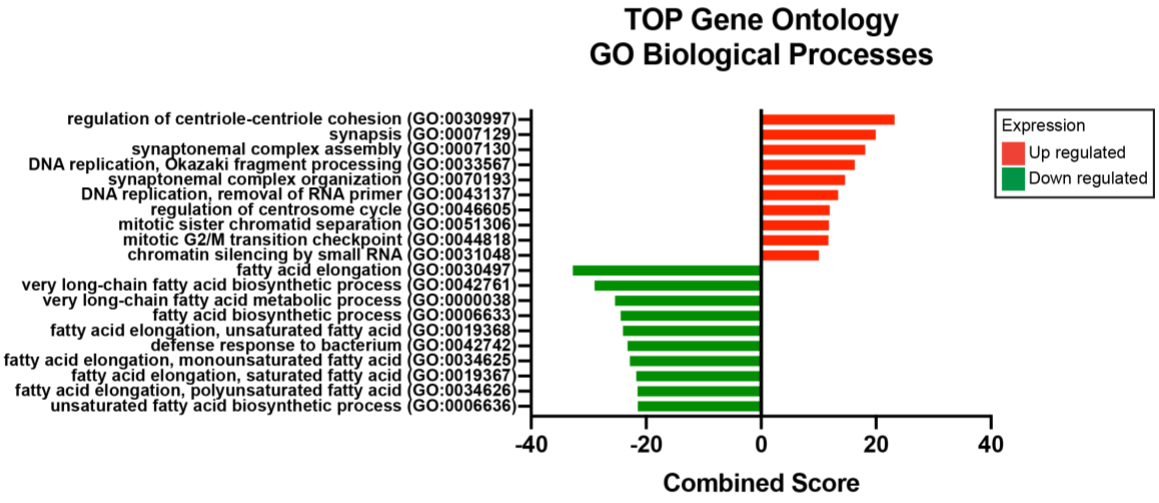

D

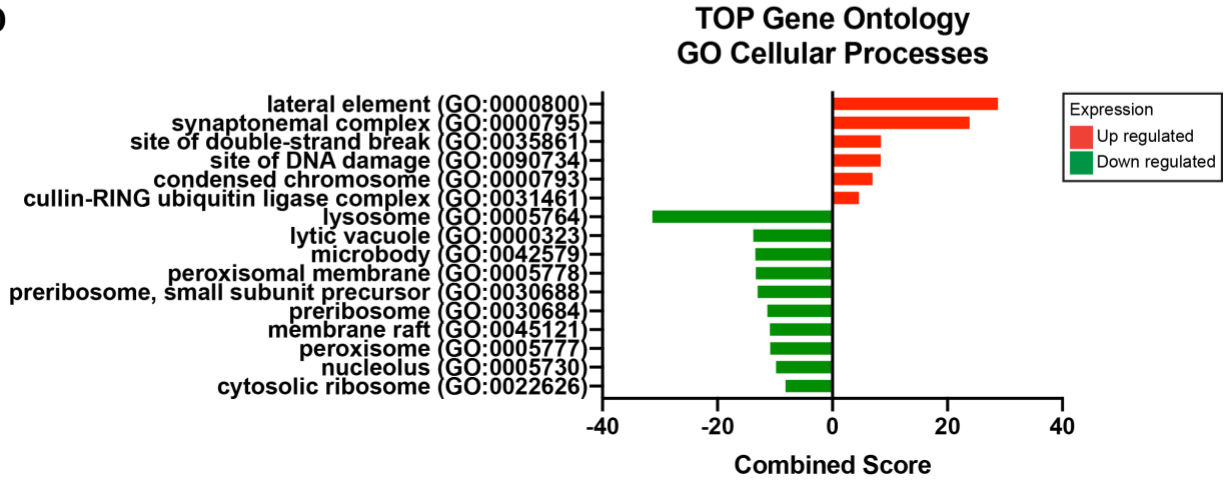

Figure S3: **Differential gene expression *spr-1*, *met-2*, and *met-2; spr-1* progeny compared to wild type.** (A) Table summary of differentially expressed genes (DEGs) in *spr-1, met-2, and met-2; spr-1* progeny from DeSEQ2 analysis (significance cut-off of p-adj< 0.05). (B) Overlap of differentially expressed genes between *spr-1, met-2, and met-2; spr-1* L1 progeny. Gene Ontology analysis showing Biological Processes (C) and Cellular Components (D) amongst genes that were up-regulated (red) and down-regulated (green) in *met-2; spr-1* progeny compared to wild-type. Combined Score was computed to determine gene category enrichment (Chen et al., 2013).

Supplementary Figure 4

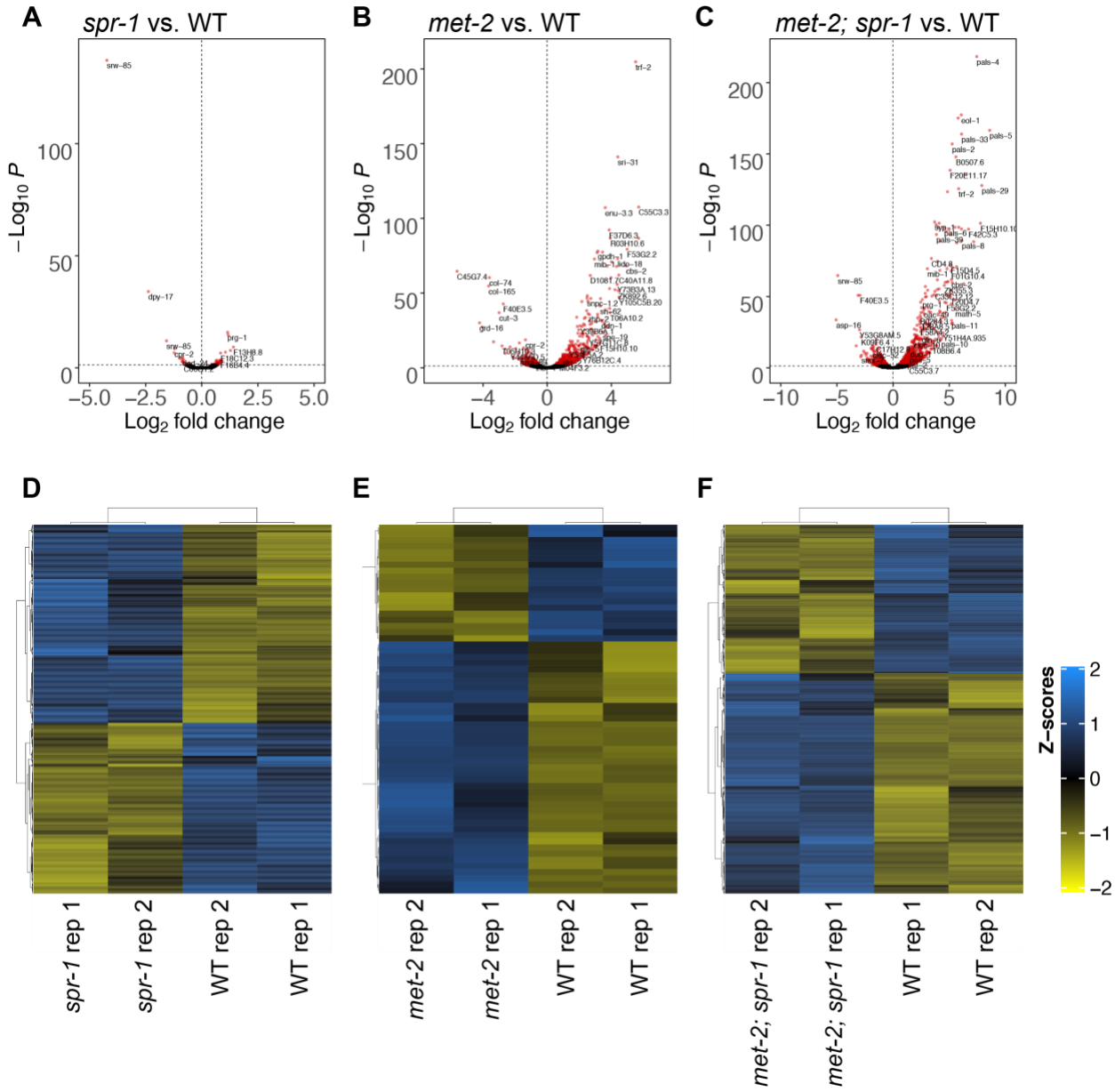

Figure S4: **Differential expression and replicate comparison of RNAseq experiments performed on wild type, *spr-1*, *met-2*, and *met-2; spr-1* progeny.** Volcano plot of log2 fold changes in gene expression (x-axis) by statistical significance (-Log_{10} P-value; y-axis) in *spr-1* (A), *met-2* (B), and *met-2; spr-1* (C) L1 Progeny compared to wild type (WT). Heatmap of differentially expressed RNA-seq transcripts between WT and *spr-1* (D), *met-2* (E), and *met-2; spr-1* (F). Data was scaled and hierarchical clustering was performed using complete linkage algorithm, with distance measured by calculating pairwise distance. Higher (blue) and lower (yellow) expression is reported as a z-score.

Supplementary Figure 5

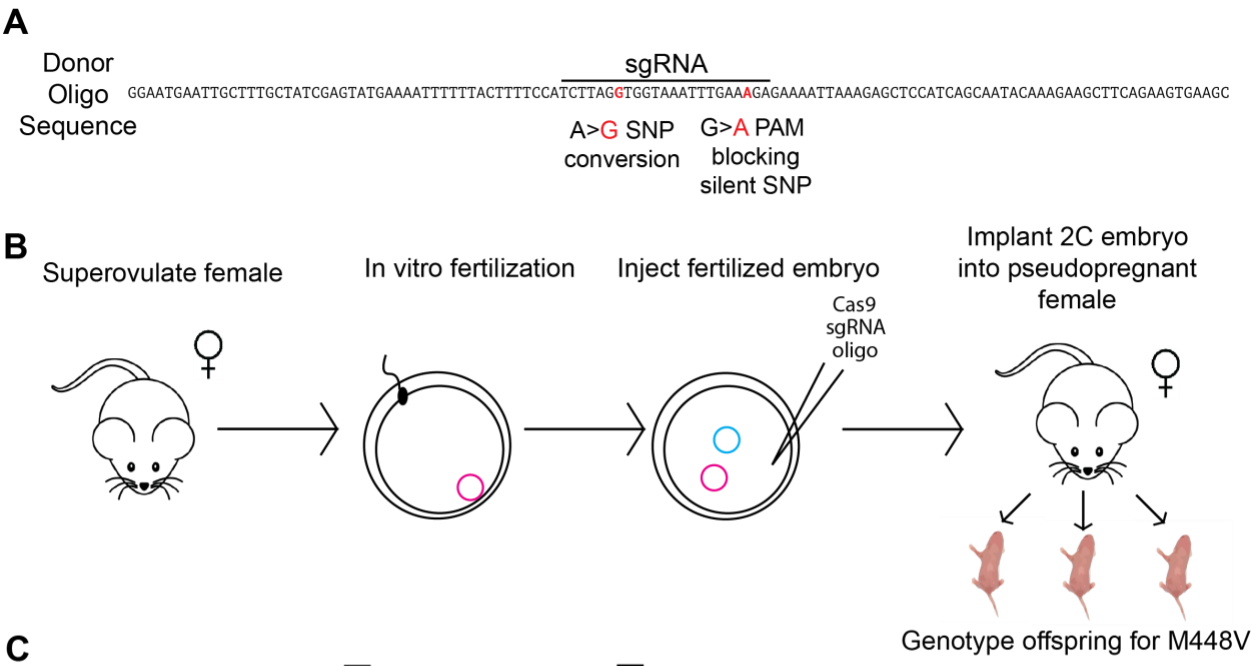

Figure S5. Generation of M448V hypomorphic allele. (A) Donor oligo sequence with the sgRNA sequence denoted. Two point mutations being introduced are colored in red: A>G SNP and G>A PAM blocking silent SNP. (B) Workflow for introducing M448V mutation into mice. (C) Wild-type chromatogram versus validated A>G SNP and G>A silent SNP in the newly generated mutant.

A

		Expected Percentage	Actual Percentage
$Lsd1^{+}$	+	50	44
	+	50	56
$Lsd1^{M448V}$	+	50	54
	+	50	46

Figure S6. Percent survival by genotype per experimental condition. *Lsd1*$^{+}$ n=50 animals genotyped. *Lsd1*^{M448V} n=87. Statistical analyses performed using chi square test, no significant difference between expected and actual percentages for either experimental condition.

Supplemental files

Supplemental file 1. List of individual litters analyzed for embryonic lethality in Figure 5.

Chapter 5:

LSD1 is required for neural stem cell development *in vivo* in mice

David Katz and Dexter Myrick conceived and designed this study. D.M., Claudia Fallini, and I performed experiments under the direction of D.K. D.M. and I analyzed data and interpreted results. I wrote the manuscript.

Introduction

Stem cell (SC) populations have the unique ability to self-renew as well as differentiate into various cell types. Lysine 4 of histone H3 (H3K4) methylation is typically associated with active gene expression and has been shown function as an epigenetic memory, maintaining transcriptional states over time and through cell divisions. This transcriptional memory function is important in the maintenance of cell fates, including stem cell programs (Mito et al., 2005; Muramoto et al., 2010; Ng & Gurdon, 2008). As a result, transcriptional memory needs to be erased in order for differentiation to occur. LSD1 is an H3K4 demethylase that uses an amine oxidase reaction to specifically remove mono- and di-methylation (me1/2) (Shi et al. 2004). LSD1 plays an essential role in mouse embryonic stem cells (mESCs) to decommission the active enhancer modification H3K4me1 (Whyte et al. 2012). Without LSD1, H3K4 methylation is not removed at critical SC gene promoters and enhancers, resulting in the inappropriate expression of SC genes during mESC differentiation. Therefore, the removal of H3K4 methylation by LSD1 is required for changes in cell fate.

The function of LSD1 in decommissioning enhancers has been shown to have a similar function *in vivo* in hematopoietic (Kerenyi et al. 2013), trophoblast (Zhu et al. 2014), testis (Lambrot et al. 2015, Myrick et al. 2017), naïve B (Haines et al. 2018), and

satellite SCs (Tosic et al. 2018). The knockout of LSD1 in all of these cell types has been shown to significantly reduce the ability of those SCs to properly undergo differentiation.

LSD1's function in neural stem cells (NSCs) has also been described. NSCs give rise to the central nervous system during embryonic development. LSD1 is expressed in NSCs, and that expression decreases with differentiation, which coincides with elevated H3K4me2 (Sun et al., 2010). Sun et al. also showed that chemical inhibition and siRNA knockdown in NSCs led to inhibition of NSC proliferation in cell culture and in the hippocampus of adult mice. Taken together, these data indicate the importance of LSD1 during NSC differentiation in mice. However, no work has been done to examine the function of *Lsd1* in NSCs during embryonic development *in vivo*.

To address that gap, our lab utilized the *Nestin Cre* transgene to delete *Lsd1* in NSCs during embryonic development. The *Nestin Cre* transgene is strongly expressed in neuronal tissues from embryonic day 10.5 (e10.5) through adulthood, when NSCs begin to proliferate into various progenitor cell populations. These mice will hereafter be referred to as $Lsd1^{NSC}$. While $Lsd1^{NSC}$ animals make it out to birth, 100% of them die before weaning. Prior to death, $Lsd1^{NSC}$ mice show a dramatic reduction in size compared to controls and exhibit motor defects. These defects are associated with abnormal brain morphology. Additionally, when motor neurons are cultured from $Lsd1^{NSC}$ mice, they continue to inappropriately express SC genes, including *Sox2* and *Nestin*. These data indicate that LSD1 functions in the proper differentiation of embryonic NSCs, analogous to LSD1's function in other stem cell populations.

Materials and Methods

Mouse husbandry and genotyping

The following mouse strains were used: *Lsd1*$^{fl/fl}$ MGI: 3711205 (Wang et al., 2007) and *Nestin-Cre* MGI: 4412413. Primers for Cre F: GAACCTGATGGACATGTTCAGG, Cre R: AGTGCGTTCGAACGCTAGAGCCTGT, Cre ctrl F: TTACGTCCATCGTGG ACAGC Cre ctrl R: TGGGCTGGGTGTTAGCCTTA. If Cre+, this results in a 302 bp product, and Cre ctrl F/R primers are an internal control that yields a 250bp product. Primers for Lsd1 forward (F): GCACCAACACTAAAGAGTATCC, Lsd1 reverse (R): CCACAGAACTTCAAATTACTAAT. A wild type allele of Lsd1 results in a 720 base pair (bp) product, the floxed allele is 480 bp, and the deleted allele is 280 bp. All mouse work was performed under protocols approved by the Emory University Institutional Animal Care and Use Committee.

Histological methods

For immunofluorescence on embryos, we set up timed matings. Pregnant females were sacrificed using cervical dislocation and embryos were fixed for 1-3 hours at 4°C in 4% paraformaldehyde, followed by a 2 hour PBS wash and then transferred to 30% sucrose overnight at 4°C. The tissue was then embedded in O.C.T. compound (Tissue-Tek) and stored at -80°C. 10μm sections were incubated with primary antibody in wash solution (1% heat-inactivated goat serum, 0.5% triton X-100 in PBS) overnight at 4°C in a humidified chamber. Slides were incubated in secondary antibody (1:500 in wash solution) at room temperature for 2 hours in humidified chamber. Antibodies used

include: KDM1A polyclonal (1:200, ab17721), CRE (1:200 ab188568),HB9 (1:1000 ab79541), and OLIG2 (1:100 ab109186).

For immunofluorescence on cell, cells were fixed at 3 DIV with 4% paraformaldehyde in PBS and stained with anti-TAU (1:5000, Aves), anti-NESTIN (1:200, Abcam), and anti-SOX2 (1:200, Epitomics) antibodies overnight at 4°C. Cy3-, Cy2- or Cy5-conjugated secondary antibodies (Jackson Immunoresearch) were incubated for 1 hour at room temperature.

For Hematoxylin and eosin staining, it was performed according to standard procedures. Briefly, sections were dewaxed with xylenes and serial ethanol dilutions then stained with Eosin using the Richard-Allan Scientific Signature Series Eosin-Y package (ThermoScientific).

Primary motor neuron culture and transfection

Primary motor neurons from E13.5 mouse embryos were isolated, cultured, and transfected by magnetofection as previously described (Fallini et al., 2010; Fallini et al., 2011). For high resolution imaging, a 60x objective (1.4 NA) was used. Z-series (5 to 10 sections, 0.2 µm thickness) were acquired with an epifluorescence microscope (Ti, Nikon) equipped with a cooled CCD camera (HQ2, Photometrics). For axon length measurement, motor neurons were transfected with GFP to highlight the entire cell. Low magnification images were acquired with a 10x or 20x phase objective. Overlapping images of a single cell were reassembled if necessary using Photoshop (Adobe). The ImageJ plug-in NeuronJ (Meijering et al., 2004) was used to measure the length of the axon, identified as the longest process.

Results

LSD1 is expressed in neural stem cells *in vivo*

To determine whether LSD1 functions in neural stem cells (NSCs) in mice, we first looked at whether it was expressed in *Nestin Cre* positive NSCs. *Nestin Cre* is strongly expressed in neural tissues beginning at e10.5, during which time NSCs are beginning to proliferate into various progenitor cell populations (Dubois et al., 2006). We performed immunofluorescence for LSD1 and CRE to detect protein levels in the neural tube at embryonic day 12.5 (e12.5). These data show that LSD1 is robustly expressed in most cell types in the neural tube at this time point, and there is a high degree of overlap of expression with CRE protein (Fig. 1A-G).

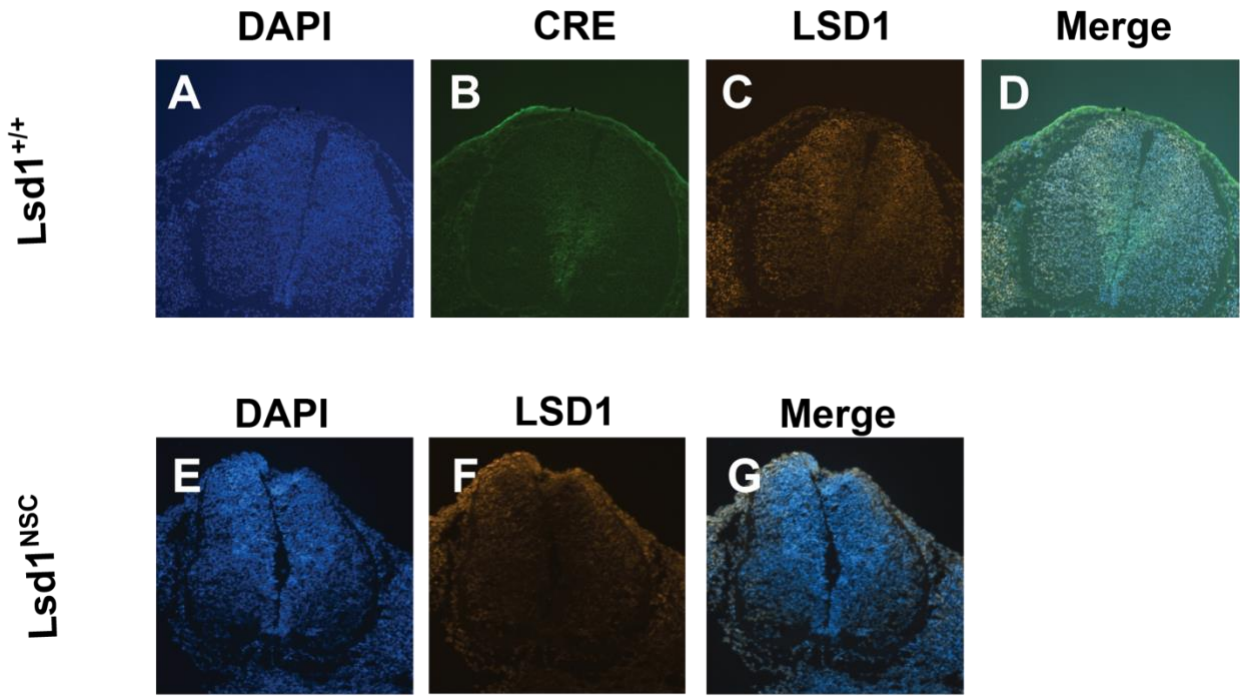

Figure 1. LSD1 is expressed in neural stem cells. Immunofluorescence at e12.5 of *Lsd1*$^{+/+}$ (A-D) and *Lsd*^{NSC} (E-G) embryos.

***Lsd1*$^{-/-}$ animals die postnatally with motor defects**

To determine whether there is a phenotype when *Lsd1* is deleted from NSCs, we conditionally deleted *Lsd1* with *Nestin Cre*, hereafter referred to as *Lsd1*^{NSC}mice. Controls were littermates of *Lsd1*^{NSC} animals that were *Cre*-, hereafter referred to as *Lsd1*^{NSC} controls. We first performed immunofluorescence at e12.5 to determine whether the expression of LSD1 in NSCs at e12.5 is specific. We found that there was a loss in LSD1 signal in *Lsd1*^{NSC} mutants, but not in *Lsd1*^{NSC} controls, suggesting that LSD1 is specifically expressed in NSCs (Fig. 1A-U).

Next, we observed the survival of *Lsd1*^{NSC} mutants compared to controls. *Lsd1*^{NSC} mutants were born at expected Mendelian ratios (data not shown), suggesting there was no embryonic lethality. In addition, *Lsd1* heterozygotes were observed at the expected frequency at weening. However, by postnatal day 21 (P21), there were zero viable *Lsd1*^{NSC} mutants observed, compared to the expected frequency of 15.8% (Fig. 2A). This indicates that 100% of *Lsd1*^{NSC} mutants died prior to weaning. Most of *Lsd1*^{NSC} animals died between 2-5 days postnatally, with a couple of animals surviving until 8-11 days.

To examine the cause of death, we observed *Lsd1*^{NSC} mutants after birth. *Lsd1*^{NSC} mutant animals had severely stunted growth compared to controls. Additionally, mutants appeared to show difficulty walking steadily, and engaged in stargazing, in which the pup's head points upward (Fig 2B, Supplemental Video 1). Taken together,

these data show that loss of LSD1 in NSCs results in stunted growth and gross motor defects prior to perinatal lethality.

A

	Expected Frequency	Actual Frequency
Cre+; +/+	15.8	12.7
Cre-; +/+	9.2	15.2
Cre+; fl/+	25.2	27.8
Cre-; fl/+	25.2	29.1
Cre+; fl/fl	15.8	0.0
Cre-; fl/fl	15.8	15.2

B

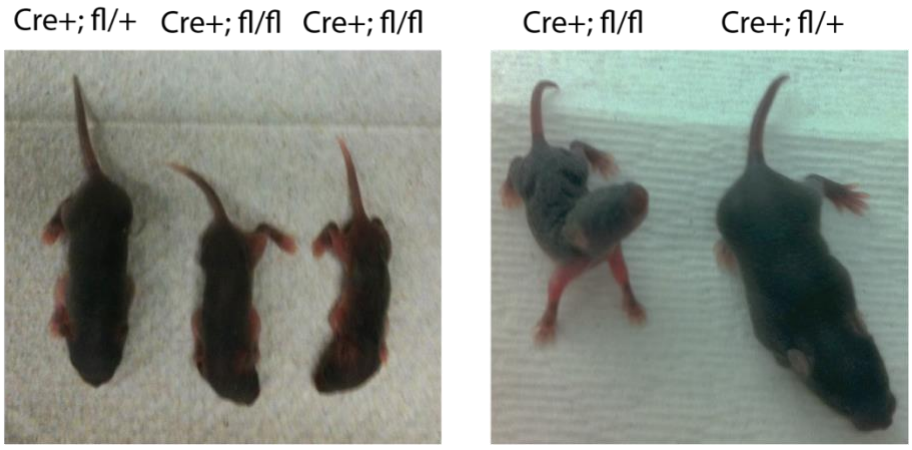

Figure 2. *Lsd1*^{NSC} animals do not survive past weaning and show stunted growth. A) Chi square calculations for expected frequencies versus actual frequencies of each possible genotype. B) Representative images of control and mutant littermates taken at the same time point in development.

Due to the gross motor phenotypes observed in *Lsd1*^{NSC} mutants, we wanted to test whether the differentiation of motor neurons embryonically was affected in *Lsd1*^{NSC} mutant embryos. To test this, we performed immunofluorescence at e12.5 and e14.5

using two markers of motor neuron differentiation: HB9 and Olig2. There did not appear to be a difference in the location or quantity of HB9- or Olig-2-positive neurons at those time points between mutants and controls, indicating that motor neuron specification was normal (Fig. 3A-P).

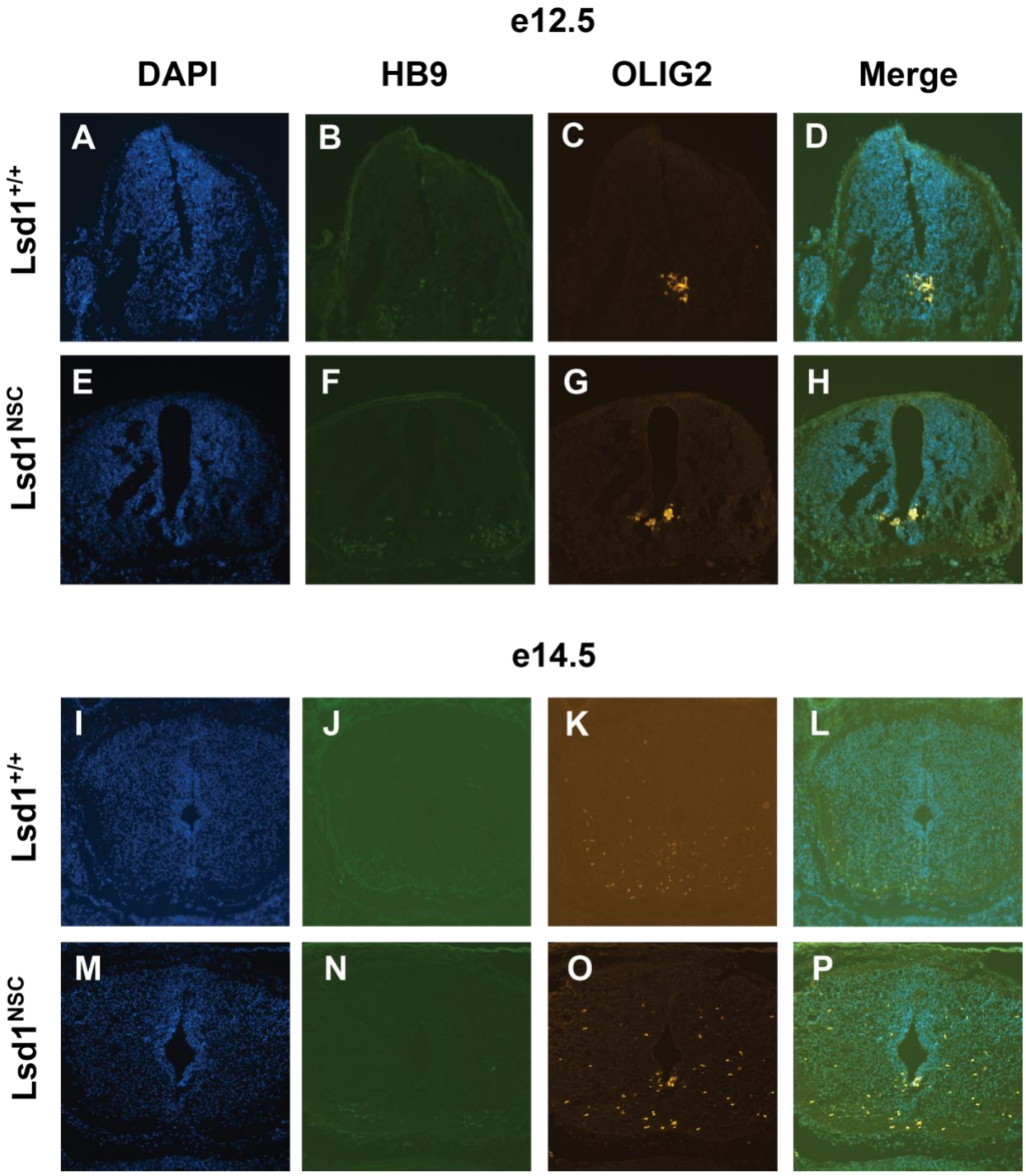

Figure 3. Differentiation of motor neurons in *Lsd1^{NSC}* animals do not appear to be affected. Immunofluorescence at e12.5 (A-H) and e14.5 (I-P) of *Lsd1$^{+/+}$* and *Lsd1^{NSC}* embryos.

Motor neurons differentiated from LSD1-deficient NSCs inappropriately express stem cell genes

To further investigate whether LSD1-deficient NSCs had defects when differentiating into motor neurons, we cultured iPSCs derived from *Lsd1^{NSC}* mutant animals *in vitro*. Motor neurons derived from *Lsd1^{NSC}* mutants appeared morphologically normal. However, motor neurons derived from LSD1-deficient NSCs continue to inappropriately express NSC genes. Normally cultured motor neurons either do not express or very weakly express two NSC proteins: SOX2 and NESTIN. However, upon loss of LSD1 in NSCs, differentiated motor neurons continued to robustly express SOX2 and NESTIN. This resulted in a significant increase in the percentage of nuclei scored as positive for these two NSC genes compared to controls (Fig. 4A-T).

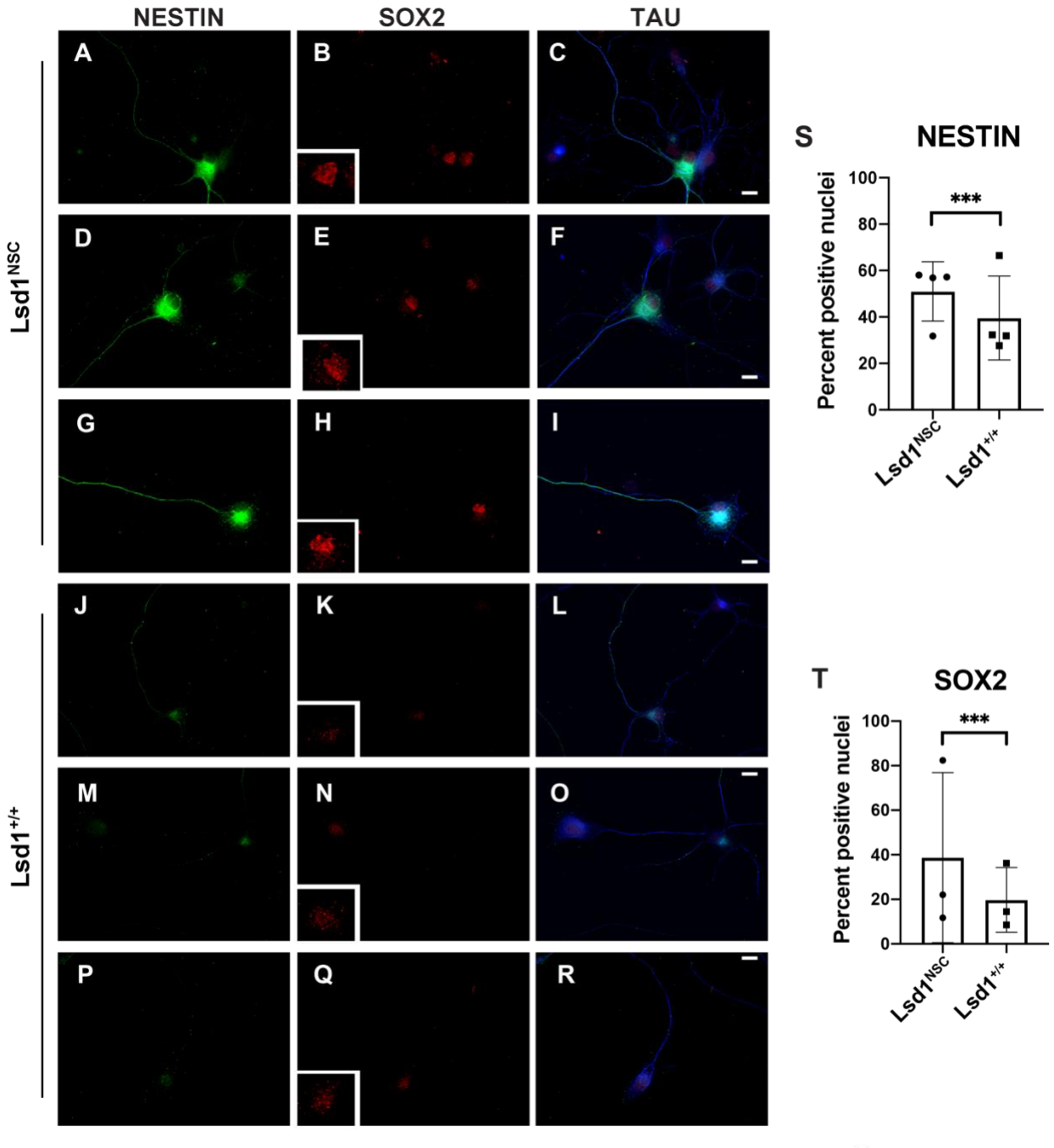

Figure 4. *Lsd1*^{NSC}-derived motor neurons inappropriately express stem cell genes. iPSCs were cultured and differentiated in to motor neurons from *Lsd1*$^{-/-}$ (A-I) and *Lsd1*$^{+/+}$ (J-R) animals, and immunofluorescence was performed. S-T) Quantification of percent positive nuclei for Nestin (S) and Sox2 (T) expression. *** = p<.001, p values calculated using an unpaired t test.

Postnatal *Lsd1^{NSC}* mutants show abnormal brain morphology *in vivo*

Postnatal *Lsd1^{NSC}* mutants have gross motor defects. To determine if defects in NSC differentiation give rise to overall defects in brain morphology, we performed hemotoxylin & eosin (H&E) staining on the brains of *Lsd1^{NSC}* animals that died perinatally. Several brain regions of *Lsd1^{NSC}* mutants looked disorganized compared to controls, including in the hippocampus and cerebellum (Fig. 5A-L). Additionally, the cerebellum of *Lsd1^{NSC}* mutants were smaller than controls when compared at the same magnification (Fig. 5A-D). At a higher magnification of 40X, the nuclei in the hippocampus and cerebellum of *Lsd1$^{-/-}$* mutants occasionally looked denser and pyknotic compared to controls (Fig. 5M-T).

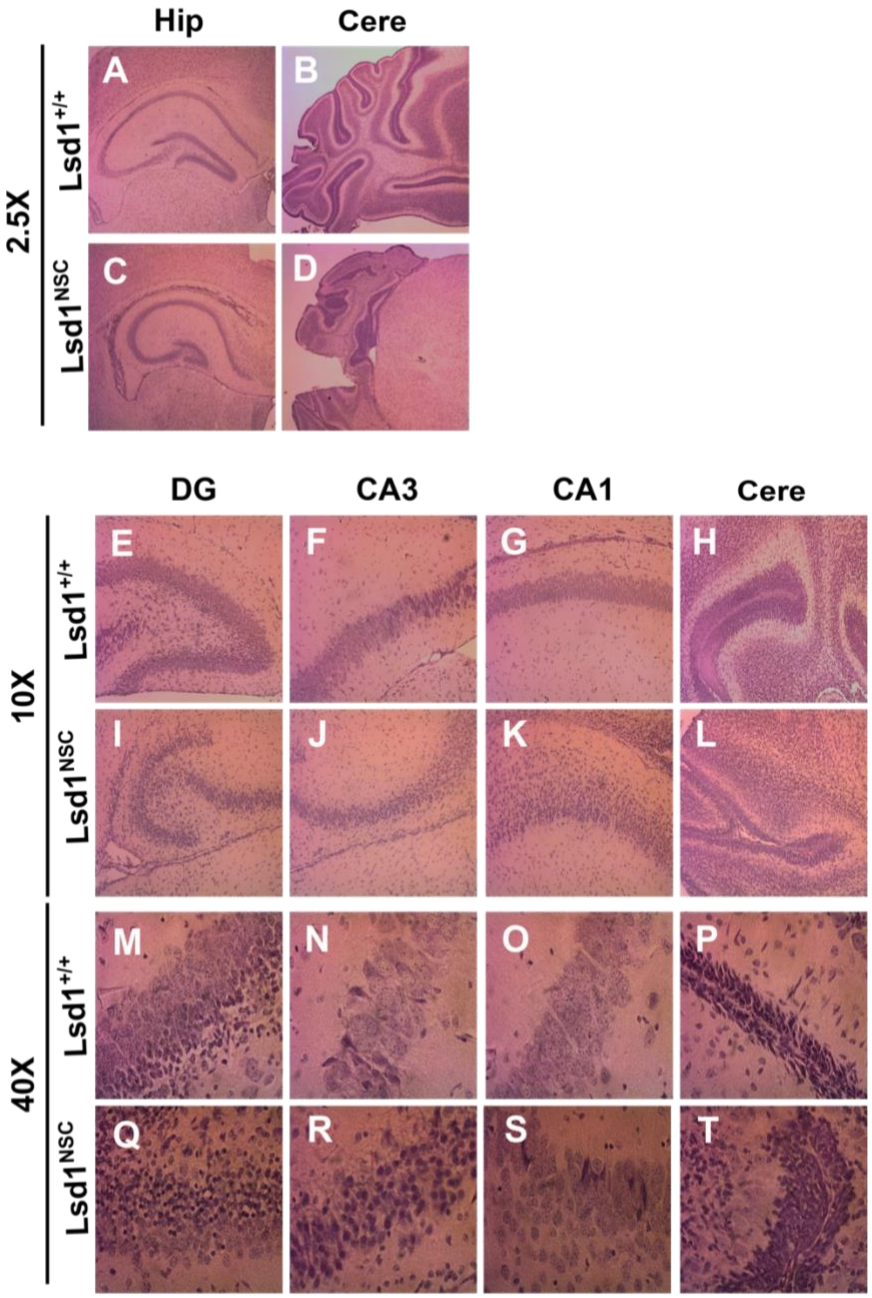

Figure 5. *Lsd*$^{NSC-}$ animals show brain morphology defects *in vivo*. H&E staining of *Lsd1*$^{+/+}$ and *Lsd1*$^{-/-}$ postnatal animals. DG= dentate gyrus, hip= hippocampus, cere= cerebellum.

Discussion

Our data show that LSD1 is expressed in embryonic NSCs. To determine whether LSD1 functions in NSC differentiation *in vivo* in mice, we conditionally deleted *Lsd1* in NSCs using *Nestin Cre.* We find that loss of LSD1 results in perinatal lethality with motor defects. This suggests that LSD1 is required for the proper establishment of the nervous system. Most of the $Lsd1^{NSC}$ animals survived beyond 24 hours and grew. This indicates that $Lsd1^{NSC}$ mutants can breathe and feed. However, $Lsd1^{NSC}$ animals have severely stunted growth, indicating a defect in obtaining proper nutrition.

To investigate the underlying causes of these phenotypes, we examined motor neuron differentiation *in vivo* and *in vitro*, along with brain morphology of the pups that died perinatally. We found that the normal number of motor neurons were established *in vivo*. However, when motor neurons were differentiated *in vitro*, we observed that NSC genes remained robustly expressed in the terminally differentiated motor neurons. This suggests that LSD1 is required for proper NSC differentiation. Previously, LSD1 has been shown to decommission enhancers at critical stem cell genes during mouse embryonic stem cell differentiation. Our data indicate that LSD1 may function similarly in NSC differentiation. Intriguingly, the failure to shut off the expression NSC genes did not prevent motor neurons from establishing normal morphology with elongated axons. This indicates that downregulation of the NSC program may be decoupled from establishment of the motor neuron program.

Ultimately, the brain morphology of $Lsd1^{NSC}$ pups was abnormal with the regions appearing smaller and containing pyknotic nuclei. These phenotypes occur despite the

normal number of motor neurons being properly specified and obtaining normal morphology *in vitro*. Based on these observations, we speculate that terminally differentiated neurons may be dying in *Lsd1*^{NSC} perinatal pups. If terminally differentiated neurons are dying, this may be due to the inability to down regulate the NSC program.

Taken together, we have shown that LSD1 is required in NSCs for survival and proper formation on the central nervous system. Similar to what has been shown in other stem cell populations, LSD1 may enable NSC differentiation by repressing the expression of critical genes associated with the undifferentiated cell fate.

Chapter 6:

A discussion on LSD1 and its role during developmental processes

Major findings

In summary, I have shown a novel role for LSD1 in neural stem cells and maternally in the oocyte. In NSCs *in vivo*, LSD1 is required to repress the stem cell program and for viability postnatally. This fits with the role that has been described for LSD1 in other stem cell populations (Haines et al., 2018; Kerenyi et al., 2013; Lambrot et al., 2015; Myrick et al., 2017; Tosic et al., 2018; Zhu et al., 2014). Previously, it was unknown which complex LSD1 was acting through maternally in the oocyte. Our work from both mouse and worm have demonstrated that LSD1 is partially dependent on CoREST for its maternal function. Finally, I have generated a hypomorphic allele of *Lsd1* that reduces its function *in vitro* and *in vivo*. I have shown that maternally hypomorphic LSD1 leads to perinatal lethality. This phenotype is modified by maternal age. Additionally, there are potential imprinting defects, as well as abnormal behavior that is only seen in certain genetic backgrounds.

Future experiments

My work establishes an exciting new model wherein H3K4 methylation is not completely erased between generations. This gives us a chance to test whether histone methylation can be inappropriately inherited between generations, and whether the phenotypes we observe are due to that ectopic H3K4 methylation. If this were the case, it would open the door to a new mechanism through which diseases may be inherited.

Instead of requiring a mutation, I believe that human disease could be occurring due to epigenetic reprogramming proteins in the oocyte that are slightly affected. Changes in protein levels are something that may be occurring naturally with age; LSD1 levels decrease in the oocyte with maternal age in mice (Shao et al., 2015). This, and a change in other epigenetic modifying proteins, could be a contributor to why the risk of having a child with neurodevelopmental disabilities increase with parental age (Newschaffer et al., 2007). A long-term direction of the lab could be to understand *why* LSD1 levels in the oocyte decrease with maternal age. Understanding the mechanism underlying this process could provide opportunities to intervene.

Due to the potential implications in humans, we are very interested in determining whether there is ectopic H3K4 methylation in maternally hypomorphic LSD1 mutants. To test this, ChIP sequencing will be performed on mutant and control blastocysts to determine whether there are changes in H3K4 methylation in mutants. These sequencing results can be compared to the RNA sequencing results to determine whether there is a corresponding change in gene expression at sites of ectopic methylation. Additionally, the RNA sequencing dataset from blastocysts can be compared to the maternal LSD1 null 2-cell arrested embryo dataset; the overlap in these datasets would give targets that continue to be misexpressed from post-fertilization to early embryogenesis. These putative targets would be a promising place to start in trying to determine what is underlying the lethality phenotype later on in development. Additionally, we know that the lethality phenotype is modified by maternal age. Therefore, we could perform these ChIP and RNA seq experiments on blastocysts

from early, middle, and late maternal age to see whether there is a correlation in severity of gene expression changes.

Prior work has shown that LSD1 homologs in worms, *spr-5* mutants, display increasing sterility across ~30 generations (Katz et al., 2009). Additionally, mutants for the H3K9 methyltransferase, *met-2*, also show sterility across many generations (Kerr et al., 2014). When *spr-5* and *met-2* mutants are combined, there is a synergistic phenotype of sterility within a single generation (Carpenter et al., 2021; Kerr et al., 2014). This suggests that SPR-5 and MET-2 are working together to reprogram the embryo. The next step is to determine whether this is also the case in mice. The orthologs of SPR-5 and MET-2 are LSD1 and SETDB1, respectively. A complete loss of either gene maternally results in similar phenotypes: early embryonic arrest (Eymery et al., 2016; Kim et al., 2016). This raises the possibility that these enzymes are also functioning together maternally in mammals. From my thesis work, we know that maternally hypomorphic LSD1 animals are able to bypass that lethality and make it out to birth, but many die perinatally. If LSD1 and SETDB1 are functioning together maternally in mammals, we might expect a reduction in SETDB1 to further exacerbate this phenotype, similar to what we have observed in *C. elegans*. This can be tested by making *Setdb1* heterozygous in the oocyte and looking at the phenotype of offspring. The potential interaction between LSD1 and SETDB1 maternally can also be tested by making both genes heterozygous exclusively in the mother's oocyte. I would predict either of these combinations would result in embryonic lethality. This would suggest that LSD1 and SETDB1 are functioning together maternally in mammals. I have almost finished generating these mutant combinations and expect to know the outcome soon.

Another exciting result has been that maternally hypomorphic mutants show some signs of imprinting defects. We chose to look at imprinted genes because imprinted loci are highly sensitive to epigenetic perturbations. Our discovery that theoretically perturbed H3K4 methylation in maternal LSD1 hypomorphic mutants led to changes in DNA methylation at the *Zac1* gene has implications for the relationship between histone methylation and DNA methylation. This could occur either directly due to H3K4 methylation blocking the *de novo* acquisition of DNA methylation via DNMT3A, or indirectly through the perturbation of proteins that regulate imprinted loci, such as STELLA. Regardless, these defects are very long lasting since perturbations at fertilization are conserved faithfully through millions of cell divisions into adulthood.

I propose that the epigenetic landscape is altered by the partial loss of function of maternal LSD1 post-fertilization, which causes downstream effects on DNA methylation. These defects are propagated in the early embryo and contribute to the phenotypes we see later on in development. Human mutations in *Lsd1* have been described as resulting in individuals with developmental delay, craniofacial defects, and abnormal behavior (Chong et al., 2016; Tunovic et al., 2014). However, their DNA methylation at imprinted genes has never been examined. It is possible that the mutations in LSD1 are also affecting DNA methylation in humans, and could be responsible for some of the phenotypes that are observed. Imprinting disorders in humans often lead to neurodevelopmental phenotypes, similar to what is described in *Lsd1* patients. For example, individuals with multi-locus imprinting disorders (MLID) have mutations that alter multiple imprinted gene clusters, and they often display neurodevelopmental phenotypes (Sanchez-Delgado et al., 2016). One known cause of MLID is variants of

Zfp57, which is a gene that was also altered in the 2-cell arrested embryo dataset from a complete maternal loss of *Lsd1* in mice (Sparago et al., 2019; Wasson et al., 2016). Therefore, testing the DNA methylation patterns at multiple loci in the human *Lsd1* mutation patients would help elucidate whether defective imprinting underlies some of the phenotypes that are observed.

Moving forward, we are very interested in determining whether imprinting is affected in certain tissues more than others. Therefore, we have acquired a GFP imprinting reporter mouse that tags the imprinted gene *Snrpn* with GFP (Figure 1A) (Stelzer et al., 2016). When the GFP allele is inherited maternally, we should be able to see GFP expression by tissue and even on a cell by cell basis. We have validated this method in our hands (Figure 1B-H). If we combine the GFP allele maternally with hypormorphic *Lsd1*, we may see changes in fluorescence if there are imprinting defects at that locus. Alternatively, if we bring in the GFP allele from the paternal side, we would expect in wild type mice that there would be no GFP expression in any cells, since *Snrpn* is silenced paternally (Figure 1I). Thus, in the mutant background, we may see a gain of GFP expression (Figure 1J). In this way, the tagged *Snrpn* allele will serve as a sort of lineage tracer, enabling us to tell which tissues or lineages are most susceptible to imprinting defects, as well as how consistent these defects are between replicates.

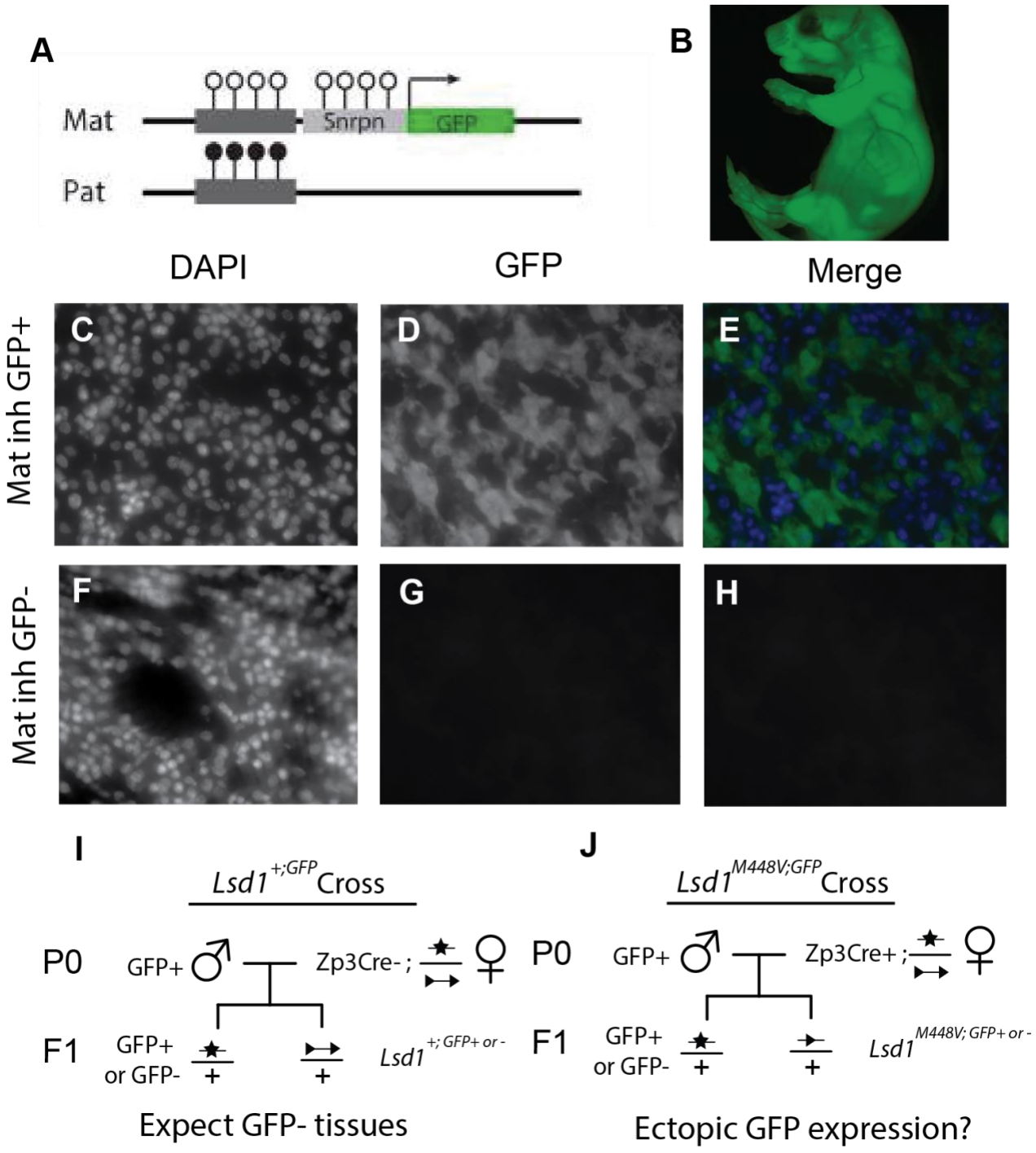

Figure 1. Schematic of GFP imprinting reporter mice (A) Expression of the GFP tagged allele with maternal inheritance and wild type genomic imprinting. Closed circles signify methylation and open circles signify a lack of methylation. (B) GFP expression

from whole pup that had maternally inherited GFP allele (C-E) DAPI (C), GFP (D) and Merge (E) immunofluorescence imaging for mouse tissue with maternally inherited GFP. (F-H) DAPI (F), GFP (G) and Merge (H) immunofluorescence imaging for mouse tissue with GFP negative maternally inherited allele. (I) Genetic cross showing wild-type *Lsd1* (+), loxP sites (triangles), and M448V alleles (star). In the P0 *Lsd1*$^{+;GFP}$ cross, mothers are *Zp3Cre*-, contributing one wild-type and one hypomorphic *Lsd1* allele maternally, while fathers provide GFP tagged allele (J) In the P0 *Lsd1* $^{M448V;GFP}$ cross, mothers are *Zp3Cre*+, contributing only the hypomorphic *Lsd1* allele maternally. Fathers provide GFP tagged allele.

The novel *Lsd1* hypomorphic allele I generated was used to specifically interrogate the function of LSD1 in the oocyte. However, using this allele, there are now opportunities to make LSD1 hypormorphic in essentially any cell type that has a specific *Cre*. I am particularly excited about the possibility of making LSD1 hypomorphic in NSCs; I have shown that completely removing LSD1 from NSCs leads to lethality prior to weaning. It is possible that making LSD1 hypomorphic in NSCs will allow animals to bypass that lethality and make it out to adulthood. From there, many behavioral phenotypes could be assessed. In addition, we could determine whether partial loss of LSD1 in NSCs may phenocopy any of the defects observed in the corresponding human patients, including repetitive behavior or intellectual disability.

Implications in humans

We have shown that having partial LSD1 function in the oocyte can lead to long term phenotypic defects in offspring. One of the reasons we made that partial function allele was to mimic having a partial loss of protein quantity, an event that occurred very rarely in our past experiments using the leaky *Vasa-Cre*. We wanted to see whether partial LSD1 function in the oocyte would mimic the phenotypes we saw when there was a partial loss of the amount of the protein. These phenotypes included perinatal lethality, abnormal behavior, and imprinting defects. Excitingly, we were able to confirm these phenotypes in our partial function mutants. Taken together, this indicates that the amount of LSD1 deposited in the oocyte could have implications for the health of the offspring in humans. Additionally, in mice it has been shown that LSD1 protein levels decrease with maternal age (Shao et al., 2015), which is something that may also be occurring in humans. This information could be important when considering assisted reproductive technologies such as in vitro fertilization (IVF). Given a pool of potential oocytes to be fertilized, one could choose the oocytes with the highest levels of LSD1, and other important epigenetic reprogramming enzymes, to give the embryo the best chance of developing normally.

In both worms and mouse, we have shown that LSD1 is partially dependent on CoREST to perform its reprogramming function at fertilization. In mouse, a mutation in the CoREST binding site of LSD1 phenocopies a partial loss of LSD1 protein. This suggests that human mutations in CoREST may also phenocopy LSD1 mutations. There are not currently any mutations in CoREST that have been described, but if it is added to genetic screening panels, we may be able to identify novel CoREST mutations that could contribute to abnormal development or neurodevelopmental phenotypes.

A model for maternal LSD1 and maternal age

I have shown that hypomorphic maternal LSD1 causes phenotypes such as perinatal lethality, abnormal behavior, and defective imprinting. The severity of the perinatal lethality phenotype is modified by maternal age. Taken together, I propose a model in which LSD1 levels are affected by maternal age (Figure 2). While it is known that LSD1 decreases with maternal age, I propose that at a young maternal age LSD1 may be decreased as well. This would be relatively straight forward to test. While I have not tested the imprinting or behavioral defects at various maternal ages, I propose that those would increase in severity as well. This model is consistent with data in humans that show that both younger and advanced parental age confer a higher risk of having a child with neurodevelopmental disabilities (Newschaffer et al., 2007). Additionally, it could explain why some human mutations in LSD1 do not display any phenotypes; it may require a 'second hit' to reduce LSD1 function enough at the critical reprogramming step, which could be through maternal age, genetic background, or other environmental factors.

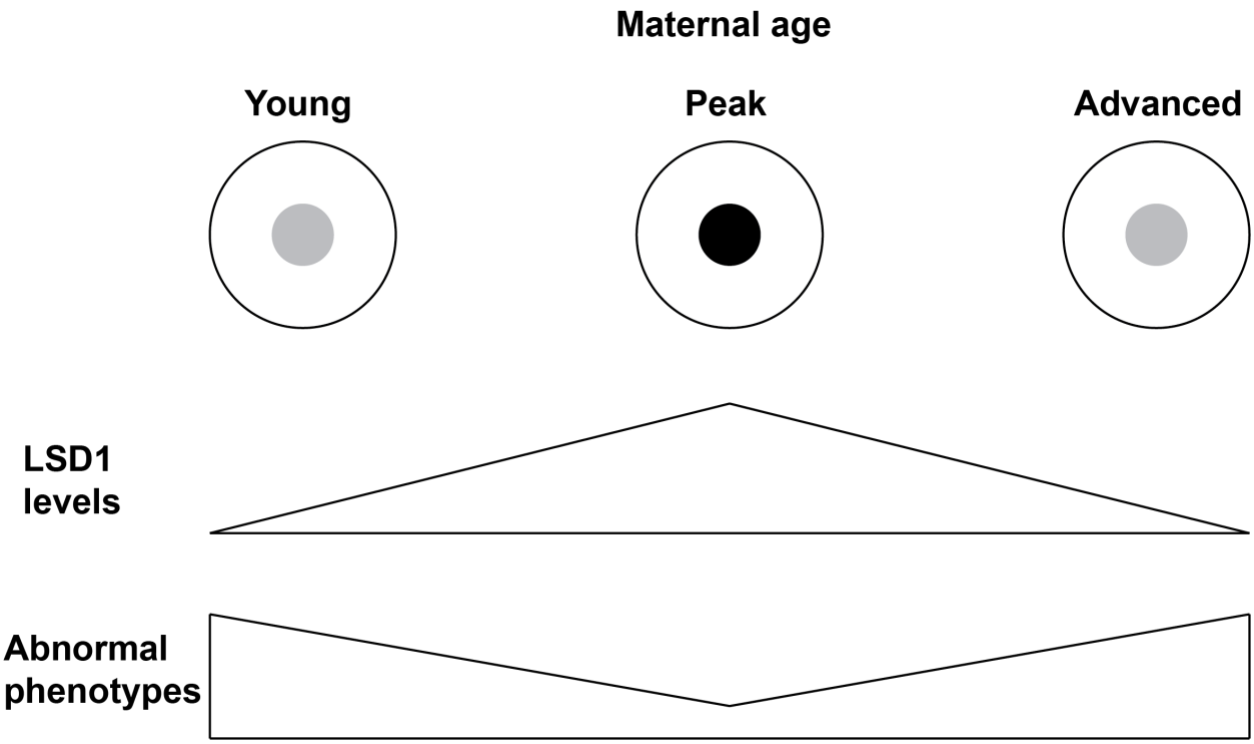

Figure 2. A model for the relationship between LSD1 and maternal age. I propose that LSD1 levels are lowest in the oocyte at young and advanced maternal ages, which is anticorrelated with the chances of having abnormal phenotypes in offspring.

References

Amente, S., Lania, L., & Majello, B. (2013). The histone LSD1 demethylase in stemness and cancer transcription programs. *Biochim Biophys Acta*, *1829*(10), 981-986. https://doi.org/10.1016/j.bbagrm.2013.05.002

Ancelin, K., Syx, L., Borensztein, M., Ranisavljevic, N., Vassilev, I., Briseno-Roa, L., Liu, T., Metzger, E., Servant, N., Barillot, E., Chen, C. J., Schule, R., & Heard, E. (2016). Maternal LSD1/KDM1A is an essential regulator of chromatin and transcription landscapes during zygotic genome activation. *Elife*, *5*. https://doi.org/10.7554/eLife.08851

Andersen, E. C., & Horvitz, H. R. (2007). Two C. elegans histone methyltransferases repress lin-3 EGF transcription to inhibit vulval development. *Development*, *134*(16), 2991-2999. https://doi.org/10.1242/dev.009373

Andreu-Vieyra, C. V., Chen, R., Agno, J. E., Glaser, S., Anastassiadis, K., Stewart, A. F., & Matzuk, M. M. (2010). MLL2 is required in oocytes for bulk histone 3 lysine 4 trimethylation and transcriptional silencing. *PLoS Biol*, *8*(8). https://doi.org/10.1371/journal.pbio.1000453

Arnaud, M., Barat-Houari, M., Gatinois, V., Sanchez, E., Lyonnet, S., Touitou, I., & Geneviève, D. (2015). [Kabuki syndrome: Update and review]. *Arch Pediatr*, *22*(6), 653-660. https://doi.org/10.1016/j.arcped.2015.03.020 (Le syndrome Kabuki : mise au point et revue de la littérature.)

Au Yeung, W. K., Brind'Amour, J., Hatano, Y., Yamagata, K., Feil, R., Lorincz, M. C., Tachibana, M., Shinkai, Y., & Sasaki, H. (2019). Histone H3K9 Methyltransferase G9a in Oocytes Is Essential for Preimplantation Development but Dispensable for CG Methylation Protection. *Cell Rep*, *27*(1), 282-293.e284. https://doi.org/10.1016/j.celrep.2019.03.002

Bannister, A. J., Schneider, R., Myers, F. A., Thorne, A. W., Crane-Robinson, C., & Kouzarides, T. (2005). Spatial distribution of di- and tri-methyl lysine 36 of histone H3 at active genes. *J Biol Chem*, *280*(18), 17732-17736. https://doi.org/10.1074/jbc.M500796200

Barski, A., Cuddapah, S., Cui, K., Roh, T. Y., Schones, D. E., Wang, Z., Wei, G., Chepelev, I., & Zhao, K. (2007). High-resolution profiling of histone methylations in the human genome. *Cell*, *129*(4), 823-837. https://doi.org/10.1016/j.cell.2007.05.009

Bartolomei, M. S. (2009). Genomic imprinting: employing and avoiding epigenetic processes. *Genes Dev*, *23*(18), 2124-2133. https://doi.org/10.1101/gad.1841409

Baujat, G., & Cormier-Daire, V. (2007). Sotos syndrome. *Orphanet J Rare Dis*, *2*, 36. https://doi.org/10.1186/1750-1172-2-36

Benayoun, B. A., Pollina, E. A., Ucar, D., Mahmoudi, S., Karra, K., Wong, E. D., Devarajan, K., Daugherty, A. C., Kundaje, A. B., Mancini, E., Hitz, B. C., Gupta, R., Rando, T. A., Baker, J. C., Snyder, M. P., Cherry, J. M., & Brunet, A. (2014). H3K4me3 breadth is linked to cell identity and transcriptional consistency. *Cell*, *158*(3), 673-688. https://doi.org/10.1016/j.cell.2014.06.027

Berger, S. L., Kouzarides, T., Shiekhattar, R., & Shilatifard, A. (2009). An operational definition of epigenetics. *Genes Dev*, *23*(7), 781-783. https://doi.org/10.1101/gad.1787609

Berndsen, C. E., & Denu, J. M. (2008). Catalysis and substrate selection by histone/protein lysine acetyltransferases. *Curr Opin Struct Biol*, *18*(6), 682-689. https://doi.org/10.1016/j.sbi.2008.11.004

Bernstein, B. E., Humphrey, E. L., Erlich, R. L., Schneider, R., Bouman, P., Liu, J. S., Kouzarides, T., & Schreiber, S. L. (2002). Methylation of histone H3 Lys 4 in coding regions of active genes. *Proc Natl Acad Sci U S A*, *99*(13), 8695-8700. https://doi.org/10.1073/pnas.082249499

Bernstein, B. E., Kamal, M., Lindblad-Toh, K., Bekiranov, S., Bailey, D. K., Huebert, D. J., McMahon, S., Karlsson, E. K., Kulbokas, E. J., 3rd, Gingeras, T. R., Schreiber, S. L., & Lander, E. S. (2005). Genomic maps and comparative analysis of histone modifications in human and mouse. *Cell*, *120*(2), 169-181. https://doi.org/10.1016/j.cell.2005.01.001

Brykczynska, U., Hisano, M., Erkek, S., Ramos, L., Oakeley, E. J., Roloff, T. C., Beisel, C., Schubeler, D., Stadler, M. B., & Peters, A. H. (2010). Repressive and active histone methylation mark distinct promoters in human and mouse spermatozoa. *Nat Struct Mol Biol*, *17*(6), 679-687. https://doi.org/10.1038/nsmb.1821

Burton, A., & Torres-Padilla, M. E. (2014). Chromatin dynamics in the regulation of cell fate allocation during early embryogenesis. *Nat Rev Mol Cell Biol*, *15*(11), 723-734. https://doi.org/10.1038/nrm3885

Carpenter, B. S., Lee, T. W., Plott, C. F., Rodriguez, J. D., Brockett, J. S., Myrick, D. A., & Katz, D. J. (2021). Caenorhabditis elegans establishes germline versus soma by balancing inherited histone methylation. *Development*, *148*(3). https://doi.org/10.1242/dev.196600

Chen, Y., Yang, Y., Wang, F., Wan, K., Yamane, K., Zhang, Y., & Lei, M. (2006). Crystal structure of human histone lysine-specific demethylase 1 (LSD1). *Proc Natl Acad Sci U S A*, *103*(38), 13956-13961. https://doi.org/10.1073/pnas.0606381103

Chong, J. X., Yu, J. H., Lorentzen, P., Park, K. M., Jamal, S. M., Tabor, H. K., Rauch, A., Saenz, M. S., Boltshauser, E., Patterson, K. E., Nickerson, D. A., & Bamshad, M. J. (2016). Gene discovery for Mendelian conditions via social networking: de novo variants in KDM1A cause developmental delay and distinctive facial features. *Genet Med*, *18*(8), 788-795. https://doi.org/10.1038/gim.2015.161

Ciccone, D. N., Su, H., Hevi, S., Gay, F., Lei, H., Bajko, J., Xu, G., Li, E., & Chen, T. (2009). KDM1B is a histone H3K4 demethylase required to establish maternal genomic imprints. *Nature*, *461*(7262), 415-418. https://doi.org/10.1038/nature08315

Coleman, R. T., & Struhl, G. (2017). Causal role for inheritance of H3K27me3 in maintaining the OFF state of a Drosophila HOX gene. *Science*, *356*(6333). https://doi.org/10.1126/science.aai8236

Dawlaty, M. M., Breiling, A., Le, T., Raddatz, G., Barrasa, M. I., Cheng, A. W., Gao, Q., Powell, B. E., Li, Z., Xu, M., Faull, K. F., Lyko, F., & Jaenisch, R. (2013). Combined deficiency of Tet1 and Tet2 causes epigenetic abnormalities but is compatible with postnatal development. *Dev Cell*, *24*(3), 310-323. https://doi.org/10.1016/j.devcel.2012.12.015

Domanitskaya, E., & Schüpbach, T. (2012). CoREST acts as a positive regulator of Notch signaling in the follicle cells of Drosophila melanogaster. *Journal of cell science*, *125*(Pt 2), 399-410. https://doi.org/10.1242/jcs.089797

Du, J., Johnson, L. M., Jacobsen, S. E., & Patel, D. J. (2015). DNA methylation pathways and their crosstalk with histone methylation. *Nat Rev Mol Cell Biol*, *16*(9), 519-532. https://doi.org/10.1038/nrm4043

Dubois, N. C., Hofmann, D., Kaloulis, K., Bishop, J. M., & Trumpp, A. (2006). Nestin-Cre transgenic mouse line Nes-Cre1 mediates highly efficient Cre/loxP mediated

recombination in the nervous system, kidney, and somite-derived tissues. *Genesis*, *44*(8), 355-360. https://doi.org/10.1002/dvg.20226

Eimer, S., Lakowski, B., Donhauser, R., & Baumeister, R. (2002). Loss of spr-5 bypasses the requirement for the C.elegans presenilin sel-12 by derepressing hop-1. *EMBO J*, *21*(21), 5787-5796. https://doi.org/10.1093/emboj/cdf561

Eliazer, S., Shalaby, N. A., & Buszczak, M. (2011). Loss of lysine-specific demethylase 1 nonautonomously causes stem cell tumors in the Drosophila ovary. *Proc Natl Acad Sci U S A*, *108*(17), 7064-7069. https://doi.org/10.1073/pnas.1015874108

Engstrom, A. K., Walker, A. C., Moudgal, R. A., Myrick, D. A., Kyle, S. M., Bai, Y., Rowley, M. J., & Katz, D. J. (2020). The inhibition of LSD1 via sequestration contributes to tau-mediated neurodegeneration. *Proc Natl Acad Sci U S A*, *117*(46), 29133-29143. https://doi.org/10.1073/pnas.2013552117

Eymery, A., Liu, Z., Ozonov, E. A., Stadler, M. B., & Peters, A. H. (2016). The methyltransferase Setdb1 is essential for meiosis and mitosis in mouse oocytes and early embryos. *Development*, *143*(15), 2767-2779. https://doi.org/10.1242/dev.132746

Fallini, C., Bassell, G. J., & Rossoll, W. (2010). High-efficiency transfection of cultured primary motor neurons to study protein localization, trafficking, and function. *Mol Neurodegener*, *5*, 17. https://doi.org/10.1186/1750-1326-5-17

Fallini, C., Zhang, H., Su, Y., Silani, V., Singer, R. H., Rossoll, W., & Bassell, G. J. (2011). The survival of motor neuron (SMN) protein interacts with the mRNA-binding protein HuD and regulates localization of poly(A) mRNA in primary motor neuron axons. *J Neurosci*, *31*(10), 3914-3925. https://doi.org/10.1523/JNEUROSCI.3631-10.2011

Forneris, F., Binda, C., Adamo, A., Battaglioli, E., & Mattevi, A. (2007). Structural basis of LSD1-CoREST selectivity in histone H3 recognition. *J Biol Chem*, *282*(28), 20070-20074. https://doi.org/10.1074/jbc.C700100200

Foster, C. T., Dovey, O. M., Lezina, L., Luo, J. L., Gant, T. W., Barlev, N., Bradley, A., & Cowley, S. M. (2010). Lysine-specific demethylase 1 regulates the embryonic transcriptome and CoREST stability. *Mol Cell Biol*, *30*(20), 4851-4863. https://doi.org/10.1128/MCB.00521-10

Furuhashi, H., Takasaki, T., Rechtsteiner, A., Li, T., Kimura, H., Checchi, P. M., Strome, S., & Kelly, W. G. (2010). Trans-generational epigenetic regulation of C. elegans primordial germ cells. *Epigenetics Chromatin*, *3*(1), 15. https://doi.org/10.1186/1756-8935-3-15

Gaydos, L. J., Wang, W., & Strome, S. (2014). Gene repression. H3K27me and PRC2 transmit a memory of repression across generations and during development. *Science*, *345*(6203), 1515-1518. https://doi.org/10.1126/science.1255023

Greenberg, M. V. C., & Bourc'his, D. (2019). The diverse roles of DNA methylation in mammalian development and disease. *Nat Rev Mol Cell Biol*, *20*(10), 590-607. https://doi.org/10.1038/s41580-019-0159-6

Greer, E. L., Beese-Sims, S. E., Brookes, E., Spadafora, R., Zhu, Y., Rothbart, S. B., Aristizabal-Corrales, D., Chen, S., Badeaux, A. I., Jin, Q., Wang, W., Strahl, B. D., Colaiacovo, M. P., & Shi, Y. (2014). A histone methylation network regulates transgenerational epigenetic memory in C. elegans. *Cell Rep*, *7*(1), 113-126. https://doi.org/10.1016/j.celrep.2014.02.044

Greer, E. L., Maures, T. J., Hauswirth, A. G., Green, E. M., Leeman, D. S., Maro, G. S., Han, S., Banko, M. R., Gozani, O., & Brunet, A. (2010). Members of the H3K4 trimethylation complex regulate lifespan in a germline-dependent manner in C. elegans. *Nature*, *466*(7304), 383-387. https://doi.org/10.1038/nature09195

Gu, T. P., Guo, F., Yang, H., Wu, H. P., Xu, G. F., Liu, W., Xie, Z. G., Shi, L., He, X., Jin, S. G., Iqbal, K., Shi, Y. G., Deng, Z., Szabo, P. E., Pfeifer, G. P., Li, J., & Xu, G. L. (2011). The role of Tet3 DNA dioxygenase in epigenetic reprogramming by oocytes. *Nature*, *477*(7366), 606-610. https://doi.org/10.1038/nature10443

Gurdon, J. B., Elsdale, T. R., & Fischberg, M. (1958). Sexually mature individuals of Xenopus laevis from the transplantation of single somatic nuclei. *Nature*, *182*(4627), 64-65. https://doi.org/10.1038/182064a0

Haines, R. R., Barwick, B. G., Scharer, C. D., Majumder, P., Randall, T. D., & Boss, J. M. (2018). The Histone Demethylase LSD1 Regulates B Cell Proliferation and Plasmablast Differentiation. *J Immunol*, *201*(9), 2799-2811. https://doi.org/10.4049/jimmunol.1800952

Hakimi, M. A., Dong, Y., Lane, W. S., Speicher, D. W., & Shiekhattar, R. (2003). A candidate X-linked mental retardation gene is a component of a new family of histone deacetylase-containing complexes. *J Biol Chem*, *278*(9), 7234-7239. https://doi.org/10.1074/jbc.M208992200

Hammoud, S. S., Nix, D. A., Zhang, H., Purwar, J., Carrell, D. T., & Cairns, B. R. (2009). Distinctive chromatin in human sperm packages genes for embryo development. *Nature*, *460*(7254), 473-478. https://doi.org/10.1038/nature08162

Heintzman, N. D., Stuart, R. K., Hon, G., Fu, Y., Ching, C. W., Hawkins, R. D., Barrera, L. O., Van Calcar, S., Qu, C., Ching, K. A., Wang, W., Weng, Z., Green, R. D., Crawford, G. E., & Ren, B. (2007). Distinct and predictive chromatin signatures of transcriptional promoters and enhancers in the human genome. *Nat Genet*, *39*(3), 311-318. https://doi.org/10.1038/ng1966

Hemberger, M., Dean, W., & Reik, W. (2009). Epigenetic dynamics of stem cells and cell lineage commitment: digging Waddington's canal. *Nat Rev Mol Cell Biol*, *10*(8), 526-537. https://doi.org/10.1038/nrm2727

Howell, C. Y., Bestor, T. H., Ding, F., Latham, K. E., Mertineit, C., Trasler, J. M., & Chaillet, J. R. (2001). Genomic imprinting disrupted by a maternal effect mutation in the Dnmt1 gene. *Cell*, *104*(6), 829-838. https://doi.org/10.1016/s0092-8674(01)00280-x

Humphrey, G. W., Wang, Y., Russanova, V. R., Hirai, T., Qin, J., Nakatani, Y., & Howard, B. H. (2001). Stable histone deacetylase complexes distinguished by the presence of SANT domain proteins CoREST/kiaa0071 and Mta-L1. *J Biol Chem*, *276*(9), 6817-6824. https://doi.org/10.1074/jbc.M007372200

Hyun, K., Jeon, J., Park, K., & Kim, J. (2017). Writing, erasing and reading histone lysine methylations. *Exp Mol Med*, *49*(4), e324. https://doi.org/10.1038/emm.2017.11

Jin, L., Hanigan, C. L., Wu, Y., Wang, W., Park, B. H., Woster, P. M., & Casero, R. A. (2013). Loss of LSD1 (lysine-specific demethylase 1) suppresses growth and alters gene expression of human colon cancer cells in a p53- and DNMT1(DNA methyltransferase 1)-independent manner. *Biochem J*, *449*(2), 459-468. https://doi.org/10.1042/BJ20121360

Jukam, D., Shariati, S. A. M., & Skotheim, J. M. (2017). Zygotic Genome Activation in Vertebrates. *Dev Cell*, *42*(4), 316-332. https://doi.org/10.1016/j.devcel.2017.07.026

Kaneshiro, K. R., Rechtsteiner, A., & Strome, S. (2019). Sperm-inherited H3K27me3 impacts offspring transcription and development in C. elegans. *Nat Commun*, *10*(1), 1271. https://doi.org/10.1038/s41467-019-09141-w

Katz, D. J., Edwards, T. M., Reinke, V., & Kelly, W. G. (2009). A C. elegans LSD1 demethylase contributes to germline immortality by reprogramming epigenetic memory. *Cell*, *137*(2), 308-320. https://doi.org/10.1016/j.cell.2009.02.015

Kawakami, M., & Yamamura, K.-I. (2008). Cranial bone morphometric study among mouse strains. *BMC evolutionary biology*, *8*, 73-73. https://doi.org/10.1186/1471-2148-8-73

Kerenyi, M. A., Shao, Z., Hsu, Y. J., Guo, G., Luc, S., O'Brien, K., Fujiwara, Y., Peng, C., Nguyen, M., & Orkin, S. H. (2013). Histone demethylase Lsd1 represses hematopoietic stem and progenitor cell signatures during blood cell maturation. *Elife*, *2*, e00633. https://doi.org/10.7554/eLife.00633

Kerr, S. C., Ruppersburg, C. C., Francis, J. W., & Katz, D. J. (2014). SPR-5 and MET-2 function cooperatively to reestablish an epigenetic ground state during passage through the germ line. *Proc Natl Acad Sci U S A*, *111*(26), 9509-9514. https://doi.org/10.1073/pnas.1321843111

Kim, H. M., Beese-Sims, S. E., & Colaiacovo, M. P. (2018). Fanconi Anemia FANCM/FNCM-1 and FANCD2/FCD-2 Are Required for Maintaining Histone Methylation Levels and Interact with the Histone Demethylase LSD1/SPR-5 in Caenorhabditis elegans. *Genetics*, *209*(2), 409-423. https://doi.org/10.1534/genetics.118.300823

Kim, J., Singh, A. K., Takata, Y., Lin, K., Shen, J., Lu, Y., Kerenyi, M. A., Orkin, S. H., & Chen, T. (2015). LSD1 is essential for oocyte meiotic progression by regulating CDC25B expression in mice. *Nat Commun*, *6*, 10116. https://doi.org/10.1038/ncomms10116

Kim, J., Zhao, H., Dan, J., Kim, S., Hardikar, S., Hollowell, D., Lin, K., Lu, Y., Takata, Y., Shen, J., & Chen, T. (2016). Maternal Setdb1 Is Required for Meiotic Progression and Preimplantation Development in Mouse. *PLoS Genet*, *12*(4), e1005970. https://doi.org/10.1371/journal.pgen.1005970

Kubota, T., Miyake, K., & Hirasawa, T. (2013). Epigenetics in Neurodevelopmental and Mental Disorders. *Medical Epigenetics*, *1*(1), 52-59. https://doi.org/10.1159/000354718

Lambrot, R., Lafleur, C., & Kimmins, S. (2015). The histone demethylase KDM1A is essential for the maintenance and differentiation of spermatogonial stem cells and progenitors. *FASEB J*, *29*(11), 4402-4416. https://doi.org/10.1096/fj.14-267328

Lee, M.-C., & Spradling, A. C. (2014). The progenitor state is maintained by lysine-specific demethylase 1-mediated epigenetic plasticity during Drosophila follicle cell development. *Genes & development*, *28*(24), 2739-2749. https://doi.org/10.1101/gad.252692.114

Lee, T. W., David, H. S., Engstrom, A. K., Carpenter, B. S., & Katz, D. J. (2019). Repressive H3K9me2 protects lifespan against the transgenerational burden of COMPASS activity in C. elegans. *Elife*, *8*. https://doi.org/10.7554/eLife.48498

Lee, T. W., & Katz, D. J. (2020). Hansel, Gretel, and the Consequences of Failing to Remove Histone Methylation Breadcrumbs. *Trends Genet*, *36*(3), 160-176. https://doi.org/10.1016/j.tig.2019.12.004

Li, E. (2002). Chromatin modification and epigenetic reprogramming in mammalian development. *Nat Rev Genet*, *3*(9), 662-673. https://doi.org/10.1038/nrg887

Li, X., Ito, M., Zhou, F., Youngson, N., Zuo, X., Leder, P., & Ferguson-Smith, A. C. (2008). A maternal-zygotic effect gene, Zfp57, maintains both maternal and paternal imprints. *Dev Cell*, *15*(4), 547-557. https://doi.org/10.1016/j.devcel.2008.08.014

Li, X. Y., Thomas, S., Sabo, P. J., Eisen, M. B., Stamatoyannopoulos, J. A., & Biggin, M. D. (2011). The role of chromatin accessibility in directing the widespread, overlapping patterns of Drosophila transcription factor binding. *Genome Biol*, *12*(4), R34. https://doi.org/10.1186/gb-2011-12-4-r34

Ma, P., Pan, H., Montgomery, R. L., Olson, E. N., & Schultz, R. M. (2012). Compensatory functions of histone deacetylase 1 (HDAC1) and HDAC2 regulate transcription and apoptosis during mouse oocyte development. *Proc Natl Acad Sci U S A*, *109*(8), E481-489. https://doi.org/10.1073/pnas.1118403109

Macinkovic, I., Theofel, I., Hundertmark, T., Kovac, K., Awe, S., Lenz, J., Forne, I., Lamp, B., Nist, A., Imhof, A., Stiewe, T., Renkawitz-Pohl, R., Rathke, C., & Brehm, A. (2019). Distinct CoREST complexes act in a cell-type-specific manner. *Nucleic Acids Res*, *47*(22), 11649-11666. https://doi.org/10.1093/nar/gkz1050

Maiques-Diaz, A., & Somervaille, T. C. (2016). LSD1: biologic roles and therapeutic targeting. *Epigenomics*, *8*(8), 1103-1116. https://doi.org/10.2217/epi-2016-0009

Mayer, W., Niveleau, A., Walter, J., Fundele, R., & Haaf, T. (2000). Demethylation of the zygotic paternal genome. *Nature*, *403*(6769), 501-502. https://doi.org/10.1038/35000656

Meijering, E., Jacob, M., Sarria, J. C., Steiner, P., Hirling, H., & Unser, M. (2004). Design and validation of a tool for neurite tracing and analysis in fluorescence microscopy images. *Cytometry A*, *58*(2), 167-176. https://doi.org/10.1002/cyto.a.20022

Messerschmidt, D. M., de Vries, W., Ito, M., Solter, D., Ferguson-Smith, A., & Knowles, B. B. (2012). Trim28 is required for epigenetic stability during mouse oocyte to embryo transition. *Science*, *335*(6075), 1499-1502. https://doi.org/10.1126/science.1216154

Mito, Y., Henikoff, J. G., & Henikoff, S. (2005). Genome-scale profiling of histone H3.3 replacement patterns. *Nat Genet*, *37*(10), 1090-1097. https://doi.org/10.1038/ng1637

Moehrle, A., & Paro, R. (1994). Spreading the silence: epigenetic transcriptional regulation during Drosophila development. *Dev Genet*, *15*(6), 478-484. https://doi.org/10.1002/dvg.1020150606

Morgan, H. D., Santos, F., Green, K., Dean, W., & Reik, W. (2005). Epigenetic reprogramming in mammals. *Hum Mol Genet*, *14 Spec No 1*, R47-58. https://doi.org/10.1093/hmg/ddi114

Mozzetta, C., Boyarchuk, E., Pontis, J., & Ait-Si-Ali, S. (2015). Sound of silence: the properties and functions of repressive Lys methyltransferases. *Nat Rev Mol Cell Biol*, *16*(8), 499-513. https://doi.org/10.1038/nrm4029

Muramoto, T., Müller, I., Thomas, G., Melvin, A., & Chubb, J. R. (2010). Methylation of H3K4 Is required for inheritance of active transcriptional states. *Curr Biol*, *20*(5), 397-406. https://doi.org/10.1016/j.cub.2010.01.017

Myrick, D. A., Christopher, M. A., Scott, A. M., Simon, A. K., Donlin-Asp, P. G., Kelly, W. G., & Katz, D. J. (2017). KDM1A/LSD1 regulates the differentiation and maintenance of spermatogonia in mice. *PLoS One*, *12*(5), e0177473. https://doi.org/10.1371/journal.pone.0177473

Nakamura, T., Arai, Y., Umehara, H., Masuhara, M., Kimura, T., Taniguchi, H., Sekimoto, T., Ikawa, M., Yoneda, Y., Okabe, M., Tanaka, S., Shiota, K., & Nakano, T. (2007). PGC7/Stella protects against DNA demethylation in early embryogenesis. *Nat Cell Biol*, *9*(1), 64-71. https://doi.org/10.1038/ncb1519

Newschaffer, C. J., Croen, L. A., Daniels, J., Giarelli, E., Grether, J. K., Levy, S. E., Mandell, D. S., Miller, L. A., Pinto-Martin, J., Reaven, J., Reynolds, A. M., Rice, C. E., Schendel, D., & Windham, G. C. (2007). The epidemiology of autism spectrum disorders. *Annu Rev Public Health*, *28*, 235-258. https://doi.org/10.1146/annurev.publhealth.28.021406.144007

Ng, H. H., Robert, F., Young, R. A., & Struhl, K. (2003). Targeted recruitment of Set1 histone methylase by elongating Pol II provides a localized mark and memory of recent transcriptional activity. *Mol Cell*, *11*(3), 709-719. https://doi.org/10.1016/s1097-2765(03)00092-3

Ng, R. K., & Gurdon, J. B. (2008). Epigenetic memory of an active gene state depends on histone H3.3 incorporation into chromatin in the absence of transcription. *Nat Cell Biol*, *10*(1), 102-109. https://doi.org/10.1038/ncb1674

Nicholson, T. B., Singh, A. K., Su, H., Hevi, S., Wang, J., Bajko, J., Li, M., Valdez, R., Goetschkes, M., Capodieci, P., Loureiro, J., Cheng, X., Li, E., Kinzel, B., Labow, M., & Chen, T. (2013). A hypomorphic lsd1 allele results in heart development defects in mice. *PLoS One*, *8*(4), e60913. https://doi.org/10.1371/journal.pone.0060913

Ooi, S. K., Qiu, C., Bernstein, E., Li, K., Jia, D., Yang, Z., Erdjument-Bromage, H., Tempst, P., Lin, S. P., Allis, C. D., Cheng, X., & Bestor, T. H. (2007). DNMT3L connects unmethylated lysine 4 of histone H3 to de novo methylation of DNA. *Nature*, *448*(7154), 714-717. https://doi.org/10.1038/nature05987

Oswald, J., Engemann, S., Lane, N., Mayer, W., Olek, A., Fundele, R., Dean, W., Reik, W., & Walter, J. (2000). Active demethylation of the paternal genome in the mouse zygote. *Curr Biol*, *10*(8), 475-478. https://doi.org/10.1016/s0960-9822(00)00448-6

Qiao, Y., Yang, X., & Jing, N. (2016). Epigenetic regulation of early neural fate commitment. *Cell Mol Life Sci*, *73*(7), 1399-1411. https://doi.org/10.1007/s00018-015-2125-6

Quenneville, S., Verde, G., Corsinotti, A., Kapopoulou, A., Jakobsson, J., Offner, S., Baglivo, I., Pedone, P. V., Grimaldi, G., Riccio, A., & Trono, D. (2011). In embryonic stem cells, ZFP57/KAP1 recognize a methylated hexanucleotide to affect chromatin and DNA methylation of imprinting control regions. *Mol Cell*, *44*(3), 361-372. https://doi.org/10.1016/j.molcel.2011.08.032

Rechtsteiner, A., Ercan, S., Takasaki, T., Phippen, T. M., Egelhofer, T. A., Wang, W., Kimura, H., Lieb, J. D., & Strome, S. (2010). The histone H3K36 methyltransferase MES-4 acts epigenetically to transmit the memory of germline gene expression to progeny. *PLoS Genet*, *6*(9), e1001091. https://doi.org/10.1371/journal.pgen.1001091

Rudenko, A., Dawlaty, M. M., Seo, J., Cheng, A. W., Meng, J., Le, T., Faull, K. F., Jaenisch, R., & Tsai, L. H. (2013). Tet1 is critical for neuronal activity-regulated gene expression and memory extinction. *Neuron*, *79*(6), 1109-1122. https://doi.org/10.1016/j.neuron.2013.08.003

Sanchez-Delgado, M., Riccio, A., Eggermann, T., Maher, E. R., Lapunzina, P., Mackay, D., & Monk, D. (2016). Causes and Consequences of Multi-Locus Imprinting Disturbances in Humans. *Trends Genet*, *32*(7), 444-455. https://doi.org/10.1016/j.tig.2016.05.001

Seisenberger, S., Andrews, S., Krueger, F., Arand, J., Walter, J., Santos, F., Popp, C., Thienpont, B., Dean, W., & Reik, W. (2012). The dynamics of genome-wide DNA methylation reprogramming in mouse primordial germ cells. *Mol Cell*, *48*(6), 849-862. https://doi.org/10.1016/j.molcel.2012.11.001

Shao, G. B., Wang, J., Zhang, L. P., Wu, C. Y., Jin, J., Sang, J. R., Lu, H. Y., Gong, A. H., Du, F. Y., & Peng, W. X. (2015). Aging alters histone H3 lysine 4 methylation in mouse germinal vesicle stage oocytes. *Reprod Fertil Dev*, *27*(2), 419-426. https://doi.org/10.1071/RD13293

Shi, Y., Lan, F., Matson, C., Mulligan, P., Whetstine, J. R., Cole, P. A., Casero, R. A., & Shi, Y. (2004). Histone demethylation mediated by the nuclear amine oxidase homolog LSD1. *Cell*, *119*(7), 941-953. https://doi.org/10.1016/j.cell.2004.12.012

Shi, Y., Sawada, J., Sui, G., Affar el, B., Whetstine, J. R., Lan, F., Ogawa, H., Luke, M. P., Nakatani, Y., & Shi, Y. (2003). Coordinated histone modifications mediated by a CtBP co-repressor complex. *Nature*, *422*(6933), 735-738. https://doi.org/10.1038/nature01550

Shi, Y. J., Matson, C., Lan, F., Iwase, S., Baba, T., & Shi, Y. (2005). Regulation of LSD1 histone demethylase activity by its associated factors. *Mol Cell*, *19*(6), 857-864. https://doi.org/10.1016/j.molcel.2005.08.027

Simon, J. A., & Tamkun, J. W. (2002). Programming off and on states in chromatin: mechanisms of Polycomb and trithorax group complexes. *Curr Opin Genet Dev*, *12*(2), 210-218. https://doi.org/10.1016/s0959-437x(02)00288-5

Slany, R. K. (2009). The molecular biology of mixed lineage leukemia. *Haematologica*, *94*(7), 984-993. https://doi.org/10.3324/haematol.2008.002436

Sparago, A., Verma, A., Patricelli, M. G., Pignata, L., Russo, S., Calzari, L., De Francesco, N., Del Prete, R., Palumbo, O., Carella, M., Mackay, D. J. G., Rezwan, F. I., Angelini, C., Cerrato, F., Cubellis, M. V., & Riccio, A. (2019). The phenotypic variations of multi-locus imprinting disturbances associated with maternal-effect variants of NLRP5 range from overt imprinting disorder to apparently healthy phenotype. *Clin Epigenetics*, *11*(1), 190. https://doi.org/10.1186/s13148-019-0760-8

Stavropoulos, P., Blobel, G., & Hoelz, A. (2006). Crystal structure and mechanism of human lysine-specific demethylase-1. *Nat Struct Mol Biol*, *13*(7), 626-632. https://doi.org/10.1038/nsmb1113

Stelzer, Y., Wu, H., Song, Y., Shivalila, C. S., Markoulaki, S., & Jaenisch, R. (2016). Parent-of-Origin DNA Methylation Dynamics during Mouse Development. *Cell Rep*, *16*(12), 3167-3180. https://doi.org/10.1016/j.celrep.2016.08.066

Stewart, K. R., Veselovska, L., Kim, J., Huang, J., Saadeh, H., Tomizawa, S., Smallwood, S. A., Chen, T., & Kelsey, G. (2015). Dynamic changes in histone modifications precede de novo DNA methylation in oocytes. *Genes Dev*, *29*(23), 2449-2462. https://doi.org/10.1101/gad.271353.115

Sun, G., Alzayady, K., Stewart, R., Ye, P., Yang, S., Li, W., & Shi, Y. (2010). Histone demethylase LSD1 regulates neural stem cell proliferation. *Mol Cell Biol*, *30*(8), 1997-2005. https://doi.org/10.1128/MCB.01116-09

Tabuchi, T. M., Rechtsteiner, A., Jeffers, T. E., Egelhofer, T. A., Murphy, C. T., & Strome, S. (2018). Caenorhabditis elegans sperm carry a histone-based epigenetic memory of both

spermatogenesis and oogenesis. *Nature Communications*, *9*(1), 4310. https://doi.org/10.1038/s41467-018-06236-8

Tessarz, P., & Kouzarides, T. (2014). Histone core modifications regulating nucleosome structure and dynamics. *Nat Rev Mol Cell Biol*, *15*(11), 703-708. https://doi.org/10.1038/nrm3890

Tosic, M., Allen, A., Willmann, D., Lepper, C., Kim, J., Duteil, D., & Schule, R. (2018). Lsd1 regulates skeletal muscle regeneration and directs the fate of satellite cells. *Nat Commun*, *9*(1), 366. https://doi.org/10.1038/s41467-017-02740-5

Tunovic, S., Barkovich, J., Sherr, E. H., & Slavotinek, A. M. (2014). De novo ANKRD11 and KDM1A gene mutations in a male with features of KBG syndrome and Kabuki syndrome. *Am J Med Genet A*, *164A*(7), 1744-1749. https://doi.org/10.1002/ajmg.a.36450

Vertino, P. M., Yen, R. W., Gao, J., & Baylin, S. B. (1996). De novo methylation of CpG island sequences in human fibroblasts overexpressing DNA (cytosine-5-)-methyltransferase. *Mol Cell Biol*, *16*(8), 4555-4565. https://doi.org/10.1128/MCB.16.8.4555

Waddington, C. H. (1942). CANALIZATION OF DEVELOPMENT AND THE INHERITANCE OF ACQUIRED CHARACTERS. *Nature*, *150*(3811), 563-565. https://doi.org/10.1038/150563a0

Wang, J., Scully, K., Zhu, X., Cai, L., Zhang, J., Prefontaine, G. G., Krones, A., Ohgi, K. A., Zhu, P., Garcia-Bassets, I., Liu, F., Taylor, H., Lozach, J., Jayes, F. L., Korach, K. S., Glass, C. K., Fu, X. D., & Rosenfeld, M. G. (2007). Opposing LSD1 complexes function in developmental gene activation and repression programmes. *Nature*, *446*(7138), 882-887. https://doi.org/10.1038/nature05671

Wasson, J. A., Simon, A. K., Myrick, D. A., Wolf, G., Driscoll, S., Pfaff, S. L., Macfarlan, T. S., & Katz, D. J. (2016). Maternally provided LSD1/KDM1A enables the maternal-to-zygotic transition and prevents defects that manifest postnatally. *Elife*, *5*. https://doi.org/10.7554/eLife.08848

Wei, X., Calvo-Vidal, M. N., Chen, S., Wu, G., Revuelta, M. V., Sun, J., Zhang, J., Walsh, M. F., Nichols, K. E., Joseph, V., Snyder, C., Vachon, C. M., McKay, J. D., Wang, S. P., Jayabalan, D. S., Jacobs, L. M., Becirovic, D., Waller, R. G., Artomov, M., Viale, A., Patel, J., Phillip, J., Chen-Kiang, S., Curtin, K., Salama, M., Atanackovic, D., Niesvizky, R., Landgren, O., Slager, S. L., Godley, L. A., Churpek, J., Garber, J. E., Anderson, K. C., Daly, M. J., Roeder, R. G., Dumontet, C., Lynch, H. T., Mullighan, C. G., Camp, N. J., Offit, K., Klein, R. J., Yu, H., Cerchietti, L., & Lipkin, S. M. (2018). Germline Lysine-Specific Demethylase 1 (LSD1/KDM1A) Mutations Confer Susceptibility to Multiple Myeloma. *Cancer Res*, *78*(10), 2747-2759. https://doi.org/10.1158/0008-5472.CAN-17-1900

Wen, C., Levitan, D., Li, X., & Greenwald, I. (2000). spr-2, a suppressor of the egg-laying defect caused by loss of sel-12 presenilin in Caenorhabditis elegans, is a member of the SET protein subfamily. *Proc Natl Acad Sci U S A*, *97*(26), 14524-14529. https://doi.org/10.1073/pnas.011446498

Whyte, W. A., Bilodeau, S., Orlando, D. A., Hoke, H. A., Frampton, G. M., Foster, C. T., Cowley, S. M., & Young, R. A. (2012). Enhancer decommissioning by LSD1 during embryonic stem cell differentiation. *Nature*, *482*(7384), 221-225. https://doi.org/10.1038/nature10805

Wu, H., & Zhang, Y. (2011). Mechanisms and functions of Tet protein-mediated 5-methylcytosine oxidation. *Genes Dev*, *25*(23), 2436-2452. https://doi.org/10.1101/gad.179184.111

Wu, S. F., Zhang, H., & Cairns, B. R. (2011). Genes for embryo development are packaged in blocks of multivalent chromatin in zebrafish sperm. *Genome Res*, *21*(4), 578-589. https://doi.org/10.1101/gr.113167.110

Xu, Q., Xiang, Y., Wang, Q., Wang, L., Brind'Amour, J., Bogutz, A. B., Zhang, Y., Zhang, B., Yu, G., Xia, W., Du, Z., Huang, C., Ma, J., Zheng, H., Li, Y., Liu, C., Walker, C. L., Jonasch, E., Lefebvre, L., Wu, M., Lorincz, M. C., Li, W., Li, L., & Xie, W. (2019). SETD2 regulates the maternal epigenome, genomic imprinting and embryonic development. *Nat Genet*, *51*(5), 844-856. https://doi.org/10.1038/s41588-019-0398-7

Xu, R., Li, C., Liu, X., & Gao, S. (2021). Insights into epigenetic patterns in mammalian early embryos. *Protein & cell*, *12*(1), 7-28. https://doi.org/10.1007/s13238-020-00757-z

Yang, M., Gocke, C. B., Luo, X., Borek, D., Tomchick, D. R., Machius, M., Otwinowski, Z., & Yu, H. (2006). Structural basis for CoREST-dependent demethylation of nucleosomes by the human LSD1 histone demethylase. *Mol Cell*, *23*(3), 377-387. https://doi.org/10.1016/j.molcel.2006.07.012

Yao, H., Goldman, D. C., Nechiporuk, T., Kawane, S., McWeeney, S. K., Tyner, J. W., Fan, G., Kerenyi, M. A., Orkin, S. H., Fleming, W. H., & Mandel, G. (2014). Corepressor Rcor1 is essential for murine erythropoiesis. *Blood*, *123*(20), 3175-3184. https://doi.org/10.1182/blood-2013-11-538678

Yoder, J. A., Soman, N. S., Verdine, G. L., & Bestor, T. H. (1997). DNA (cytosine-5)-methyltransferases in mouse cells and tissues. Studies with a mechanism-based probe. *J Mol Biol*, *270*(3), 385-395. https://doi.org/10.1006/jmbi.1997.1125

You, A., Tong, J. K., Grozinger, C. M., & Schreiber, S. L. (2001). CoREST is an integral component of the CoREST- human histone deacetylase complex. *Proceedings of the National Academy of Sciences of the United States of America*, *98*(4), 1454-1458. https://doi.org/10.1073/pnas.98.4.1454

Zheng, H., Huang, B., Zhang, B., Xiang, Y., Du, Z., Xu, Q., Li, Y., Wang, Q., Ma, J., Peng, X., Xu, F., & Xie, W. (2016). Resetting Epigenetic Memory by Reprogramming of Histone Modifications in Mammals. *Mol Cell*, *63*(6), 1066-1079. https://doi.org/10.1016/j.molcel.2016.08.032

Zhu, D., Holz, S., Metzger, E., Pavlovic, M., Jandausch, A., Jilg, C., Galgoczy, P., Herz, C., Moser, M., Metzger, D., Gunther, T., Arnold, S. J., & Schule, R. (2014). Lysine-specific demethylase 1 regulates differentiation onset and migration of trophoblast stem cells. *Nat Commun*, *5*, 3174. https://doi.org/10.1038/ncomms4174

Zylicz, J. J., Borensztein, M., Wong, F. C., Huang, Y., Lee, C., Dietmann, S., & Surani, M. A. (2018). G9a regulates temporal preimplantation developmental program and lineage segregation in blastocyst. *Elife*, *7*. https://doi.org/10.7554/eLife.33361